UNIVERSIDADE D
COIMBRA

Maria José Gueidão Costa

REVEALING THE ROLE OF NEOCORTICAL CIRCUIT DEFECTS IN COGNITIVE ALTERATIONS IN AUTISM SPECTRUM DISORDER

Dissertação no âmbito do Mestrado em Biologia Celular e Molecular, orientada pela Doutora Melanie Ginger e pela Doutora Ana Luísa Carvalho e apresentada ao Departamento de Ciência da Vida da Faculdade de Ciência e Tecnologia da Universidade de Coimbra.

Outubro de 2020

MARIA JOSÉ GUEIDÃO COSTA

REVEALING THE ROLE OF NEOCORTICAL CIRCUIT DEFECTS IN COGNITIVE ALTERATIONS IN AUTISM SPECTRUM DISORDER

Supervised by Doctor Melanie Ginger[1] and Doctor Ana Luísa Carvalho[2]

[1] Cortical Plasticity Team | Neurocentre Magendie – INSERM U1215

[2] Department of Life Sciences – Faculty of Science and Technology of the University of Coimbra

Master's in Cellular and Molecular Biology, specialization in Neurobiology

Department of Life Sciences, Faculty of Science and Technology of the University of Coimbra

October 2020

I would like to thank everyone who somehow contributed to make this work come to a successful conclusion:

to my supervisors, to my classmates and lab colleagues (and friends),
to my family, especially my sister, to my boyfriend, and to my friends.
For their unconditional support and unlimited patience,
thank you.

ABSTRACT

Autism spectrum disorder is a complex neurodevelopmental disorder associated with a range of early-onset social, behavioural and cognitive impairments. Atypical neuronal connectivity underlies one of the most consistent theories to explain the neurobiological basis of ASD. Increasing evidence of dysfunctional long-range connectivity of the prefrontal cortex (PFC) places this brain region at the core of this theory. The PFC is a major hub for connectivity, and both clinical and preclinical studies on ASD have correlated alterations in PFC structure with a range of symptoms related to its function, including deficits in executive, emotional and cognitive features such as working memory, decision-making, inhibitory control, social communication and attention. Accumulating evidence point to a requirement for attention, mediated in part by the anterior cingulate cortex (ACC; a part of the PFC) during trace fear conditioning (TFC) in mice, as well as in humans. Notably, *Fmr1* knock-out (KO) mice, a model for studying fragile X syndrome, which is the most common and best characterized genetic cause of ASD, exhibits defects in TFC, coupled to a decrease in long-term potentiation within the ACC. To date, no study has directly related cognitive deficits to changes in ACC circuits in ASD. Thus, the main goal of this study was to identify and quantify the specific structural and functional alterations of ACC connectivity in the *Fmr1*KO mouse model. To address this question, we employed a novel strategy using rabies virus-mediated mono-trans-synaptic tracing, combined with c-fos-based tet-tagging to label the inputs into ACC neurons implicated in TFC. Using rapid acquisition scanning microscopy and custom-made quantification approaches, these neural connections were mapped to identify alterations in the input maps of ACC neurons in *Fmr1*KO mice. Functional consequences of altered connectivity on behavioural outcome were explored by DREADD-dependent manipulation of specific pathways providing input into ACC neurons. Our findings suggest both an increase and a reduction in inputs from specific thalamic nuclei. Yet, our analysis regarding the implication of this specific input disruption on *Fmr1*KO phenotype is preliminary and nonconclusive. Further experiments should be carried out.

Keywords: Autism spectrum disorder; Anterior cingulate cortex; Cognition; Fragile X syndrome; Neural circuits

RESUMO

O transtorno do espectro do autismo (ASD) é um conjunto de distúrbios do neurodesenvolvimento caracterizados por aterações sociais, comportamentais e cognitivas precoces. A existência de alterações na conectividade neuronal apresenta-se como uma das teorias mais consistentes para explicar a base neurobiológica do ASD. Evidências crescentes que sugerem a prevalência de uma conectividade de longo alcance disfuncional no córtex pré-frontal (PFC), colocam esta região do cérebro no centro desta teoria. O PFC é um centro fundamental de conectividade cerebral, e estudos sobre ASD, quer sejam clínicos ou pré-clínicos, têm correlacionado alterações na estrutura do PFC com uma série de sintomas associados à sua função, incluindo deficiências nos processos executivos, emocionais e cognitivos, tais como a memória de trabalho, a capacidade de tomar decisões, o controlo inibitório, a comunicação social e a atenção. Estudos anteriores apontam para a necessidade de atenção, mediada em parte pelo córtex do cíngulo anterior (ACC; uma parte do PFC) durante *trace fear conditioning* (TFC), tanto em modelos animais como em seres humanos. O ratinho Fmr1 knock-out (*Fmr1*KO) – usado no estudo da síndrome do X-Frágil, amplamente descrita como sendo a causa genética mais comum do ASD – apresenta defeitos em TFC, associados a uma diminuição da potenciação de longa duração ao nível do ACC. Até à data, nenhum estudo relativo ao ASD relacionou diretamente os défices cognitivos com alterações nos circuitos neuronais do ACC. O principal objetivo deste estudo foi identificar e quantificar as alterações estruturais e funcionais específicas da conectividade do ACC nos ratinhos *Fmr1*KO. Para isso, foi aplicada uma nova estratégia que combina *rabies virus-mediated mono-trans-synaptic tracing* e *c-fos-based tet-tagging* para identificar os eferentes dos neurónios do ACC implicados no TFC. Estas conexões neurais foram mapeadas para identificar alterações no circuito neuronal do ACC do *Fmr1*KO. As consequências funcionais que estas alterações podem ter no fenótipo do *Fmr1*KO foram exploradas através da manipulação (dependente da expressão DREADDs) de circuitos específicos que representam inputs nos neurónios do ACC ativados durante TFC. Os resultados sugerem, tanto um aumento, como uma diminuição nas projeções neuronais que partem de núcleos talâmicos específicos. Contudo, a análise efetuada sobre a implicação desta alteração do circuito neuronal do *Fmr1*KO no seu comportamento é preliminar e inconclusiva. Outros estudos devem ser levados a cabo.

Palavras-chave: Circuitos neuronais; Cognição; Córtex cíngulo anterior; Síndrome do X-Frágil; Transtorno do espectro do autismo

CONTENTS

LIST OF FIGURES

ABBREVIATION LIST

A/P: Anterior/posterior

AAV: Adeno-associated Virus

ACC: Anterior cingulate cortex

AM: Anteromedial thalamic nucleus

APC: Adenomatous polyposis coli gene

ASD: Autism spectrum disorder

CDH: Chromodomain-helicase-DNA-binding

ChR: Channelrhodopsin

CNO: Clozapine-N-Oxide

CNTNAP2: Contactin associated protein- Like 2

CTNNB1: Catenin beta-1

D/V: Dorsal/ventral

DAPI: 4',6'-Diamidino-2-phenylindole

DNA: Deoxyribonucleic acid

Dox: Doxycycline

DREADD: Designer receptor exclusively activated by designer drug

DSM: Diagnostic and statistical manual of mental disorders

EEG: Electroencephalography

EM: Electron microscopy

EnvA/B: Envolop A/B protein

ER: Estrogen receptor

ErbB4: Erb-B2 receptor tyrosine kinase 4

FMR1: Fragile X mental retardation 1 gene

fMRI: Functional magnetic resonance imaging

FMRP: Fragile X mental retardation protein

FXS: Fragile X syndrome

GABA: Gamma-AminoButyric acid

GFP: Green fluorescent protein

GIRK: G-protein-gated inwardly rectifying potassium channel

GPCR: G protein-coupled receptor

HSV: Herpes simplex virus

hSyn: Human synapsin 1 gene promoter

IEG: Immediate-early gene

IL: Infralimbic cortex

ITI: Inter-trial interval

KO: Knockout

L/M: Lateral/medial

LM: Light microscopy

LPFC: Lateral prefrontal cortex

LSFM: Light-sheet fluorescence microscopy

MCC: Midcingulate cortex

MD: Mediodorsal thalamic nucleus

MEA: Medial amygdalar nucleus

MECP2: Methyl CpG Binding Protein 2

MEG: Magnetoencephalography

MOs: Secondary motor cortex

mPFC: Medial prefrontal cortex

MRI: Magnetic resonance imaging

mRNA: Messenger ribonucleic acid

mTOR: Mammalian target of Rapamycin

NDB: Diagonal band nucleus

NF1: Neurofibromatosis

NLGN3: Neuroligin 3

NLGN4X: Neuroligin 4 X- Linked

NMDA: N-Methyl-D-Aspartate Receptor

NRXN1: Neurexin-1-Alpha

PCR: Polymerase chain reaction

PDD-NOS: Pervasive development disorder- not otherwise specified

PET: Positron emission tomography

PFA: Paraformaldehyde

PFC: Prefrontal cortex

PL: Prelimbic cortex

PO: Posterior complex of the thalamus

PSEM: Pharmacologically slective effector molecule

PTEN: Phosphatase and tensin homolog

RABV ΔG: Glycoprotein gene-deleted RABV

RABV: Rabies virus

RG: RABV envelop glycoprotein

RSP: Retrosplenial cortex

SHANK2/3: SH3 and multiple ankyrin repeat domains 2/3

STP: Serial two-photon tomography

TFC: Trace fear conditioning

TRE: Tetracycline-dependent promotor

TSC: Tuberous sclerosis gene

TVA/B: Avian receptor protein A/B

WGA-HRP: Wheat germ agglutinin-horseradish peroxidase

WT: Wildtype

1. INTRODUCTION

Autism spectrum disorder (ASD) is a genetically and clinically heterogeneous neurodevelopmental disorder, clinically characterized by early-onset deficits in social behaviour, and verbal and non-verbal communication, restrictive interests, and repetitive behaviour [1–3].

The clinical features of ASD represent a worrying, significant cause of lifetime neuropsychiatric morbidity due to their lifelong persistence and high level of associated comorbidities [4,5], as well as the absence of effective treatment strategies. Additionally, the worldwide prevalence of this disorder is substantially increasing [6].

ASD diagnosis is mainly based on the clinical evaluation of behaviour together with the assessment of developmental levels (by testing cognition, language, speech and motor function, for example), and medical and family history information. Nevertheless, genetic and neuroimaging studies also provide strong support for a neurobiological cause underlying this behavioural biomarker [1,7]. Atypical neuronal connectivity is one of the most consistent theories for explaining the neurobiological basis of ASD [8,9] and has particular pertinence for forward and reverse translational studies in human subjects. In particular, a pattern of reduced long-range connectivity and increased local connectivity has been suggested to explain the behavioural and cognitive features of the disorder [8,10].

As a major hub for brain connectivity [11–13], prefrontal cortex (PFC) structure and function has demonstrated to be relevant for the understanding of the neurobiological underpinnings of ASD. Clinical and preclinical results have correlated alterations of this brain area with deficits in executive, emotional and cognitive features such as working memory, decision-making, inhibitory control, social communication and attention [8,9,14,15].

The anterior cingulate cortex (ACC) is a prefrontal region consistently reported as functional and structural modified in imaging and *post-mortem* analysis of ASD patients [1,7,16,17]. Interestingly, ACC has been extensively implicated in a range of functions strongly related to a number of core features of ASD as well as related comorbidities. Namely, social interaction, emotional learning, long-term socio-emotional attachments, adaptive responses to changing conditions, conflict processing and motor coordination [16–20].

This first chapter aims to review the existing knowledge in the field of ASD neurobiology, with a special focus on the disruption of neural circuits associated with altered PFC function.

1.1 AUTISM SPECTRUM DISORDER

1.1.1. CLINICAL FEATURES AND DIAGNOSIS

In 1943, Leo Kanner used for the first time the term “autism” (previously created by Eugen Bleuler to define symptoms of schizophrenia) in its modern meaning while clinically describing 11 young people who presented affective disturbances and had pronounced social isolation [1].

From the 1950s to the 1970s, autism was essentially considered a form of psychosis similar to childhood schizophrenia [1]. It was only with the publication of the DSM-3 that autism began to be qualified as a development disorder and that specific diagnostic criteria were suggested [1].

In 2013, when the DSM-5 was published, the category “Autism Spectrum Disorder” was adopted to include the notion of a spectrum encompassing distinct etiologies and pathophysiological entities with multiple genetic and environmental contributions [1,21]. Thus, the extensive categorization of ASD combines numerous disorders that were previously separated into Kanner’s Autism, Asperger’s Syndrome, Childhood Autism, Atypical Autism, Heller’s Syndrome and Pervasive developmental disorder – not otherwise specified (PDD-NOS) [21].

Currently, according to DSM-5, the diagnostic criteria for ASD are (1) «persistent deficits in social communication and social interaction across multiple contexts»; (2) «restricted, repetitive patterns of behaviour, interests or activities»; (3) «the presence of symptoms in early developmental period»; (4) «core symptoms must cause significant impairment in social, occupational, or other important areas of current functioning»; and (5) «cannot be better explained by intellectual disability or global developmental delay» [1,21]. The first criterion includes deficits in social-emotional reciprocity like the decrease of sharing facts such as interests or sensations like emotions and affection; deficits in nonverbal communicative behaviours used for social interaction; and deficits in developing, maintaining, or even understanding relationships. The second refers to stereotyped or repetitive motor movements, use for objects or speech; insistence on sameness, inflexible adherence to routines or customary patterns, and/or verbal nonverbal behaviour; extremely restricted and fixated interests that are regarded with unexpected and uncommon intensity or focus; and hyper- or hyporeactivity to sensory input and/or unusual interests in sensory aspects of the environment [21]. As a result of this revised definition, a delay in the development of linguistic capacities (previously considered a main criterion) now has reduced importance and it is included in the deficits in social interactions criterion [21].

The severity and nature of the deficit in social interactions may differ with age and developmental stages but it frequently compromises interactions in a familiar environment, at school and in the community [21]. Clinical heterogeneity is present not only in symptom severity, but also in language ability, cognitive functioning, co-occurring diagnosis, and functional outcome [1,21–23].

DSM-5 also incorporates the utilization of specifiers that aim at a more detailed diagnosis of ASD, particularly when there is an association with intellectual impairment; language impairment; another neurodevelopmental, mental or behavioural disorder; a known medical or genetic conditions (such as Down Syndrome, Rett Syndrome and Fragile X Syndrome) or an exposure to environmental risk factors [21].

1.1.2. EPIDEMIOLOGY

The most recent epidemiological studies indicate that ASD prevalence is increasing globally. For instance, it is estimated that that 1 in 59 children in the United States and on average 1 in 89 children in Europe (varying among countries) have ASD [6,24,25]. These numbers can be explained not only by improved awareness and reporting, better diagnostic tools and changes in diagnostic criteria, but also by an increase in risk factors, particularly environmental pollution and advanced paternal age [1,7,24,25].

According to the same studies, a strong male bias has also been observed, with male-to-female registered ratios of 4 to 1 (4 affected males for every 1 affected female) [1,7,26,27]. This male predominance in ASD might result from differences in phenotypic presentation, meaning that, for example, fewer restricted and repetitive behaviours have been observed by in female subjects [1,26]. Evidence suggests that sex chromosomal gene dosage and/or sex hormone levels, especially testosterone, may modulate the presentation of the autistic phenotype [1,26,27]. Yet, future work is needed for a better understanding of the biological basis of this sex-differential risk [1,26].

1.1.3. ETIOLOGY

ASD is considered a multi-factorial disorder resulting from genetic, epigenetic and non-genetic risk factors, and their interaction [1,7,28,29]. Twin and family studies support the notion that ASD susceptibility is highly heritable [7,28–30]. Early signs of ASD in siblings of individuals with autism were detected with a recurrence rate of 10%-20% [1,29,31]. The concordance rate increases to 82%-92% in monozygotic, compared with only 20% in dizygotic twins [1,29,31]. The lack of a complete concordance in monozygotic twins points to an interaction between genetic, epigenetic and/or environmental risk

factors in the pathogenesis of ASD [29–31]. In addition, it could also be explained by situations in which the monozygotic twin presents some of the features associated with ASD but doesn't meet all the criteria required for a full diagnosis [29–31].

Although there is clearly a strong genetic contribution to ASD, the underlying etiology of ASD is complex, involving many genes, some of which represent common genetic variations that affect limited biological pathways of brain development and plasticity [7,28,30,32]. Genetic studies have identified gene mutations and chromosomal anomalies – frequently gene copy-number variations – that specifically interfere with multiple cellular pathways. Such pathways impinge on mRNA translation, cell metabolism, synaptogenesis and axonal mobility and thus lead to the disruption of neuronal connections, brain growth and synaptic/dendritic morphology [1,7,28,30,32]. The expression of ASD-related genes is widely detected throughout the brain, explaining the variety of symptoms observed in ASD subjects [32].

Secondary forms of ASD (also referred as syndromic autism) have been correlated with genetic diseases, namely tuberous sclerosis (*TSC1* and *TSC2* genes), neurofibromatosis (*NF1* gene), Rett syndrome (*MECP2* gene), Cowden syndrome (*PTEN* gene, involved on the regulation of mTOR signaling), Phelan-McDermid syndrome (*SHANK3* gene), cortical dysplasia-focal epilepsy syndrome (*CNTNAP2* gene) and Fragile X syndrome (*FMR1* gene) [7,27,29,31–35].

Fragile X syndrome (FXS) is the most common and best characterized genetic cause of ASD (between 2 and 5% of ASD cases are attributed to FXS) [29,31,32,36]. This neurodevelopmental disorder is caused by a trinucleotide expansion in the *FMR1* gene, which leads to the loss or significant reduction in the expression of the fragile X mental retardation protein (FMRP) [29,31,32,36]. FMRP is a RNA-binding protein that regulates a myriad of different RNA transcripts, thus implicated in a number of pathological pathways inherent to ASD etiology [29,31,32,36].

Non-syndromic forms of autism involve mutations in synaptic genes such as *NLGN3*, *NLGN4X*, *SHANK2* or *NRXN1* [7,27,37,38,28–35]. Recent exome sequencing analysis have detected *de novo* or noninherited mutations in both the *CDH5* and *CDH8* genes – which encode DNA helicases that act as chromatin remodeling factors and regulate transcription –, confirming that epigenetic events also contribute to ASD development [29,32,33]. Another example is the pronounced correlation between ASD and alterations in the ß-catenin network, revealing mutations in *CTNNB1* (the ß-catenin gene), and ß-catenin interacting proteins (Shank3 and APC) and transcriptional regulator (CDH8) [33,37].

It is estimated that a total of 1000 or more genes may be linked to ASD, meaning that each gene may contribute to less than 1% of the cases [7,28,30–32]. The relevance of

the vast majority of the identified genetic variants remains unknown, in particular due to of the diversity of sample size, study designs, control subjects, and statistical models used for genomic assays [39]. In addition, multiple variants of a candidate gene may present its own associated risk [7,27,37,38,28–35]. Further quantitative assessment of ASD risk genes through the transmission and *de novo* association (TADA) analysis, and whole exome sequencing (WES) studies of ASD genetic samples, partially overcome this diversity [39,40]. A number of strategies have been developed in order to evaluate the importance and contribution of risk genes. For example, the SFARI gene platform (https://gene.sfari.org/) provides a curated database of ASD risk genes, using scoring criteria mainly based on relative value of sample size, statistical significance, replication and functional evidence, to assess the significance for ASD [41]. This database accords particular value to human genomic studies[41] thus classifying genes associated with ASD into six main categories: «high confidence», «strong candidate», «suggestive evidence», «minimal evidence», «hypothesized but untested», and «evidence does not support a role» [41]. A total of 25 genes, including FMR1, *PTEN*, *SHANK3* and *CDH8*, are classify as «high confidence genes»; and 66 genes as «strong candidate», including *CNTNAP2*, *SHANK2*, *NLGN3*, *NRXN1* [41].

Alongside, pre-, peri- and post-natal non-genetic factors also contribute to ASD [1,30,31]. Environmental factors can affect gene expression during critical periods of embryo development through epigenetic mechanisms, such as DNA methylation, changes in histone proteins and expression of noncoding RNA [1,7,30,42]. Maternal physical and mental health, exposure to thalidomide or valproic acid, viral infections, abnormal gestational age, low birth weight and size, hypoxia, or post-natal autoimmune disease are examples of environmental risk factors involved in the incidence of ASD [1,7,30,31,42].

1.1.4. NEUROBIOLOGY

Post-mortem histological analyses and neuroimaging studies have provided important macro- and microscopic insights into the neuropathological changes underlying ASD clinical features [1,22,43–45].

Clinical and pre-clinical studies on ASD have identified widespread alterations on neuronal morphology, function and connectivity, as consequence of an early, abnormal brain maturation. The affected stages of neurodevelopment include prenatal events of neuronal migration and axonal pathfinding, and postnatal dendritic development, synaptogenesis and pruning [22,23,43–46]

Preliminary morphometric and structural neuroimaging data revealed that both brain size and head circumference are increased during early childhood in ASD patients, when compared to normal age-based values, [22,23,43,45,47]. Subsequent *post-mortem* studies support the notion that this phenotype reflects an augmentation of cerebral grey and white matter tracts – even though an increase in pathway volume and fiber number was observed in the absence of brain volume alterations [22,23,43,45,48]. The grey and white matter thickness and organization are altered as a consequence of developmental alterations in neuronal and glial density and size, axonal guidance, synaptogenesis, axonal pruning, and neuronal myelination [22,23,43,45]. The presence of these neurodevelopmental impairments in ASD was confirmed by results from magnetic resonance spectroscopy, which revealed that molecular markers of enhanced neuronal and synaptic density are often decreased [23].

Cortical dysplasia and nodules of neuronal heterotopy are the most consistent abnormalities reported in *post-mortem* microscopic analysis [10,23,44,45]. These defects point to alterations in precursor proliferation, programmed cell death, axodendritic outgrowth, and neuronal migration and maturation [23,44].

In ASD patients, neocortical minicolumns – vertical structural arrays of inter-connected neurons comprising the basic modular units for information processing – are small and present in larger numbers compared with typically developing individual (see Casanova *et al*., 2002) [49]. At the histological level these columns exhibit reduced neuropil space, and are constituted by more dispersed neurons with smaller soma and nucleus [22,23,44,45,49]. Minicolumnar pathology can explain grey and white matter abnormalities, the imbalance between neuronal excitation and inhibition, or excess local connectivity [22,44–49].

As alluded to above, alterations in excitatory/inhibitory (E/I) balance (including altered GABAergic function and glutamatergic hypofunction) are popular alternative theories for explaining the autism phenotype [50,51] . Changes in the E/I balance involving the circuits that mediate language, and social behaviour has been hypothesized as a neurobiological cause for ASD [46,50–52]. Early evidence of altered EI balance come from data revealing decreased levels of neuronal synchronization during response inhibition tasks [50,53]. In addition, a reduction of the neuropil space occupied by inhibitory interneurons, as a consequence of minicolumn narrowing, can reflect a deficit in cortical inhibition [23,45,50]. Clinical and preclinical molecular studies have identified downregulation of inhibitory biomarkers and receptors, genetic mutations involved with the outgrowth of inhibitory neurons and inhibitory synaptogenesis and a reduction in interneuron numbers (e.g.: El Idrissi *et al*., 2005; Gibson *et al*, 2008; Gogolla *et al*., 2011; Peñagarikano *et al.*, 2011; Hashemi *et al*., 2017) [54–58]. As a

corollary, alterations in E/I can be expected to impact on many aspects of neuronal circuit function, including the maturation of neuronal circuits.

Current research also indicates that cerebellar dysfunction leads to the functional disruption of specific cerebellar circuits, which contribute to cognitive, motor and social reward deficits in ASD [59,60]. Cerebellar hypoplasia, reduced number of Purkinje cells, age-related changes in cerebellar nuclei and inferior olive, smaller cerebellar volume and altered activation of cerebello circuits during task-based fMRI are some of the evidence supporting this theory [23,60].

Concomitantly, atypical neuronal connectivity is one of the most consistent theories explaining the neurobiological basis of ASD [10,22,46,61,62]. Specifically, a pattern of reduced long-range connectivity and increased local connectivity has been suggested to explain the social, behavioural and cognitive phenotype of the disorder [8,10,22,46,61–63]. From a neurobiological perspective, differences in brain connectivity may be a consequence of the previous described abnormalities in white matter tracts, specifically decreased axon diameter and/or decreased myelination that reduce axon volume/axon density [22,45,61]. Yet, neurophysiological basis and genetic etiologies underlying alterations of neuronal connectivity are poorly known [61,63,64].

ASD children show reduced functional cortico-cortical and cortico-subcortical connectivity (long-range connectivity), and aberrant our excessive activation and increased synchrony within specific brain networks (local connectivity) during distinct task-based fMRI and resting state studies [8,10,22,61,63]. Structural imaging data has also revealed alterations in deep white matter tracts, suggesting compromised composition and/or structural integrity of long-distance pathways [8,10,22,61,63]; and expanded white matter volume related to fibres connecting neighbouring regions, suggesting local overconnectivity [22,23,43,45,48]. While numerous clinical studies support this notion, other studies point to a more heterogenous or nuanced pattern of connectivity changes. For instance, functional and structural neuroimaging results have also showed long-range overconnectivity, or a mixture of local over- and underconnectivity [22,64–69]. According to Vasa, *et al*. (2016), these inconsistent findings can be explained by possible artefacts related to each connectivity measure, methodological heterogeneity, and the pronounced variability of clinical phenotype and etiology in ASD [22,63]. To those it can also be added factors like the choice of control group, age or deliberate decisions to only include specific ASD subgroups e.g. high performing ASD patients [22,63]. In recent years, the development of methodology (such as small animal MRI or sophisticated viral tracing approaches) has permitted the study of mesoscale changes in connectivity in animal models of ASD.

1.1.5. BIOMARKERS

ASD is characterized by significant clinical and etiological heterogeneity. This heterogeneity reinforces the need for biomarkers – parameters that can be objectively measured and evaluated – as sensitive, valid and reliable outcome measures for an earlier and reproducible diagnosis [70–73]. Moreover, ASD biomarkers permit the stratification of ASD patients according to etiology or neuropathological pathways thereby improving clinical treatment response, drug dosage and treatment evaluation in clinical trials [70–73].

Potential ASD biomarkers include genetic, epigenetic, hormonal, metabolic, behavioural, and brain anatomy and activity markers [72–74]. Genetic and epigenetic markers refer, respectively, to genetic tests based on the clustering of genes presenting a strong correlation with ASD and to the recognition of DNA methylation patterns. Hormonal markers, on the other hand, indicate imbalances such as decreases in plasma levels of oxytocin and/or melatonin. Metabolic markers can range from indicators of immune dysregulation, to fatty acid analysis, to markers of oxidative stress, mitochondrial dysfunction or neurotransmitter function. Behavioural markers include intelligence quotient tests (e.g.: Wechsler Adult Intelligence Scale), verbal language and social deficits scores (e.g.: Social Responsiveness Scale and Behaviour Rating Inventory of Executive Function-Adult), evaluation of sensory processing (e.g.: Adolescent/Adult Sensory Profile) and the Autism Diagnostic Interview [72–74]. Lastly, markers of brain anatomy and activity refer to morphometric and functional neuroimaging, and EEG (summarized in Ruggeri *et al*., 2013) [73].

A major limitation of most of the previous described biomarkers is their lack of reproducibility. For instance, Goldani *et al*. (2014) defends that ASD biomarkers translate genetic, epigenetic or neurobiological changes/processes that are present/activate during a specific time-window, thus they do not define the disorder, only the underlying mechanism [74]. Additionally, common genetic variants, beyond known ASD forms related to genetic syndromes, have not been consistently identified [73–75]; and metabolic biomarkers, for example, only provide a baseline for evaluating disease progression over time [74].

Excluding significant interindividual differences, neuroanatomical findings across groups tend to be characteristic, objectively measurable and reflect the underlying neuropathobiology of the disorder. Neuroanatomical findings can thus overcome variations due to gene or chromosomal mutations [73,75]. Emerging data from functional brain connectivity analysis support a role for brain connectivity as a ASD biomarker, describing it as a tool for early diagnosis and prognosis of children with ASD [75–78]. For

instance, Anderson, *et al*. (2011) conclude that functional connectivity MRI is a feasible diagnostic assay for ASD [79]. Keown, *et al*. (2013) have correlated symptomatology severity with different patterns of local connectivity using the same imaging technique [78].

1.1.6. EXPERIMENTAL MODELS

In order to correlate risk factors for ASD with the disease neurobiology, different molecules, cells, and circuits can be dissected through the employment of computational, cellular, and animal model systems. Their use is particularly important in the understanding of how and when risk factors can affect brain development and contribute to subsequent changes in behaviour and physiology.

Recently introduced techniques using human cell lines are being used to explore the molecular consequences of genetic risk variants. Human models consist of cells derived from patients that have been reprogrammed into induced pluripotent stem cells and then differentiated into individual neuronal lineages. They allow the identification of deficits and the evaluation of therapeutic interventions, and represent testable targets and hypotheses for clinical research trials [31,80]. For example, Yi et al (2016) used gene editing to introduce a mutation associated with Phelan-McDermid syndrome [81]. By comparing the physiological phenotype of induced neurons carrying this mutation with isotype controls, they described a novel non-synaptic mechanism which might be amenable to pharmacological interventions [81]. In addition, brain organoids derived from human pluripotent stem cells are being used for ASD modeling [82]. These are three-dimensional cell cultures composed of progenitor, neuronal and glia cell types thus able to generally recapitulate the brain development and circuit structure (i.e.: greater degree of complexity; details in Qian *et al*., 2019) [82,83]. While it must be stated that these models are more similar to human neurons than other kinds of differentiated neuronal-like cultures, these ‘induced’ neurons have until now been confined to early stages of brain development, represent a limited number of cell types, sometimes suffer from lack of reproducibility and lack isotype controls (unless gene editing techniques are used) [31,81].

Animal models permit an elucidation of the consequences of a genetic variant or environmental manipulation on brain structures and cell types. Since each ASD core symptom domain is characterized by a multifactorial etiology and an extensive phenotypic diversity, it is clear and understandable that there is no single animal model that can capture all cellular, molecular, or systems-level features of ASD. Because of the complexity of this disorder, researchers focused on the use of approaches that

allow the investigation of specific aspects of the disorder as well as an examination of the underlying mechanisms.

The value of information derived from this type of experimental models mainly depends on their validity. The validation process of an animal model usually considers three major aspects: construct validity, face validity and predictive validity [84]. Construct validity refers to the similarity between the mechanism underlying the disease phenotype in the experimental model, and the known disease etiology in humans; face validity evaluates how well an animal model replicates the diseases phenotype in humans; and predictive validity establishes the value that an outcome obtained in a model has to predict currently unknown aspects of the modeled condition [84].

Beside its small size, low-cost, high fertility rate and rapid development, zebrafish is consider a relevant model of ASD, in particular because of its ability to display social behavioural phenotypes from early life onwards [85,86]. Alterations in zebrafish sociability are easily observed thus multiple tests have been developed to define ASD-like behavioural phenotypes based, for example, on zebrafish predisposition to swim toward other fish, engage in dominance or freeze [85]. Moreover, the transparency of larvae and some adult strains make zebrafish a good model for imaging approaches evaluating the consequences of neural genetic manipulation on behaviour outcome [85,86]. Zebrafish is also a very useful model for pharmacological studies given that drug administration is simple (e.g.: drug diffuses through the gill into the bloodstream) [85]. Nonetheless, the lack of correlation between the behavioural phenotype detected in zebrafish models of ASD and the human behaviour (i.e.: lack of face validity), as well as the significant anatomical differences between species limits its translational value [85,86].

Drosophila has been widely used in studies of many ASD-associated genes involved on synaptic structure and turn-over (reviewed in Tian, *et al*., 2017) [87]. In fact, *Drosophila* is a low-cost, highly prolific and genetically accessible animal model that conserves many molecular, cellular and synaptic processes present in higher organisms [87,88]. For instance, *Drosophila* neuromuscular junctions share many features with synapses of vertebrates' central nervous system. Its multidendritric neurons permit an analysis of the developmental, morphological and functional alteration of dendrites. In additions, the reduced complexity of its brain simplifies electrophysiological recordings and calcium imaging. Finally, the mushroom body (composed of cell axons) has been implicated in learning and memory processes during olfactory and courtship conditioning paradigms [88]. Thereby *Drosophila* models for ASD enable the elucidation of important molecular, cellular and behavioural aspects of the ASD pathophysiology.

Primate and rodent models have a higher biological resemblance to humans and can display behaviour that better corresponds to social or repetitive human behaviours. Even though primate models are the most similar in biology and behaviour to humans, their high cost combined with several ethical issues and the long timeframe needed to evaluate the progression of the disorder have limited their extensive application [31,89]. For that reason, researchers opt for mouse models which, although having a brain that is less complex than the human brain, allow the recapitulation of a human gene variant in a more cost-efficient and time-saving way while still providing a developmental context required to observe the effect of risk factors on specific cells, tissues, and organs [31,90].

The development of a substantial number of mouse models that contribute to the validation of the genetic pathways is an important aspect of preclinical research. Studies in genetically modified mouse models are important not only for linking the loss of function of specific risk genes to core neuropathological, and social, cognitive and behavioural features of ASD, but also for identifying common phenotypes among different genetic causes [91]. For instance, Huguet*, et al*. (2013) observed that models carrying mutations in genes *MECP2*, *CNTNAP2*, *SHANK2*, and *SHANK3* display both decreases and increases in the density of synapses [29]. Simultaneously, these four mouse models presented behavioural impairments related to ASD core diagnostic criteria, suggesting that the implicated genes are crucial to the neural circuits involved in both social communication and repetitive behaviours [29]. In fact, alterations in the number and morphology of dendritic spines (which were previously identified in clinical research [92,93]) may compromise the strength and stability of synaptic transmission and thereby impair neuronal plasticity and connectivity [92–94]. Since changes in both neuronal plasticity and connectivity are suggested to explain the social, behavioural and cognitive phenotype of the disorder, such changes in dendritic spine morphology may be strongly correlated with other aspects of ASD pathophysiology [10,22,46,50,52,61,62].

Since FXS patients display a range of symptoms which overlap with those of ASD, mice modeling loss of function of the *Fmr1* gene (*FMR1* in humans), have been commonly used to model the disorder [36,44,60]. *Fmr1* knockout (*Fmr1*KO) mice exhibits multiple ASD-like behavioural alterations (e.g.: hyperactivity, perseverative and repetitive behaviour, atypical sensory responsiveness, as well as cognitive deficits such as decreased spatial learning abilities and reduced fear memory), and usually display age-dependent spine length and density abnormalities [44,95–97]. Histological and anatomical neocortical abnormalities have also been reported in this mouse model [9,44,60,95], as well as evidence of altered neocortical connectivity [15,62].

Beside genetic models, models of environmental risk – obtained through prenatal exposure to sodium valproate, maternal autoantibodies administration or maternal immune activation – can be used in ASD- related studies. Pregnant women exposed to sodium valproate (usually prescribed as an anti-epileptic drug or mood stabilizer, and known as a human teratogen), exhibit nearly three times the risk of having a child with ASD. Therefore, rodent models with prenatal valproic acid exposure have been exploited in numerous studies and ASD-like behavioural phenotypes have been reported [98,99]. Additionally, ASD has also been associated with prenatal exposure to maternal antibodies against fetal brain proteins [100,101]. The exposure of experimental mice to maternal autoantibodies *in utero* show, during cortical neurogenesis, increased cell proliferation and, in adulthood, increased neuronal and brain size [102], as it is described in children with autism born to mothers possessing the same autoantibodies [45]. Since autism has also been associated with early prenatal exposure to maternal infection or fever [103], rodents and non-human primates with several autism models of prenatal exposure to maternal infection have been developed. The maternal immune activation mice, for example, as demonstrated by some ASD studies, are induced by influenza- infection or synthetic double-stranded RNA to mimic viral infection [104].

Ideally mouse models of ASD demonstrate adequate face validity in addition to construct validity. Face validity may be evaluated by the expression of a behavioural phenotype recapitulating core features of the disorder – reciprocal social interactions, social communication, and repetitive behaviours and/or restricted interests including atypical sensory features. In order to evaluate behavioural abnormalities in these domains, specific tasks have been developed to evaluate behavioural features in a species-relevant manner [23,105,106]. Social interaction, social recognition and social memory are evaluated through the tendency of mice to spend time with another animal rather than non-social novel objects [23,107]; for the analysis of social communication in mice olfactory and auditory communication may be evaluated using measures such as scent marking and ultrasonic vocalizations [23,107–110]. For phenotypes recapitulating the repetitive behavioural patterns, perseveration, and narrow interests aspects of ASD, exploratory choices and reversal tasks and tests targeting innate behaviours like self-grooming, rearing, marble burying and nest building are often used [23,105,111]. Atypical sensory features may be evaluated using measures of reactivity to sensory stimuli such as acoustic and/or tactile startle (e.g. Orefice, *et al.,* 2016) [112]. It is also important to note that behavioural tests in mice may reflect symptom domains of ASD or human social cognition in general in a non-accurate way, but allow the observation of hyperactivity, repetitive behaviours, and/or learning deficits reminiscent of the human phenotype on these animals, which can be useful to evaluate, develop and promote

potential treatments for core symptoms of ASD [23,31]. Physiological measures such as EEG also provide measures of face validity that are both quantitively and highly translational between mouse and humans (e.g.: Sahin and Modi, 2017; Sinclair *et al*., 2017; Lovelace *et al*., 2018; Wen *et al*., 2019) [113–116]. Lastly, mouse models response to drugs (e.g.: risperidone, Peñagarikano *et al*, 2011) [57] and strategies (e.g.: environmental enrichment, Oddi *et al*., 2015) [117] approved for ASD therapeutic treatment supports its predictive validity.

1.2 PREFRONTAL CORTEX

1.2.1 DEFINITION, STRUCTURA AND FUNCTIONS

The prefrontal cortex (PFC) is defined as the most anterior cortical part of the frontal lobe. In agreement with its classical definition of a cortex strongly and reciprocally connected with the mediodorsal thalamic nucleus, this brain region is broadly divided into medial (mPFC), lateral (LPFC) and ventral orbital PFC [11,118]. The mPFC is further subdivided into a dorsal region (dorsal mPFC) that includes the secondary motor cortex (MOs, also known as medial agranular cortex, medial precentral cortex or second frontal area) and the anterior cingulate cortex (ACC); and a ventral region (ventral mPFC) encompassing the prelimbic (PL), infralimbic (IL) and medial orbital cortices [11,118–120]. Although PFC cytoarchitecture features (granular *vs* agranular regions) and connectivity patterns can have differences across species, its distinct subregions are identifiable in rodents, primates and humans [11,120,121]. Nevertheless, there is no consensus about what constitutes the rodent PFC, the nomenclature used to describe it, and how it correlates with the PFC of monkeys and humans [11,121,122].

Several clinical and pre-clinical studies have proven that the PFC is crucial in the higher-level control of executive, emotional and cognitive brain functions such as resistance to interference, planning and decision-making, task switching, monitoring or working memory (reviewed in Fuster, 2001 and Dalley, *et al*., 2004) [1,16,105]. It is thus not surprising that the PFC has critical implications in several neuropsychiatric disorders.

A range of functions that includes social interaction, emotional learning, long-term socio-emotional attachments, adaptive responses to changing conditions, conflict processing and motor coordination have been attributed to the mPFC and specifically to the ACC [16–20,123]. Lesions affecting the ACC result not only in apathy, loss of social skills and abnormal social responsivity, but also in an inability to maintain attention on

behavioural and cognitive tasks [19,44,118]. Moreover, functional neuroimaging data revealed ACC activity during sustained effort and concentrated attention, reflecting the need for ACC in attentional selectivity [118,123,124]; and Han, *et al*. (2003) pointed to a requirement for the ACC during trace fear conditioning (TFC) – a reliable model of attention-dependent associative learning – in mice, as well as in humans [125]. Disturbances in any of these functions can thus strongly contribute to a number of core features of ASD as well as related comorbidities (e.g.: intellectual disability, attention deficit hyperactivity disorder or motor impairments).

Due to its implications in the processing of a wide range of cognitive, social and emotional information, the ACC might be a central hub in the brain circuitry underlying ASD symptoms, and therefore it is the main focus of the follow subchapters (i.e.: *Afferent Connectivity* and *Structural and Functional Alterations related to Autism Spectrum Disorder*).

1.2.2 AFFERENT CONNECTIVITY

The PFC sends and receives axonal projections from virtually all cortical sensory and motor systems, and many subcortical structures [11,118]. The different prefrontal areas (i.e.: mPFC, LPFC and ventral orbital PFC) and their subregions are further intra- and interconnected [11,118,126–129].

Trancing studies in rodents have shown the afferent projections to each main mPFC subdivision [126–129]. Cortical and thalamic regions were identified as major sources of medial prefrontal inputs.

ACC primary cortical afferents came from the auditory, frontal polar, motor, parietal associative, somatosensory, retrosplenial, temporal, ventral orbital and visual cortices, other regions of mPFC (mostly PL cortex and ACC itself), and from parahippocampal cortices such as the ectorhinal, entorhinal and perirhinal cortices [126,127]. ACC also receives moderate cortical inputs from the hippocampal formation, claustrum and taenia tecta [126,127]. A significant part of ACC thalamic afferents is from anterior nuclei of the thalamus, including the anterodorsal, anteromedial, anteroventral, interanterodorsal and interanteromedial nuclei [126–128]. Additional thalamic inputs include projections from the mediodorsal nucleus; midline nuclei; central lateral, central medial, paracentral and rhomboid nuclei of the intralaminar group; posterior complex of the lateral group; and ventral medial nucleus and ventral anterior-lateral complex of the ventral thalamus [126,127].

Other ACC input sources are mainly the basolateral and basomedial amygdalar nucleus; substantia innominate and magnocellular nucleus, globus pallidus, and medial

septal nucleus of the ventral, dorsal and medial pallidum, respectively; lateral hypothalamus and posterior hypothalamic nucleus; substantia nigra, pars compacta, periaqueductal gray, and ventral tegmental area of the midbrain; and dorsal raphe nucleus and locus coeruleus of the hindbrain [126,127].

Likewise, MOs receives auditory, somatosensory, parietal, restrosplenial, orbital and visual inputs, as well as inputs from the primary motor cortex [127,130]. Its cortical afferents also include projections from the insular and frontal polar cortices[127,130]. The mediodorsal nucleus, and nuclei of the central and ventral thalamus are considered prime thalamic afferents to the MOs [127,130]. Other subcortical inputs include structures such as the claustrum, basolateral amygdalar nucleus, ventral tegmental area or substantia nigra, pars compacta [127].

Generally, the ventral mPFC (i.e.: PL, IL and medial orbital cortices) have fewer cortical afferents, especially those from sensory, motor and associative cortices, comparing to ACC [127–129]. Cortical projections to PL and IL cortices predominantly originate from limbic cortices [127,128], e.g.: agranular insular, ectorhinal, perirhinal, piriform and ventral orbital cortices, the hippocampal formation, and PL and IL cortices themselves. Major thalamic inputs to the ventral mPFC are from the midline thalamus, and amygdalar projections to these prefrontal cortices are heavily [127–129].

The development of the PFC is complex and proceeds in a number of distinct phases that are not completed before early adulthood in humans. Earliest phases of its basic connectivity formation start in the early childhood [118,131]. Thus, early aversive experiences affecting PFC have lifelong consequences on behaviour, emotion and cognition [131].

1.2.3 STRUCTURAL AND FUNCTIONAL ALTERATIONS RELATED TO AUTISM SPECTRUM DISORDER

Functional and structural alterations of the PFC have been detected in ASD subjects and experimental models, and related with executive, emotional and cognitive deficits commonly related to the disease.

Anatomical, histological and molecular alterations

Neuroimaging and neurophysiological studies indicate that the pathological brain overgrowth observed in ASD children is mainly caused by the increased volume of the frontal cortex mainly due to abnormally large white and grey matter in the PFC [8,44,61]. Histological reports reveal increased cellular density and reduced neuronal size, laminar disorganization, clusters of neurons arrested in migration, and evidence of minicolumnar pathology within the PFC [8,44,61,132]. Altered cytoarchitecture and changes

in neuronal amount and size were also observed in the ACC [16,133,134]. This evidence points to prefrontal defects in neurogenesis, synaptogenesis, neuronal migration, axonal pathfinding and myelination, and synaptic pruning.

Based on these reported changes in neuron density and morphology, and laminar and columnar distribution, it was hypothesized that subsequent prefrontal imbalance of excitation and inhibition can occur. A possible contribution to this imbalance might be the deficit of cortical inhibition resulting from the reduced neuropil space surrounding the minicolumn – where inhibitory interneurons are normally present [8,23,45,50]. Additionally, impairments of prefrontal neuronal communication is suggested by changes in spine number and maturation (which underlie grey matter abnormalities) observed in PFC, which affect density and efficiency of both excitatory and inhibitory synapses on prefrontal dendritic segments [92,93]. Notably, the *Fmr1* KO mice showed a decrease in long-term potentiation within the ACC [135,136], also coupled to impairments in trace fear conditioning (i.e.: attention-dependent associative learning) [137].

Vargas*, et al.* (2005) presented cellular and molecular proof of an ongoing neuroinflammation in the PFC of patients with ASD [138]. Since glial cells are important in neuronal migration, axonal guidance, minicolumn development and apoptosis, chronic activation of glia cells during brain development may be linked to the neuronal abnormalities observed in prefrontal regions [8,138].

Krueger, *et al*. (2010) reported that the *Fmr1* KO mouse model displays visual-spatial discrimination deficits correlated with changes in synaptic composition (decreased post-synaptic proteins and NMDA receptor subunits) within the mPFC [14]. And other molecular abnormalities have been specifically identified in the ACC of ASD subjects, reinforcing its role in the symptomatology of this disease [16]. For example, reduced density of serotonin receptors were observed in a SPECT (single photon emission computed tomography) study, and correlated with abnormal reciprocal social interaction [139]; and a PET analysis detected a decrease in glucose metabolism throughout the entire cingulate gyrus, including the ACC [140].

Neural connectivity alterations

Functional and structural imaging from ASD children and adults along with *post-mortem* data demonstrate a pattern of local overconnectivity and long-distance disconnection, specifically in prefrontal subregions. Broadly speaking, activity of long-range connections of the PFC is dysregulated, unsynchronized and reduced, causing diminished information processing in these circuits. Local connectivity, in contrast, is aberrantly activated and hyper-synchronized and both conditions are accompanied by cyto-architectural and cell morphology changes [8–10,44,48,67,141]. Visualization of individual

axons by high resolution methods revealed an increase in the amount of myelinated neurons and their axonal branching in superficial white matter below the ACC of adults with ASD, supporting local overconnectivity in this prefrontal brain region [44,46,134]. Conversely, in agreement with the long-range underconnectivity hypothesis, the number of myelinated neurons in the deep white matter below the ACC is decreased [46,48]. Axon pathology of long-range connectivity is proved to affect ACC bidirectional connections with distant brain regions (e.g.: temporal cortex and amygdala) [134,142,143].

Alterations specifically in the ACC circuitry have been related to social and cognitive tasks. Zhou, *et al*. (2016) detected ASD-related reductions in functional connectivity between the ACC and the rolandic operculum, insula, post-central gyrus, superior temporal gyrus, and the middle temporal gyrus, which are mostly sensorimotor networks involved in social behaviour [17]. Kana, *et al*. (2007) found functional underconnectivity between the ACC and both the right parietal lobe and the frontal gyrus when ASD patients performed a task implying response inhibition [144]. Despite the broadly attested role of ACC in attention for learning [118,123–125,145], ASD-related attentional/learning deficits were only been correlated with ACC plasticity alterations [137] and not directly with ACC circuitry changes.

Beyond the aforementioned impairments in neurogenesis, synaptogenesis, axonal guidance, neuronal pruning and myelinization, Courchesne and Pierce (2005) suggest that the functional under-selectivity of prefrontal minicolumns can also contribute to brain connectivity impairment. Specifically, the decrease of inhibitory control inter- and intra-minicolumns negatively affects long-range cortico-cortical communication, leading to consequent loss of connectivity. In contrast, the sustained local excitation favours local and short-distance connections [8]. Based on this, the prefrontal excitatory and inhibitory imbalance can be seen as a contributor for prefrontal connectivity aberrations.

Preclinical studies have also reported alterations of prefrontal connectivity and consequently cognitive and social behavioural deficits in different genetic mouse models of ASD. For instance, a pattern of reduced local and long-range prefrontal connectivity in the CNTNAP2 mouse model has been associated it with social impairments [134]; prefrontal underconnectivity and socio-communicative problems were correlated by Pagani, *et al*. (2018) [133]; hyperconnectivity of projections from the PFC to amygdala and social behaviour impairment were also described in the heterozygous mutant mice for *PTEN* gene [146]; heterozygous mutation in the autism-associated *NF1* gene showed increase functional prefrontal-striatal connectivity that may underlie working-memory defects detected in this genotype [147]; prefrontal hypoconnectivity with parieto-temporal regions was observed in the 16p11.2 deletion and pointed as a

contribute to cognitive and social dysfunction [148]; and Rinaldi, *et al*. (2008) reported overconnectivity on the mPFC of the valproic acid animal model of autism [149].

1.3 NEURAL CIRCUIT MAPPING AND CHARACTERIZATION

Currently it is well recognized that altered patterns of neuronal connectivity contribute for ASD neuropathology. Although numerous clinical studies support a pattern of long-range hypoconnectivity and local hyperconnectivity, findings diverge and point to the opposite or to a mixture of over- and underconnectivity[22,63,65–69]. Several methods can be applied for identification and exploring of the functional consequences of mesoscale changes in connectivity in animal models of ASD, thereby providing some clarification about neural circuit connectivity in ASD.

1.3.1 BRAIN IMAGING

Alterations in cerebral blood oxygenation, volume and flow, captured by fMRI provide indirect spatially and temporally information about neuronal activation [150–152]. Specifically, fMRI connectivity analysis detects interactions between different brain areas in a task- or stimulus-related manner, during rest (resting-state), or as a response to drug treatments [63,151]. fMRI clinical and preclinical studies have shown to be sensitive to alteration of brain circuitry function related to neuropsychiatric disorders, pharmacological manipulation and genetic differences [63,150–152]. In particular, preclinical neuroimaging allows the correlation of alterations of neural connectivity to concrete genetic and non-genetic risk factors, under controlled experimental conditions [63].

Compared with other techniques used to measure brain functional connectivity, namely EEG and MEG, fMRI has low temporal resolution, yet provides high three-dimensional spatial resolution [151]. Moreover, fMRI do not use radioactive compounds (as PET) or ionizing radiation (as computed tomography) [151]. An hybrid system combining fMRI with PET has been suggested to improve brain functional mapping sensibility [151].

Importantly, given the emphasis and relevance that connectivity has been gaining as a biomarker, the preclinical use of neuroimaging techniques for the identification of neural circuit alterations in ASD has the ability to be more directly and easily transposed onto the clinical diagnosis of the disorder [63].

1.3.2 NEUROANATOMICAL APPROCHES

Genetic approaches coupled to high resolution imaging techniques allow the identification and characterization of the neural circuits structure by targeting individual neurons for the analysis of their morphology, presynaptic partners and brain location.

Neural trans-synaptic tracing

Transneuronal tracing can be achieved using a variety of methods that make use of compounds or viruses which are able to specifically cross synapses to label synaptically connected neurons in either an anterograde or retrograde manner. Such approaches permit the visualization and manipulation of functional neuronal networks[153,154]. In the context of trans-neuronal tracing, the term anterograde refers to tracers that are either actively transported or diffuse from the cell body to the axon terminals and cross the synapse in a presynaptic to post-synaptic manner. Retrograde tracers on the other hand cross synapses from the post-synaptic neuron to the presynaptic neuron and are then transported from axon terminal to cell body.[153].

Classical transneuronal tracers – such as tritiated proline, WGA-HRP and tetanus toxin fragments – were shown poorly specific or weak. For instance, transneuronal labelling with WGA-HRP or tetanus toxin fragments often fails or only reaches second-order neurons, and may spread in a bidirectional manner, depending on the type of synapse and circuit involved, thus complicating the interpretation of labeled-pathways [154,155]. Importantly, none of the three examples spread in a truly synapse-specific manner, and may also label axons of neurons that are close but not necessarily connected by synapses [155,156]

More sensitive techniques exploit the ability of certain neurotropic viruses to be transported along axons and trans-synaptically infect neuronal pathways [153–155]. These trans-synaptic tracers are self-amplifying due to the replicative nature of viruses, overcoming the dilution of signal observed with conventional markers [153,154,156]. In addition, these labelled-neurons can be visualized through the expression of morphological markers, e.g.: fluorescent reporter molecules [154,156–158]. None-the-less, the infection efficiency of these trans-synaptic viral vectors significantly varies according to cell type, depending on the type and/or expression levels of molecules that mediate viral entry and experimental conditions [158,159].

Alpha-herpesviruses, including herpes simplex virus (HSV) type1 and pseudorabies, and a rhabdovirus (RABV) are two main classes viral tracers that spread retrogradely and in an exclusively trans-synaptic manner[155–157]. In contrast to alpha-herpesviruses, RABV is less cytotoxic, does not spread locally regardless of the dose

and time post-inoculation, and infects primate neurons [153–157]. Moreover, the insertion of foreign genes in the RABV genome does not present the instability issues observed in positive strand RNA viruses, and its life cycle is limited to the cytoplasm thus not interfering with host gene expression [154–156]. RABV vectors also present efficient long-range neural transport and high gene expression (allowing signal amplification)[154–156]. Even so, RABV and alpha-herpes viruses are polysynaptic (crossing at least two consecutive synapses) tracers creating ambiguity in determining the direct or indirect projection targets in neural pathways [156,160].

Mono-trans-synaptic tracing overcame this problem using a pseudotyped, recombinant RABV deficient in the gene required for trans-synaptic crossing, which restricts infection to a specific starter cell and, in the case of trans-complementation, to its immediate pre-synaptic inputs (see below) [161]. Due to its versatility and proven high-level expression of fluorescent proteins, genetically modified RABV (RABV ΔG) has been shown to be an important tool not only for tracing synaptic connectivity, but also for morphological analysis, and for the precise analysis of neural circuit function (classifying cell types) [161–165]. Researches have amply described RABV ΔG's ability to precisely identify presynaptic partners separated by distances ranging from micrometers to centimeters and to precisely execute the mapping of long-range connections, unlike other mono-trans-synaptic tracing techniques and assays (e.g. electron microscopy and paired electrophysiological recordings) [156,161–166]. Additionally, the genetically modified RABV technology has consistently demonstrated its potential in aiding the visualization of neuronal morphology with dimensions ranging from nano- to macroscale and has shown to be extremely helpful in visualization approaches that do not permit further signal amplification [156,161–166]. RABV ΔG's features, thus, enable the analysis of cell type, localization and number of both the initially infected cells and their immediate presynaptic partners. Besides its capacity for labelling and characterizing inputs into specific cell types, RABV may also be used as a means of delivering exogenous transgenes, meaning that this system can be employed in a synapse-specific manner for the monitoring or manipulation pf neuronal activity [167].

RABV ΔG lacks the gene coding for the RABV envelop glycoprotein (RG) [156,161,166,168]. Since RG is essential for the assembly of infectious virus particles, as well as for mediating trans-synaptic crossing of the virus, its deletion permits the replication of viral genomes and expression of viral proteins, yet prevents the assembly of infectious particles and trans-synaptic spreading [156,161,166,168]. Retrograde infection capabilities of RABV ΔG can be rescued in a highly restricted manner by the exogenous expression of RG in the targeted neuron population [156,161,166,168]. Further, the RABV ΔG vector is pseudotyped with an engineered surface protein EnvA [RABV

ΔG(EnvA)] thus limiting infection to neurons expressing TVA, a bird virus receptor that is normally absent from mammalian neurons [156,161,166,168]. Both conditions ensure that virus spreading is limited to the initial infected cells and their immediate presynaptic partners. Additionally, RABV ΔG expresses a fluorescent marker permitting neuronal visualization of both the presynaptic input population and the starting (with a second fluorescent marker) [156,166,168].

Stereotaxic injection in a specific brain region of a Cre-dependent viral vector expressing TVA/RG required for RABV ΔG(EnvA) infection and spread is one of the most commonly used approaches to achieve neuronal specificity with mono-trans-synaptic tracing [156,169]. AAV with Cre-dependent gene cassettes (TVA and RG genes flanked by lox sites) restricts the expression of transgenes to cells expressing Cre recombinase *in vivo* (i.e.: mouse lines or the previous stereotaxic injection of a viral vector encoding the enzyme under the control of a cell-type specific promoter)m [156,158,169]. Alternatively, cells undergoing neurogenesis have been specifically targeted by the use of retroviruses vectors (i.e.: Moloney murine leukemia virus expressing TVA/RG/fluorescent marker) that exclusively infect proliferating neurons [170]. In other cases neurons expressing the ErbB4 receptor have been targeted through a neuregulin1-TVB bridge protein (a protein in which the TVB receptor is fused with the ErbB4 ligand) and a RABV ΔG and a viral vector expressing RG pseudotyped with the surface protein EnvB [171,172].

The temporal regulation of the RABV ΔG(EnvA) neural tracing may be possible if TVA/RG expression is either activated by tamoxifen-induced nuclear translocation of a tamoxifen-dependent Cre recombinase (Cre-ER) [167,173], or regulated by viral tet-tagging. In tet-tagging systems, the transgene (i.e.: TVA/RG) expression is driven by a tetracycline-responsive promotor specifically activated by tetracycline-controlled transcriptional activators whose activity is activated (Tet-On system) or inactivated (Tet-Off system) by Dox administration [167,174,175]. Since upregulation *in vivo* is faster than downregulation, the Tet-On system is more accurate when compared to the Tet-Off system [176]. A major advantage of tet-tagging systems over Cre-ER is the possibility to return to a control situation by discontinuing Dox administration [167,176]. The tet-tagging approach thus restricts neural labelling to a permissive time window.

Whole-brain microscopy

Serial-selection electron microscopy (EM) enables the reconstruction of dense neural circuits with individual synapses resolution [158,177]. Although advances in EM data acquisition and analysis made possible the automated reconstruction of larger volumes of brain tissue, substantial challenges remain and difficult whole-brain imaging. These

include the long duration for imaging acquisition, data storage, and validation of EM reconstructions comparing with light microscopic [158,177].

Light microscopy (LM) methods are often utilized for sparse reconstruction of fluorescent protein-based tracers across the brain. Notably, LM automated technology for three-dimensional imaging and powerful data processing pipelines allows for speed and standardization of the process, comparing with two-dimensional imaging and manual brain mapping procedures, respectively. Currently, LM approaches for automated, 3D scanning are based on block face microscopy or on light-sheet fluorescence microscopy (LSFM) of chemically cleared tissue [178,179]. The main particularity of block-face microscopy is the mechanical removal of the imaged tissue surface (that can be collected for further analysis) [178,179]. An example is the serial two-photon tomography (STP), which combines a two-photon microscope and vibratome-based tissue sectioning for agar-embedded tissue [178,179]. Other instruments include wide-field, line-scan or confocal imaging methods or the possibility of ultramicrotome sectioning of resin-embedded tissue [163]. Microscopes based on LSFM scan chemical cleared brains without the need for mechanical tissue sectioning. Yet, a major technical downside is the weakening of neural tracers' fluorescence due to chemical clearing protocols [163].

1.3.3 NEUROFUNCTIONAL APPROACHES

In addition to structure, neuron physiological/functional properties define brain circuits. Functional mapping approaches define neural projections based on the level of activity of single neurons.

C-fos immunodetection

Analysis of *c-fos* expression pattern is commonly used to identify and map brain regions involved in specific physiological and behavioural processes that took place *in vivo* or *ex vivo* [180].

As an immediate early gene (IEG), *c-fos* expression is induced by changes in neural activity following neural stimulation. Further protein detection by immunohistochemistry or -fluorescence allows to visualize and localize these neurons across the brain [180]. Time required for protein synthesis and protein turnover should be considered to avoid under protein detection. During *in* vivo studies, is important to minimize animal manipulations to prevent unspecific neural activation (i.e.: nonrelated to the experimental condition).

Activity of immediate early gene promotors

IEG promotors such as *c-fos* and *Arc* – whose gene product is rapidly and transiently activated by neuronal activity – has been use to target neurons based on recent neuronal activation [158,181]. Specifically, IEG promoters have been used to drive the expression of tetracycline-controlled transcriptional activators (of tet-tagging systems, e.g.:Fos-tTa vector) [182,183], or Cre-recombinases (of Cre-lox systems) [184] for the expression of a fluorescent protein linked to neural activity triggered by the experimental task.

A main limitation of this technique that should be taken in account during interpretation of the results is its prolongated temporal precision, i.e., the timescale needed to capture the activated neurons is slow (when compared to others such as discrete behaviours, which only takes seconds) and takes many hours [158,182–184]. As a consequence, both neurons of interest and "background" neurons, activated during the same period of time and because of a particular experience or behavioural episode, might be labelled.

Chemogenetic

Designer Receptors Exclusively Activated by Designer Drug (DREADDs) are a chemogenetic approach derived from human muscarinic receptors thus enable the control of neuronal activity by GPCR signaling [185,186]. Different types of DREADDs activate different GPCRs signaling pathways of neuronal silencing (e.g.: Gi-based DREADDs) or activation (e.g.: Gq-based DREADDs). For instance, the hM4Di-DREADD induces neuronal hyperpolarization via Giα-mediated activation of GIRKs, and via inhibition of the presynaptic release of neurotransmitters [158,186,187]. Conversely, the hM3Dq-DREADD induces burst-like firing of neurons through Gαq-mediated activation of the phospholipase C intracellular calcium release pathway [158,185,186].

Although, the hM4Di and hM3Dq are the most commonly used DREADDs to, respectively, inhibit and activate neuronal activity, a hM4Di-neurexin variant ($hM4D^{nrxn}$) was created for selective axonal silencing [188], and two Gq-coupled DREADDs were design (i.e.: hM1Dq and hM5Dq) based on different muscarinic receptors [186]. A Gs-DREADD (rM3Ds) is employed in studies about the role of Gs signaling regardless its constitutive activity [186,189,190]. Additionally, the Gi-coupled DREADD derived from the K-opioid receptor (i.e.: KORD), activated by salvinorin B, has been reported as an efficient inhibitor of neuronal activity [191,192]. Given that KORD is activated by a different ligand, it can be co-expressed with hM3Dq, allowing the sequential chemogenetic inhibition and activation of neuronal activity [186,191].

All of the aforementioned DREADDs (except KORD) are activated by CNO [158,185,186,188]. When administered at recommended doses in mice, CNO selectively binds to DREADDs, is pharmacologically and behaviourally inert, and is not metabolized to clozapine, according to in numerous reports [158,185–188,192]. CNO also allows oral or intraperitoneal administration since it crosses the blood-brain barrier [158,185–188]. Other chemical ligands for DREADDs were developed in order to avoid the potential risk of clozapine-like side effects related to CNO metabolism, namely compound 21 and perlapine [193]. However, both CNO-alternatives are only advised for studies in which the back metabolism to clozapine is a problem, since they have lower binding affinity for DREADDs comparing to clozapine and modest off-target binding [186,193,194].

Engineered ligand-gated ion channels are an alternative chemogenetic technology for *in vivo* manipulation of neuronal activity. After PSEM (a synthetic agonist) application, neurons expressing engineered cationic channels (e.g.: pentameric nicotinic acetylcholine receptors, tetrameric ionotropic glutamate receptors or trimeric P2X purinergic receptors) depolarized and fired action potentials, while neurons expressing engineered anion-permeable channels (e.g.: pentameric $GABA_A$, $GABA_C$ and glycine receptors) are inhibited and silenced [158,192].

Chemogenetic systems represent a noninvasively approach for long-lasting (hours to days) manipulation of neurons across large brain areas [158,185,186]. Importantly, chemogenetics have a potential therapeutic application for brain disorders [158,186], including ASD [195]. Yet, Urban, *et al*. (2016) suggested that chronic drug administration (that underlies studies requiring prolonged DREADD activation) can induce neuronal adaptation (e.g.: possible non-DREADD mediated effects of CNO) [196]. Another limitation is the reported non-specific effects of the ligands [158,192].

Optogenetic

Optogenetic approaches, that make use of light-sensitive or responsive to light channel proteins, are being exploited to manipulate widely scattered but functionally defined groups of genetically modified neurons in order to investigate neuronal activity, circuits and behaviour [158,197]. That is, genetically defined neurons are selectively activated or silenced though the direct application of light of different wave lengths over a vast list of microbial opsins. Namely, the opening of channelrhodopsins (ChRs) in response to blue light leads to the neural depolarization through the influx of cations [158,197]; and neural hyperpolarization is achieved through the activation of bacteriorhodopsins by yellow light or of halorhodopsins by green light [158,197]. Further, bacteriorhodopsins opening allow the efflux of protons and halorhodopsins permit the influx of chloride anions [158,197].

The application of these optogenetic systems normally follows only one-photon excitation, that uniformly photo-stimulates tissue volumes on the order of one cubic millimeter per light source [158,197]. For the excitation of single neurons in intact tissue (a more targeted application) a two-photon stimulation and therefore more expensive and specialized equipment and lasers are necessary [158,197].

ChRs have shown to be a precise and efficient approach used in the manipulation and activation of neurons by depolarizing these cells [158]. This approach enables an adequate excitation of neurons with innocuous intensities of light and within time periods that can extend from milliseconds to seconds or longer (step opsins) [158]. Admitting 1,000s of cations per absorbed photon, the expression of these opsins can thus be achieved at modest levels.

As opposed to ChRs, cell-type-specific silencing channel proteins have generally shown slower effects on neuronal membrane potential and spike rates (100s of milliseconds), and lower efficiency [158,197]. In order to achieve an adequate stimulation of the neurons and to be correctly expressed these hyperpolarizing opsins need higher levels and more intense lighting [158,197]. Consequently, heating, toxicity and the decrease of the opsin-mediated silencing efficacy over time have been mentioned as limitations of these approaches. As an alternative, new cell-type-specific silencing approaches based on anion-conducting ChRs are being developed and used.

Usually cell transfection underlying both chemo- and optogenetics is mediated by viral vectors encoding the engineered receptors or channels, such as AAV, lentiviral and HSV vectors [186,192]. The type of promoter inserted into the viral vectors varies according to the type of cell targeted – the hSyn promotor confers highly neuron-specific transgene expression [186,192]. In addition, Cre-dependent viral vectors or RABV ΔG(EnvA)-mediated infection are used to limit the expression of engineered receptors and channels to specific subtypes of neurons (as described above for the expression of fluorescent proteins) [186,192].

Chemo- and optogenetics are frequently combined with *in* vivo or *ex* vivo electrophysiological recordings to investigate cell-type specific responses within network. Yet, both approaches *per si* are pertinent to explore the functional consequences of the manipulation of a specific circuit on behaviour outcome (i.e.: to stablish causality).

2. HYPOTHESIS

Based on previous findings related to changes in neocortical connectivity in both the *Fmr1*KO mouse (Haberl *et al*., 2015; Zerbi *et al*., 2018), and two unrelated genetic mouse models of ASD (Liska, *et al*., 2017; Huang, *et al*., 2016) we hypothesized **1) that connectivity of the ACC is altered in the *Fmr1*KO mouse and 2) that these changes underlie cognitive deficits related to ASD-related behavioural alterations.**

3. AIMS

To address our hypothesis, the present project aims to explore alterations in the connectivity of specific populations of ACC neurons in *Fmr1* KO mice and to probe the functional consequences of these alterations for behavioural outcome.

4. METHODS

4.1 EXPERIMENTAL DESIGN

Task 1 – **Whole-brain mapping of monosynaptic inputs into ACC neurons engaged during the acquisition of TFC**

To examine the input map of those neurons of the ACC that were engaged during TFC encoding in *Fmr1*KO and WT mice, we employed an innovative, intersectional strategy involving *c-fos*-mediated tet-tagging (Zhang et al., 2015) and recombinant rabies virus-based mono-trans-synaptic tracing (Wickersham et al., 2007; reviewed in Ginger et al., 2013).

Mono-trans-synaptic tracing is a viral-vector mediated approach for circuit tracing which exploits an engineered form of the vaccine strain of rabies virus, Street Alabama Dufferin (SAD B19). This vector (RABV ΔG) lacks the gene coding for the RABV envelop glycoprotein (RG). In its place, the recombinant virus expresses a fluorescent marker permitting neuronal visualization [158,166]. Since G is essential for the assembly of infectious virus particles, as well as for mediating trans-synaptic crossing of the virus, its deletion is sufficient to prevent trans-synaptic spreading [158,166] of the virus, a feature of wildtype RABV. The retrograde trans-synaptic propagation capabilities of RABV ΔG can be rescued in a highly restricted manner by the exogenous expression of RG in the targeted neuron population [166]. Furthermore, the RABV ΔG vector is pseudotyped with an engineered surface protein, EnvA [RABV ΔG(EnvA)], thus limiting infection to neurons expressing it cognate receptor, TVA, a bird virus receptor that is normally absent from mammalian neurons [166]. Both conditions ensure that virus spreading is limited to the initially infected cells — the so-called starter cells — and their immediate presynaptic partners. To narrow the mono-trans-synaptic tracing to a specific ACC neuronal population engaged during a specific task, we exploited the *c-fos* promoter, whose gene product, cFOS, is commonly used as a marker of plasticity related neuronal activity [198]. In particular, we used a conditional expression approach in which the *c-fos* promoter drives the expression of tTA – a transcription factor sensitive to the presence of Dox. Combining this with a viral vector expressing TVA/G under the control of a tetracycline-dependant promotor (TRE), allowed TVA/G expression to be linked to neuronal activity during a specific, experimentally-controlled time window (as illustrated in figure 1). No further labelling of active cells occurs outside the permissive time window/presence of Dox [166,198].

Figure 2 schematizes the timeline of this experimental design. Two weeks prior to the first surgery, mice were adapted to a diet supplemented with Dox (at a concentration of 40mg/kg). Mice then received unilateral intracerebral injections of an AAV-cfos-tTA/AAV-TRE-HTG mixture (surgery procedure described below) permitting viral mediated tet-tagging. Ten days following delivery of the AAVs the Dox-containing diet was replaced with non-supplemented food. Two and a half days later, the mice underwent conditioning (as described below), which induced *c-fos* activation and the expression of the tetracycline-dependant transgenes. Ninety minutes after the test, the food was once again replaced with Dox-supplemented food to limit expression of TRE-regulated transgenes to a specific experimental window. One day later, a second surgery was performed to the deliver the third viral vector, RABV ΔG mcherry (EnvA) into the same ACC location. Green fluorescent protein (GFP) expression identified initial infected neurons (starter cells), while mCherry expression allowed to visualize ACC inputs and quantify projection density.

As a result of this innovative approach it was possible to visualize if the anatomical input map of the neuronal ensembles engaged in TFC are altered in the *Fmr1*KO mice.

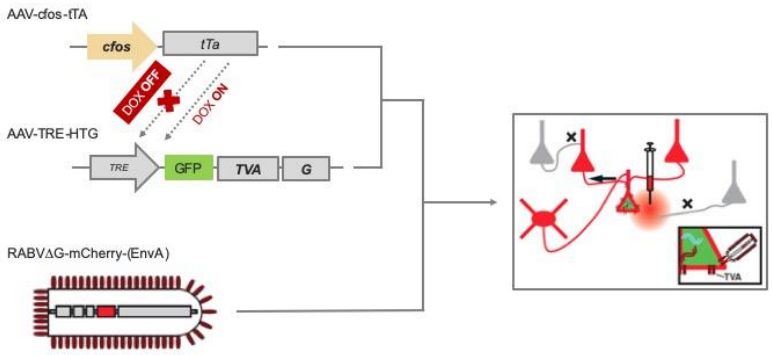

Figure 1 . Rabies virus-based mono trans-synaptic tracing combined with viral based tet-tagging.

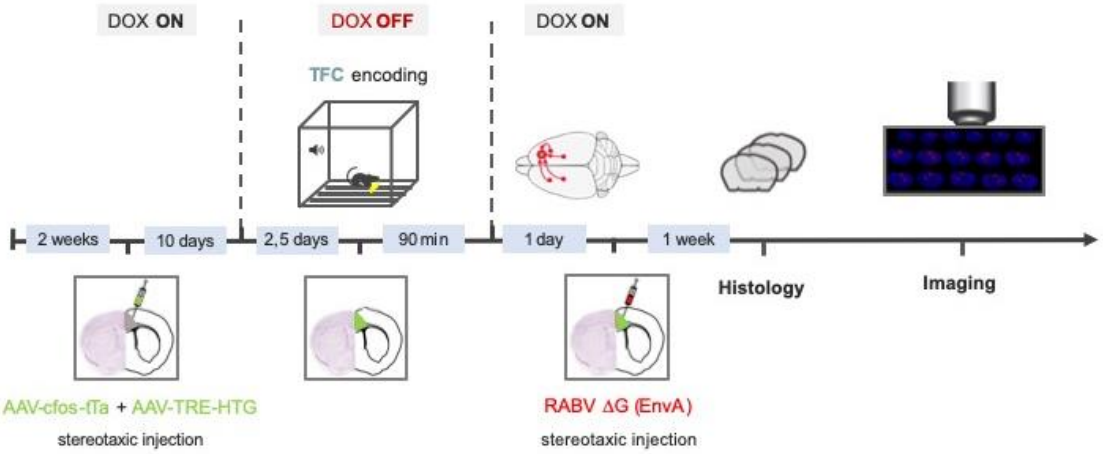

Figure 2 . Timeline of the experimental design employed to trace presynaptic neuron projecting to ACC neurons engaged during the acquisition of TFC.

Task 2 – **Pharmacogenetic manipulation of specific aspects of ACC circuits**

Functional consequences of altered ACC circuit organization on TFC outcome were explored employing an intersectional approach entailing the Cre-dependant expression of an excitatory DREADD in a specific input, accordingly with the projection diagram of the ACC obtained in the previous task.

The engineered M3 (hM3Dq) muscarinic receptors are G-coupled DREADDs designed to induce burst-like firing of neurons through activation of the phospholipase C intracellular calcium release pathway, when selectively activated by CNO [158,186]. AAV vectors where the hM3Dq DREADD gene is flanked by lox recognition sites for Cre recombinase restrict the transgene expression to cells expressing the recombinase enzyme [199,200]. Namely, AAV vectors with double-floxed inverse open reading frame constructs (AAV-DIO vectors) have the sequence of interest in an inverted, inactive orientation, and flanked by two sets of different lox sites [199,200]. Consequently, transgene expression within Cre-expressing cells occurs after two random recombination steps [200] (as schematized in figure 3). Incompatibility between the remaining lox sites prevents transgene re-inversion [200].

To selectively target a specific ACC input, the AAV-DIO-hM3Dq vector was combined with an AAV retro2 vector expressing Cre recombinase and nuclear localized eGFP. AAVretro2 infects presynaptic terminals of different classes of neurons and has an efficient retrograde transport [201]. When AAVretro2-Cre is injected into the ACC and the AAV-DIO-hM3Dq into the ACC input source area, AAVretro2 is retrogradely transported to the soma and expresses Cre recombinase within the nucleus, activating the expression of hM3Dq DREADD only in neurons projecting from the targeted source to the ACC.

Figure 4 schematizes the timeline of this experimental design. Four weeks before underwent conditioning, mice were bilaterally, intracerebrally injected with AAVretro2-Cre and AAV-DIO-hM3Dq-mCherry, allowing Cre-dependent expression of hM3Dq DREADD and mCherry. TFC encoding and retrieval (24 hours later) took place ~40 minutes after vehicle (saline solution) or CNO intraperitoneal injections, increasing the neural activity of the targeted ACC input during the behavioural task. In order to evaluate the consequences of manipulating this circuit on behavioural outcome, average freezing during the encoding and retrieval sessions was scored.

Thereby, we boosted the neural populations activity of a specific ACC input as an attempt to either reproduce the cognitive phenotype in *Fmr*1WT mice or to improve the performance of *Fmr*1KO in the TFC task.

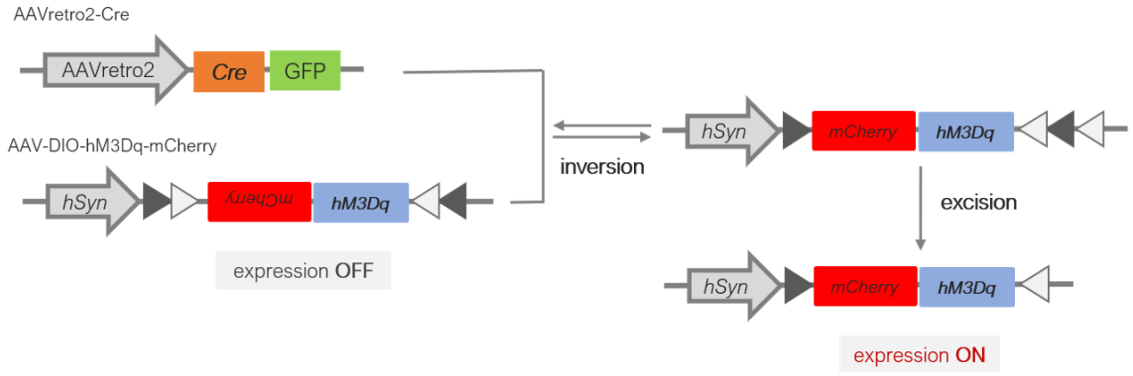

Figure 3. Cre-lox recombination system to regulate hM3Dq DREADD expression using DIO vectors.

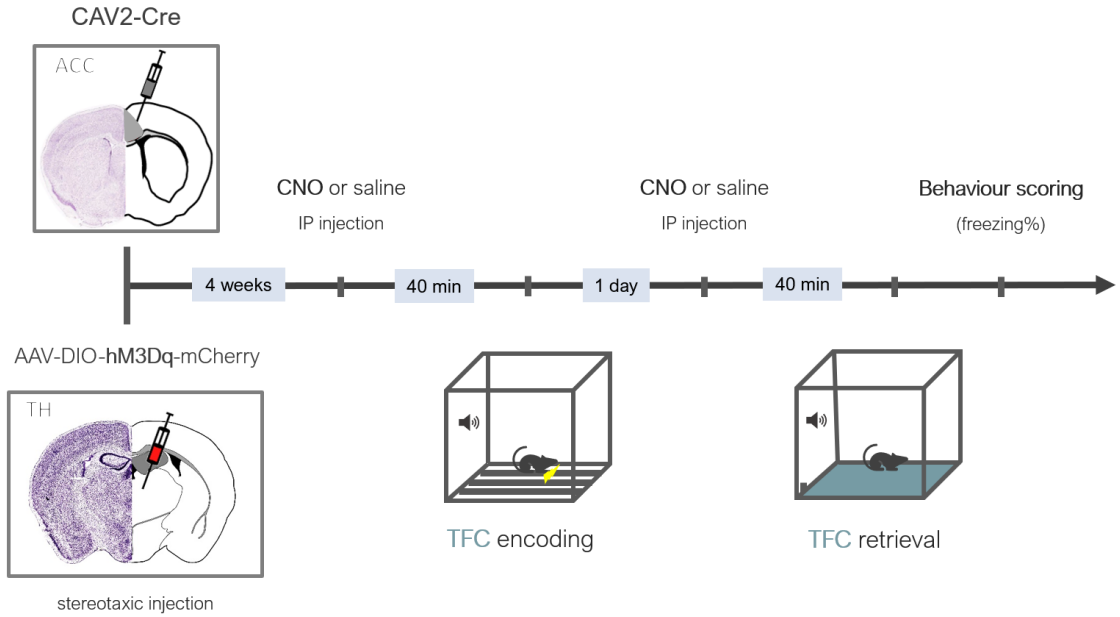

Figure 4. Timeline of the experimental design employed to pharmacologically boost the activity of a specific ACC input.

4.2 EXPERIMENTAL APPROACHES

4.2.1 MOUSE MODEL

Second-generation (Mijentes et al, 2006) 3-month-old *Fmr1*KO mice and their wild type (*Fmr1*WT) littermates were generated by crossing heterozygous *(Fmr1*$^{+/-}$) females with a *Fmr1*$^{+/y}$ (wildtype) mouse from the same genetic background. Animals were maintained in a congenic C57BI/6J background and bred in a SPF animal facility at the Neurocentre Magendie in Bordeaux, France. For these experiments only male mice were used due to the strong penetrance of the disorder in male subjects. At the end of the experiments, a tail sample was taken to reconfirm the genotype.

Mice were housed in groups of three or four *per* cage (balanced for genotype) in an experimental animal facility, kept on a 12h:12h light/dark cycle with *ad libitum* access to food and water. Cages were supplemented with minimal enrichment (cotton nestlet). Experiments were performed during the animal's light phase. All the experiments procedures were performed in agreement with the European Union directives as well as the French law and were approved by the ethics committee of Bordeaux, C2EA50; APAFIS 12856).

4.2.2 VIRAL VECTORS

The following viral vector were used in this project:

a) AAV-cfos-tTA: Adeno associated virus (AAV) expressing the trans-activator (tTA) under the control of the c-fos promoter (Zhang *et al*., 2015). The titre was estimated by genomic PCR as 1.x10^{12} vg/mL.

b) AAV-TRE-HGT: AAV expressing, under the control of tetracycline responsive promoter (TRE); i) a nuclear-targeted GFP; ii) the receptor of the avian sarcoma and leucosis virus, TVA; and iii) rabies virus glycoprotein (Miyamichi *et al*., 2011). The titre was estimated by genomic PCR as 1.x10^{12} vg/mL.

Both AAVs were packaged using a chimeric capsid containing the capsid proteins derived from AAV serotypes 1 and 2, as described by Hauck *et al*., 2003.

c) RABV ΔG mcherry (EnvA): A modified recombinant glycoprotein-deleted rabies virus vector derived from the vaccine strain of rabies virus, SADB19 (Etessami *et al*., 2000) and expressing the red fluorescent protein, mCherry. The vector (RABV ΔG mcherry) is pseudotyped with a chimeric envelop protein containing extracellular sequences derived from the glycoprotein of the avian sarcoma and leucosis virus as described in Wickersham *et al*., 2007.

d) AAVretro2-Cre-nls-GFP: AAV expressing Cre and nuclear localized GFP under the control of a CMV promoter. This vector was produced using a novel retro-2 capsid, which infects axon terminals (Tervo et al, 2016). The titre was estimated by genomic PCR as 1.2 $x10^{12}$ vg/mL.

e) AAV-DIO-hM3Dq-mCherry: AAV carrying Cre-dependent hM3Dq DREADD fused to mCherry. The titre was estimated by genomic PCR as 2.8$x10^{12}$ vg/mL.

AAV-cfos-tTA, AAVretro2-Cre-nls-GFP and RABV ΔG mcherry (EnvA) were produced by the host team. AAV-TRE-HTG was produced by the AAV facility of the Bordeaux Neurocampus. AAV-DIO-hM3Dq-mCherry was obtained from the Viral Vector Facility of the University of Zurich.

4.2.3 STEREOTAXIC SURGERY

Stereotaxic injections were performed as described in Cetin *et al*., 2007 and *Haberl et al*., 2017. Mice received an initial injection of Rimadyl (5mg/Kg, intraperitoneal non- steroidal analgesic) and were then deeply anesthetized with isoflurane (4% induction and 1.5-2% maintenance). Then, the animals were head-fixed in a stereotaxic frame, the skin of the head shaved and disinfected, and 30µL of Lurocaine delivered subcutaneously prior to incision of the skin. The skull was exposed, and the skin maintained in an open position with custom-made clamps. The craniotomy was performed at the site of injections coordinates 1.00mm anterior/posterior (A/P), 0.61 mm lateral/medial (L/M) with respect to Bregma. A pulled glass capillary (internal diameter ~15µm) was then inserted on a 20º angle at a depth of 1.06 mm (with respect to pia, targeting the ACC) and 250µL of a mixture of AAV-cfos-tTA/AAV-TRE-HTG (ratio 2:1) delivered at a rate of 50nL *per* minute. At the end of the injection, the capillary was kept in place for ~5mint before being removed. After closing the skin, mice recovered in an absorbent surface in a heated chamber. During the second injection, the animal was re-anesthetized as above and injected using the same coordinates with 500nL of RABV ΔG mCherry (EnvA) delivered at a rate of 50nL *per* minute using a 10µL glass syringe fitted with a 34G needle. The injection rate was controlled by a programmable pump (WPI Ultra Micro Pump).

For the pharmacogenetic manipulation of the altered ACC input (second experimental task), mice were anesthetized as previously described and bilaterally injected with 350nL of AAVretro2-Cre into the aforementioned coordinates (i.e.: into the ACC) and 300nL of AAV-DIO-hM3Dq-mCherry into de mediodorsal nucleus of the thalamus, injection coordinates - 1.30mm A/P, +/- 0.50mm L/M and - 3.50mm

dorsal/ventral (D/V) with respect to Bregma, at a rate of 50nL *per* minute. The needle remained in the target location for ~2mints before the start and ~5 mints after injection.

4.2.4 TRACE FEAR CONDITIONING

Trace fear conditioning was performed as described by Zhao *et al*., 2015 and Hyashi *et al*. 2007 with minor amendments to the procedure. Mice handled for five days prior to examination. On day 1, mice were brought to the training room and individually placed in the conditioning boxes (Immetronics). The box was composed of transparent outer walls with a white opaque inner wall. The base of the chamber was cleaned with 70% ethanol prior to conditioning of each mouse. Following 1 minute exploration of the chamber, the software presented a 15 second tone (80dB). A 1 second foot shock (0.7mA) was then delivered to the mouse after a trace period of 30 seconds. After 7 conditioning trials with 210 seconds inter-trial interval (ITI), mice were taken out of the conditioning boxes 90 seconds after the last foot shock. A less aversive protocol for the encoding session (day 1), which included a 2 seconds foot shock of 0.4mA, was also tested. In both situations, on the following day, mice were place in a novel chamber composed uniformly of white opaque walls and a uniform grey-coloured floor. The chamber was cleaned with 1% acetic acid prior to commencing experiments. Mice were acclimated for 1 minute followed by 7 trials of tone (80dB) and an ITI. All data were videotaped and the percentage of freezing time during each ITI was manually analysed (blind to genotype) to examine trace fear memory. Freezing was defined as the absence of movement, except for breathing movement.

4.2.5 HISTOLOGY AND IMAGING

Presynaptic neurons identified by mono-transsynaptic tracing (task1) were assessed post-mortem by microscopy. Mice were euthanized 1 week following RABV injection. Thirty minutes prior to euthanasia, the animals received an i.p. injection of rimadyl (5mg/kg). Then, after a lethal dose of sodium pentobarbital, they were transcardially perfused with Ringer's solution supplemented with heparin followed by 4% paraformaldehyde (PFA) in 0.1M Phosphate buffer pH 7.2. Dissected brains were post-fixed in 4% PFA overnight at 4ºC, embedded in 3% agarose block and then cut into 50µm coronal sections using vibrating microtome. Brain slices were then counterstained with 4′,6-diamidino-2-phenylindole (DAPI) and mounted in a mowiol-based mounting media.

Imaging of the whole brain was performed using wide-filed fluorescence microscopy and a rapid acquisition system (NanoZoomer slide scanner, Hamamatsu)

equipped with a 20x 0.75 numerical aperture objective. Brain images were acquired at seven z-positions of 7µm.

For the pharmacogenetic experiments, mice were euthanized following behaviour experiments. Injection positions of both vectors needed for DREADD expression were verified using wide-field fluorescence microscopy (Nikon inverted microscope equipped with a CCD camera).

4.2.6 MAPPING OF LABELLED NEURONS THROUGHOUT THE BRAIN

NanoZoomer images pertaining to individual brain slices were exported and converted to 16-bit Tiff-format. Each image was then overlaid with a reference atlas (based on the Allen Mouse Brain Atlas 2011) using a custom-written python script developed within the host team. Labelled neurons were manually counted with respect to brain structure, nucleus, and layer (for cortical structures). The number of labelled neurons for each structure was normalized to the total number of neurons present throughout the brain. Since rodent ACC definition in literature is not consistent, for the purpose of this project it was considered the Vogt and Paxinos' (2014) characterization of mouse ACC as Brodmann areas 24, 25 and 32 (previous 24a and 24b) [122].

4.2.7 STATISTICAL ANALYSIS

Microsoft Excel and GraphPad Prism 5.00 were applied for the data analysis and graph construction. Results are expressed as mean ± SEM. Most of the statistical comparations were performed using one- and two-way analysis of variances (ANOVA) coupled to Turkey's multiple comparison test and Bonferroni correction as post-hoc tests; or the Kruskal-Wallis test with Dunn's multiple. Unpaired t-test or Mann–Whitney U test were applied for separated individual comparations between genotypes included in the analysis of TFC data. Statistical significance was considered for $p<0.05$.

5. RESULTS

*Fmr1*KO mice display deficits in trace fear conditioning

Trace fear conditioning (TFC) is a behavioural model for attention related cognitive abilities. In this protocol the animal has to associate a conditional stimulus (the tone) and an unconditional stimulus (the foot-shock) that occurs after a certain delay, thus requiring an extended attention period to enable this associative learning. Previous studies have suggested that this paradigm may reveal crucial FXS/ASD-related behavioural phenotypes in the *Fmr1*KO mouse model [36,202]. Since behavioural phenotypes in the *Fmr1*KO model have been reported to vary across laboratories[202], we sought to establish whether this phenotype can be robustly detected in the second-generation *Fmr1KO* mouse line. To evaluate deficits in the acquisition and retrieval of the task in an unfamiliar context, we analysed freezing behaviour during the inter-trial intervals (ITI) following stimulus delivery of both encoding and novel-context sessions of TFC.

To probe cognitive deficits in *Fmr1*KO mice, we initially subjected a first experimental group of 12 mice (6 WT and 6 KO) to a strong TFC protocol ($TFC_{0.7mA}$) as previously described by Hayashi, *et al*. (2007) for the same genetic background [203]. We applied seven conditioning trials consisting of a 15 second-long tone at 80dB, followed by a 30 second trace period, a 1 second-long foot shock of 0.7mA intensity, and an ITI of 210 seconds for the encoding session (day1); and seven trials of tone followed by ITI for the novel-context session (day 2). Due to errors in the software programming, only 6 conditioning trials were performed during the encoding session (instead of 7). WT mice displayed an increase in the freezing duration from the first to the last ITI (increase from 9.365 ± 3.223% freezing during ITI-1 to 49.19 ± 7.282% freezing during ITI-6, respectively; p=0.0017), suggesting that they were able to associate the tone with an aversive event even after only 6 conditioning trials. Although *Fmr1*KO mice also exhibited increased freezing following the last conditioning trial (increase from 6.032 ± 2.05% freezing during ITI-1 to 36.22 ± 2.937% during ITI-6; p<0.0001), a significant impact of genotype on the freezing percentage of both genotypes was detected with *Fmr1*KO freezing significantly less than WT across trials (figure 5A; p=0.0009). Average freezing during all 6 ITIs (figure 5B) was also significantly reduced in *Fmr1*KO mice when compared with WT mice (WT, 39.90 ± 3.549% *vs* KO, 29.439 ± 2.829%; p=0.0155). Similarly, average freezing in the novel-context session 24 hours later was significantly reduced in *Fmr1*KO (figure 5B; WT, 33.847 ± 2.287% *vs* KO, 25.266 ± 2.409%; p=0.0086). Together, these results indicate that the *Fmr1*KO mouse model

exhibits deficits in associative fear learning in which attention is required, as well as in the expression of this fear memory.

A less aversive protocol ($TFC_{0.4mA}$) was also tested since it has been sufficient to reveal *Fmr1*KO cognitive deficits in Nolan *et al*., 2017 [204]. Thus, we decided to test this protocol since it represents a more ethical alternative compared to $TFC_{0.7mA}$ paradigm in which multiple presentations of a more aversive stimulus are required over a long time duration. In $TFC_{0.4mA}$, mice were subjected to 7 conditioning trials with a longer (2 seconds) but less intense (0.4mA) foot shock. This stimulus is similar to that used previously by the host team for contextual fear conditioning (Aloisi *et al*., 2017) [205]. In $TFC_{0.4mA}$, mice were subjected to 7 conditioning trials with a longer (2 seconds) but less intense (0.4mA) foot shock. This protocol induced an increase in the freezing score throughout conditioning trial in both genotypes (figure 5C; WT, increase from 5.222 ± 1.826% freezing during ITI-1 to 43.85 ± 16.78% freezing during ITI-7; n=3, p=0.0379; KO, increase from 5.437 ± 1.304% freezing during ITI-1 to 34.13 ± 7.470% freezing during ITI-7; n=6, p=<0.001). In contrast to our aforementioned results, genotype had no significant impact on the freezing percentage of both genotypes, meaning that *Fmr1*WT and KO increasing freezing across trials was similar (p=0.8918). In accordance, the average freezing of both *Fmr1*WT and KO during the encoding session (WT, 32.724 ± 4.797% *vs* KO, 32.220 ± 2.715%; p=0.9709) and the novel-context session (WT, 14.764 ± 1.283% *vs* KO, 14.486 ± 1.106%; p=0.8786) was not different (figure 5D). Importantly, average freezing decreases significantly (p<0.0001) from one session (encoding) to the other (novel context) not only for *Fmr1*KO but also for WT. The present results suggest that the less aversive TFC protocol is not adequate for the needs of our study in these mice (i.e. that it would not be sensitive enough to reveal the consequence of manipulating the activity of prefrontal cortex circuits).

Based on these results, the $TFC_{0.7mA}$ protocol (consisting of 7 ITIs) was employed to probe whether ACC connectivity is altered in *Fmr1*KO mice. To address this question, we used whole-brain mapping approaches to detect monosynaptic inputs into anterior cingulate cortex (ACC) neurons engaged during the encoding phase of the TFC task (day 1). During these experiments, both genotypes presented increased freezing throughout the 7 conditioning trials (figure 6A; WT, 6.286 ± 2.100% freezing during ITI-1 to 38.78 ± 11.79% freezing during ITI-7, n=3; p=0.0061; and KO, 0.8333 ± 0.5706% freezing during ITI-1 to 29.33 ± 10.30% during ITI-7; n=4, p=0.0397). As in the first round of experiments using the $TFC_{0.7mA}$ protocol, genotype had significant impact on the freezing percentage with *Fmr1*KO freezing significantly less than WT across trials (p=0.0003). In addition, the freezing average of both experimental groups

(Figure 6B) was significantly different (p=0.004). These results confirmed the *Fmr1*KO mice deficits in associative fear learning we observed before. These mice did not undergo the novel-context session since the aim was to trace ACC inputs engaged during TFC acquisition and avoid the interference of possible neural plasticity processes underlying memory.

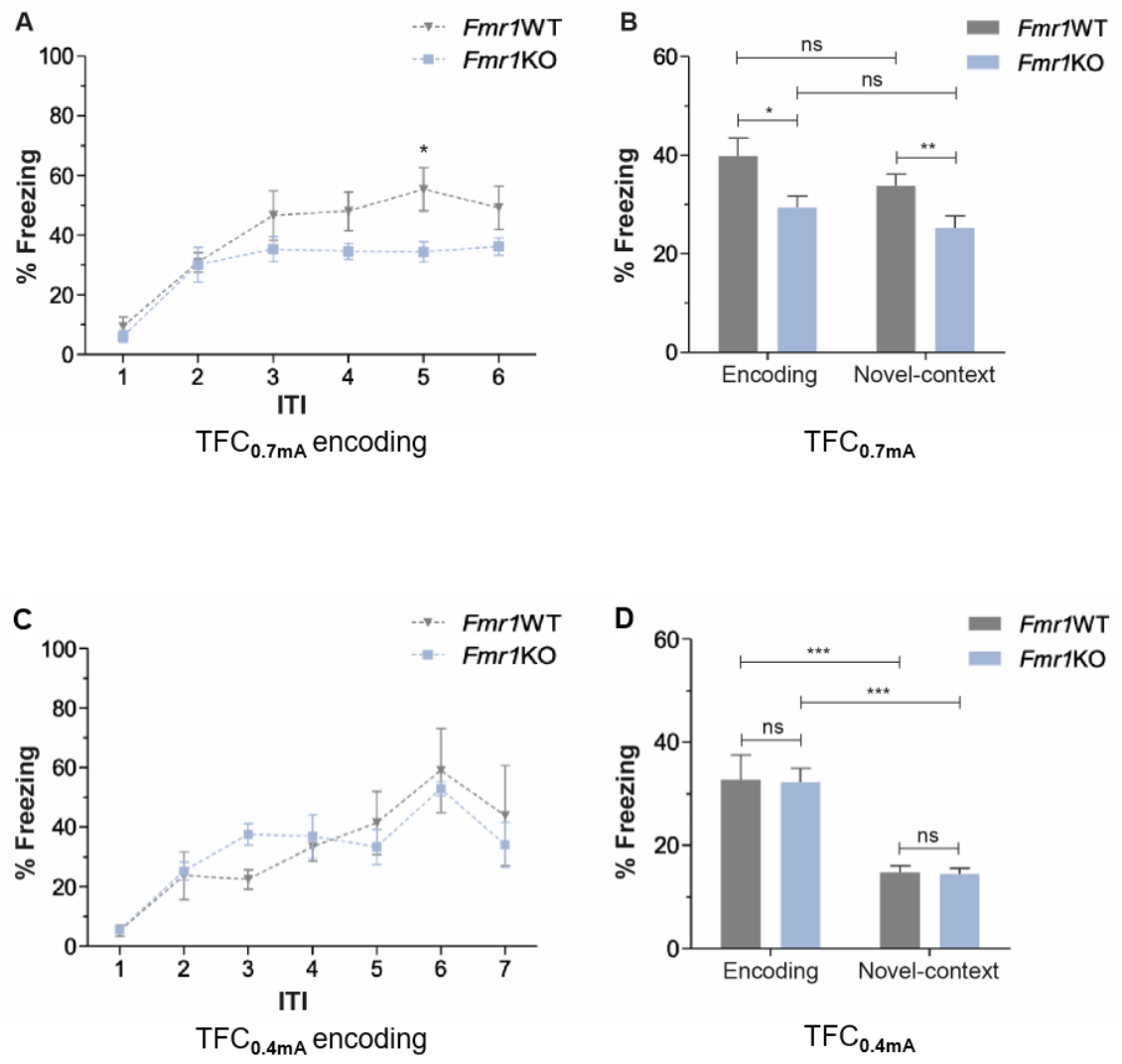

Figure 5. Percentage of time spent freezing during inter-trial intervals (ITI) in the Fmr1WT and Fmr1KO groups. (**A**) Time course of $TFC_{0.7mA}$ encoding, and (**B**) average freezing during $TFC_{0.7mA}$ encoding and novel-context sessions; (**C**) Time course of $TFC_{0.4mA}$ encoding, and (**B**) average freezing during $TFC_{0.4mA}$ encoding and novel-context sessions. ns p>0.05; *p<0.05; **p<0.01; ***p<0.001.

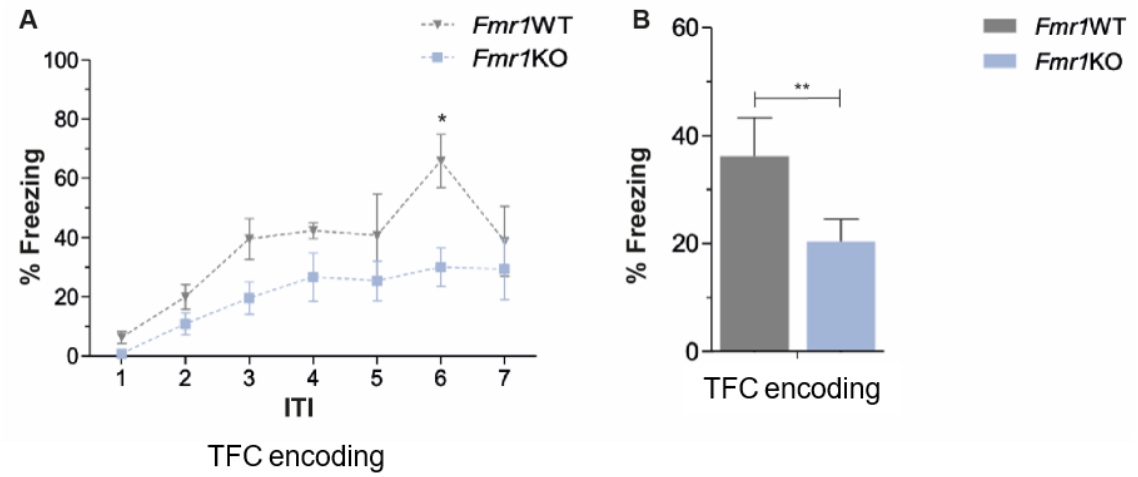

Figure 6. Percentage of time spent freezing during inter-trial intervals (ITI) in the Fmr1WT and Fmr1KO groups used for whole brain mapping. (**A**) Time course of TFC encoding, and (**B**) average freezing during TFC encoding. *p<0.05; **P<0.01.

ACC input map engaged during TFC is altered in the *Fmr1KO* mice

To assess whether ACC connectivity is altered in the *Fmr1* KO mouse model (our first hypothesis), we combined the recombinant rabies-based monosynaptic tracing technique with a c-fos-mediated tet-tagging system (see Experimental Design). This approach allowed us to target the expression of the accessory molecules (TVA and RG) specifically to ACC neurons that were engaged in TFC encoding – a behaviour task proven to demand ACC activity [125]. Seven days after mice underwent TFC followed by RABV stereotaxic injection, brains were fixed, processed for histological analysis and the resulting slices (~200 slices per brain covering the distance from 3.35mm to - 6.65mm relative to bregma; see figure 7) were then imaged using a high-throughput imaging approach. This approach allowed us to trace and detect neurons that are presynaptic to the engaged starter neurons (presynaptic neurons, mCherry+). An example of labelled neurons from two regions of interest (the ACC and thalamus) are shown in figure 8.

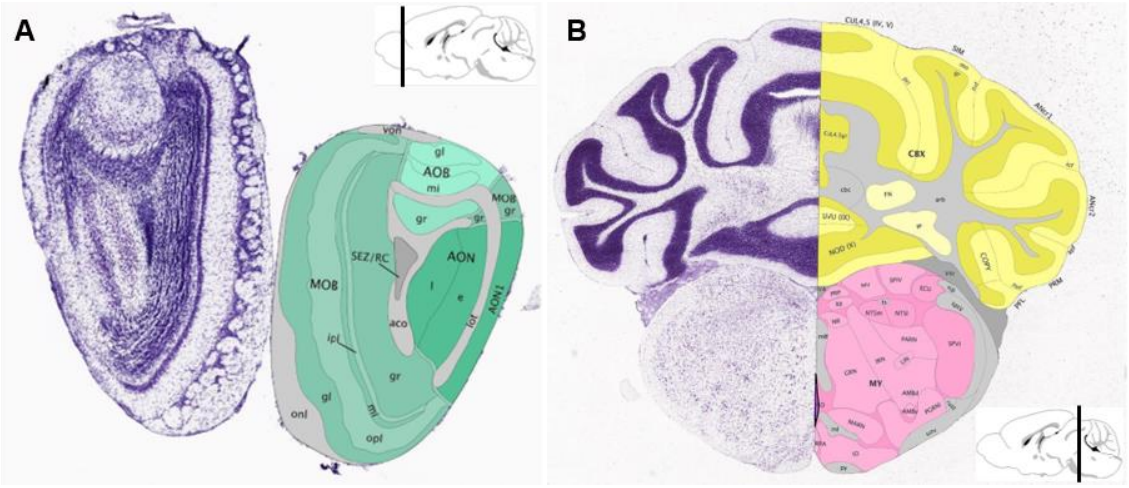

Figure 7. Inputs into engaged ACC neuros during TFC encoding were mapped from Bregma + 3.35mm (**A**) to - 6.65mm (**B**). Images from Allen Mouse Brain atlas, available online at https://mouse.brain-map.org/static/atlas.

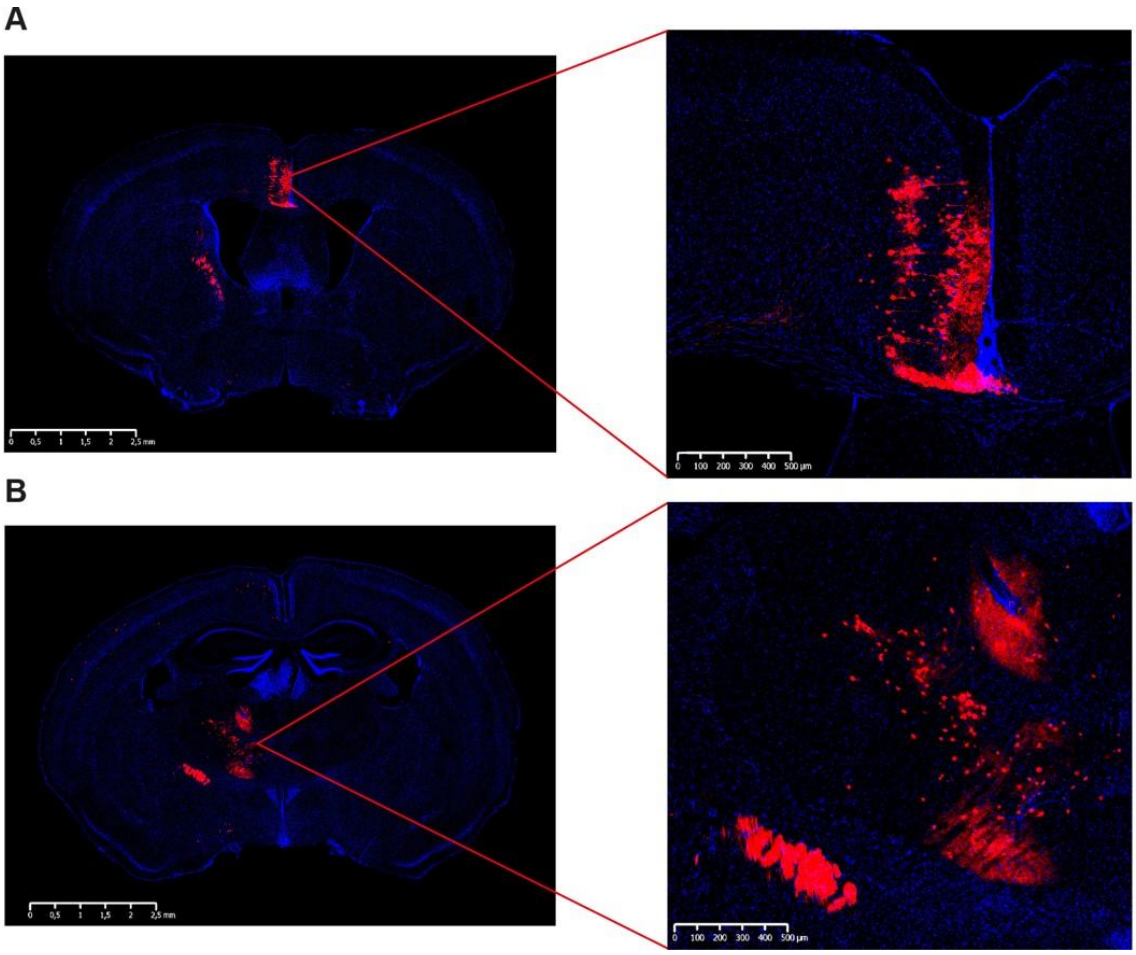

***Figure 8*.** Labelled presynaptic neurons (mCherry+) throughout the brain: (**A**) Bregma ~ +0.05mm, zoom in ACC; and (**B**) Bregma ~ -1.35mm, zoom in thalamus. Images were obtained using wide-filed fluorescence microscopy and a rapid acquisition system (NanoZoomer slide scanner, Hamamatsu) equipped with a 20x 0.75 NA objective.

The location of each labelled neuron was then mapped using one of two approaches. Subcortically labelled neurons were semi-automatically mapped using a custom-written python script that overlaid each brain slice image with a reference atlas (see Experimental Methods). Labelled neurons within the neocortex, on the other hand, were manually counted and mapped. The latter approach was necessary due to artefacts caused by the perfusion and mounting procedure that made it difficult to correctly overlay this brain region with the reference atlas. For all brain regions except the ACC, the ontology and hierarchal organization adapted by the reference atlas was maintained (Allen Mouse Brain Atlas, 2011). Based on cytoarchitectural evidence of the midcingulate cortex in the mouse (and rat) brain [122], we considered ACC as area 24, 25 and 32 (previous 24a and 24b), and the midcingulate cortex as area 24', according to Vogt and Paxinos (2014).

When performing this analysis, a number of technical and logistic challenges were encountered. First, as a consequence of the COVID-19 related confinement measures, we were able to only image the brains of five mice out of the total cohort of 7 mice. The results of our analysis are thus limited to two *Fmr1*WT brains and three *Fmr1*KO brains. Second, the site of injection was characterized by particularly dense labelling of neurons (figure 9), suggesting that a large number of inputs are derived from local connections. Due to the limitations of widefield epifluorescence microscopy — in particular the contribution of signal from outside the focal plane and light scattering in thick (50 µm) slices — it was not possible to resolve and count all the locally labelled neurons. Specifically, the following ipsilateral areas were affected: secondary motor cortex between ~3.05mm and ~0.20mm A/P; dorsal and ventral ACC from ~2.70mm to ~0.20mm A/P and ~1.30mm to ~0.20mm, respectively; prelimbic cortex between ~3.15mm and ~1.35mm A/P; infralimbic cortex from ~2.05mm to ~1.05mm A/P; medial orbital from ~3.15mm to ~2.05mm A/P; dorsal peduncular area and taenia tecta between ~1.50mm and ~1.55mm A/P, and ~1.35mm and 1.30mm A/P, respectively. For the same reasons, we were not able to resolve and count starter cells using widefield epifluorescence microscopy. Confocal microscopy would have been necessary to perform these analyses. However, we did not have access to this equipment due to the confinement measures in place at the University of Bordeaux. Access to this equipment in the immediate period after confinement was restricted to users who had already been trained to use the equipment independently. Thus, instead of normalizing the number of labelled presynaptic neurons to the number of ACC starter cells, we normalized them to the total population of labelled neuron. This approach is commonly used in this type of analysis (e.g.: Beier *et al*, 2017) to avoid

bias related to the variable number of initially labelled starter cells or to the quantity of virus injected.

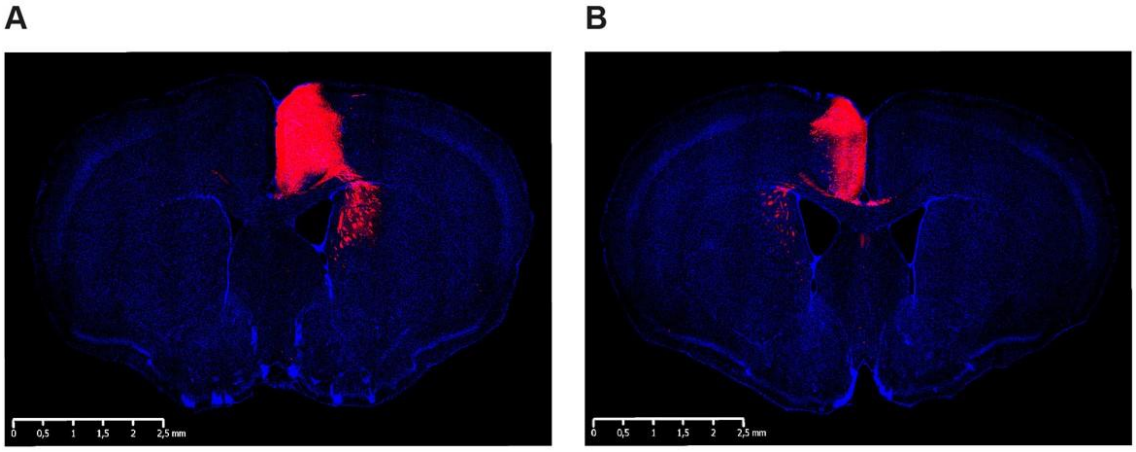

Figure 9. Highly dense neural labelling within the mPFC surrounding the site of injection (Bregma ~ + 1.00mm) in (**A**) Fmr1WT and (**B**) Fmr1KO brains. Images were obtained using wide-filed fluorescence microscopy and a rapid acquisition system (NanoZoomer slide scanner, Hamamatsu) equipped with a 20x 0.75 NA objective.

Our analysis revealed that ~85% inputs to engaged ACC neurons were localized ipsilateral to the ACC injection site (figure 10A; WT, 87.85 ± 0.2554% ipsi- *vs* 12.15 ± 0.2554% contralateral; KO, 83.20 ± 4.058% ipsi- *vs* 16.80 ± 4.058% contralateral; $p<0.0001$), and originated in many different brain regions (figure 10B; see detailed list in appendix 1). Contralateral projections (~15% of labelled neurons) were predominantly from cortical areas (WT, 94.57 ± 0.7575%; KO, 78.29 ± 6.944%).

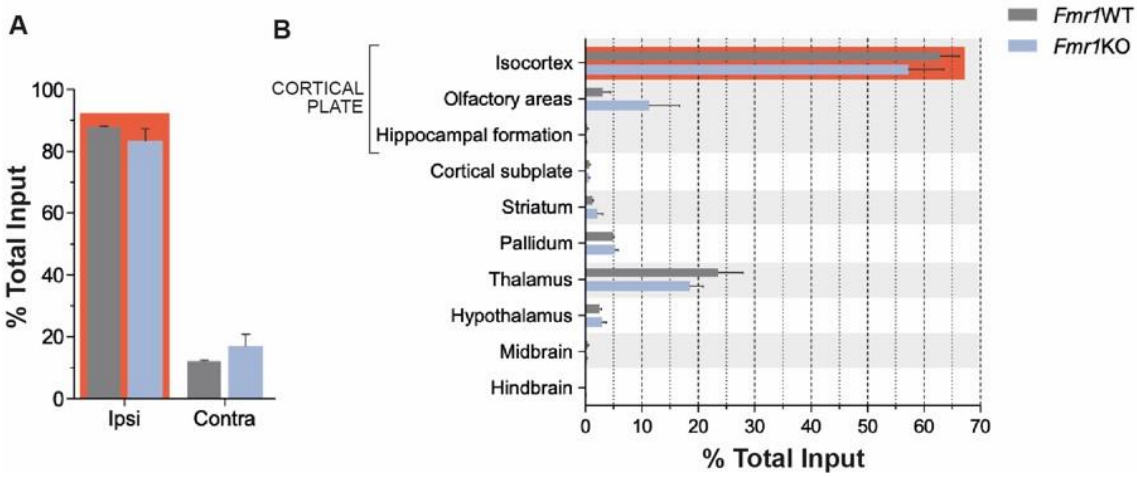

***Figure 10*.** ACC presynaptic neurons engaged during TFC encoding throughout the brain: percentage of total activated inputs (**A**) per ipsi- and contralateral side of the injection site; and (**B)** per main brain regions. Highlighted regions represent $p<0.01$ when compared to the others, independently of genotype.

As a whole, the primary source of afferents was the cortical plate (WT, 66.44 ± 4.997%; KO, 70.63 ± 2.431%), followed by the thalamus (WT, 23.53 ± 4.400%; KO, 18.40 ± 2.404%) and other subcortical regions (WT, 10.98 ± 2.286%; KO, 10.01 ± 0.6211%). The cortical plate includes isocortical and olfactory areas, and the hippocampal formation. The largest number of presynaptic neurons was identified in isocortical areas (WT, 62.82 ± 3.427% and KO, 53.13% ± 8.611% *vs* other cortical plate main regions; p=<0.001; figure 10B), namely somatosensory, somatomotor, limbic-related, auditory, associative, orbital and visual cortices (figure 11). According to our findings, the midcingulate cortex (MCC; WT: 15.54 ± 3.379%; KO: 15.93 ± 7.498%) and the ventral part of the restrosplenial cortex (RSPv; WT: 7.956 ± 1.162; KO: 8.329 ± 3.192%) present the higher proportions of cortical inputs to ACC neurons engaged during TFC. Due to the aforementioned limitations of our analysis (see above) we could not provide a full quantitative analysis of all prefrontal inputs to engaged neurons. However, the highly dense neural labelling within the mPFC surrounding the site of injection (figure 9) suggests that a large percentage of ACC inputs are local (i.e.: afferents from other medial prefrontal regions and ACC intraprojections). Indeed, as mentioned above neurons in these regions (spatial range specified above) were not included in this analysis since it was impossible to clearly differentiate individual neurons due to the technical limitations of widefield microscopy. Consequently, our analysis of mPFC inputs represents an undersampling of inputs from this area. A more detailed neural counting requiring confocal imaging is necessary to provide a full analysis. With respect to the olfactory cortex, labelled presynaptic neurons were generally in the dorsal taenia tecta (figure 11; TTd; WT: 1.734 ± 0.641%; KO: 5.782 ± 3.95%) and dorsal peduncular area (DP; WT: 1.007 ± 0.529%; KO: 2.284 ± 1.158%). Finally, afferents from the hippocampal formation included few neurons (figure 11; WT: 0.5012 ± 0.24%; KO: 0.2877 ± 0.1887%) located within the CA1 and CA3 fields, and the entorhinal (ENT) retrohippocampal area. Differences between genotypes regarding the proportion of ACC inputs from cortical plate structures did not have statistical significance.

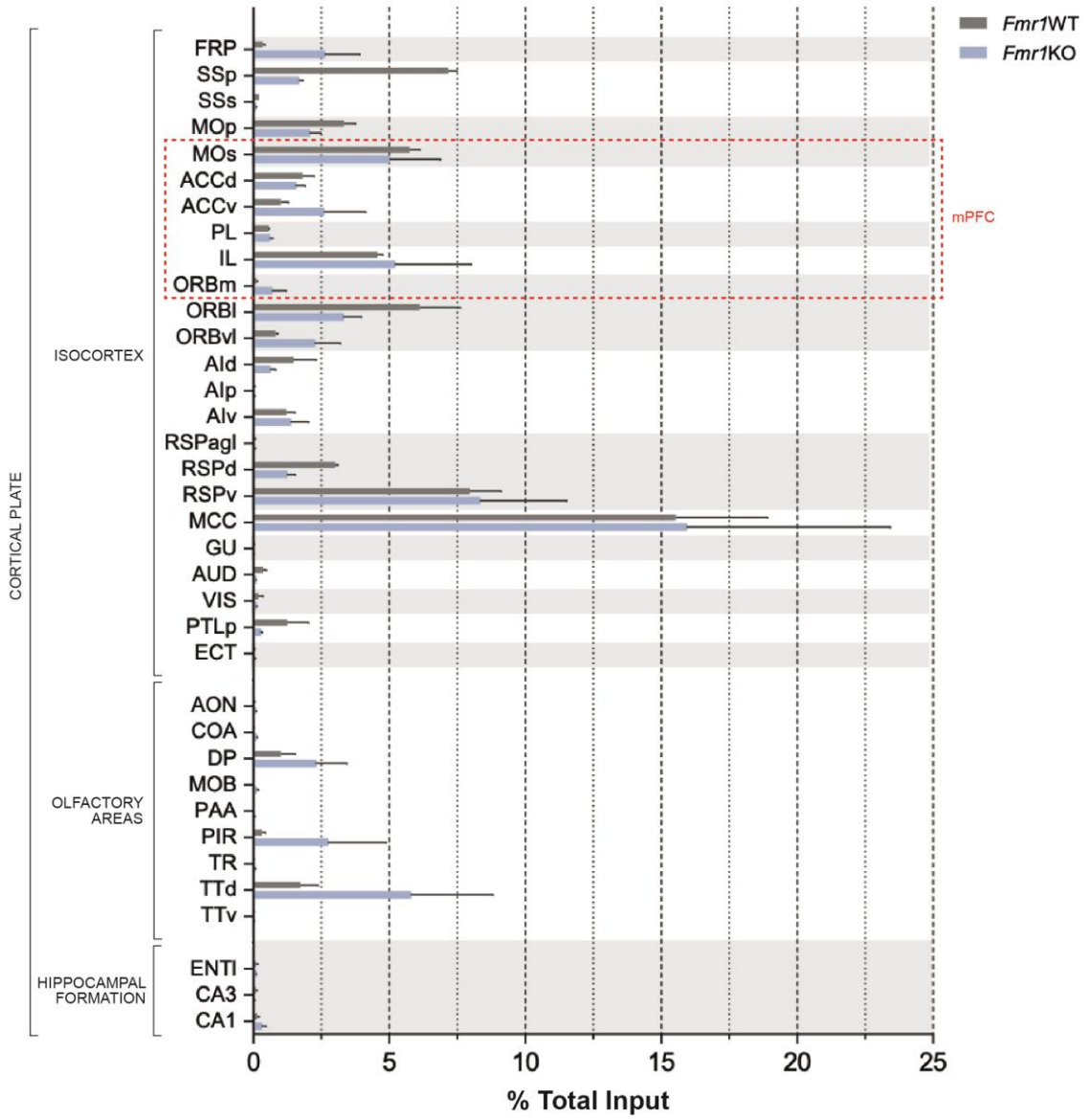

Figure 11. ACC presynaptic neurons engaged during TFC encoding throughout cortical plate substructures. FRP, frontal pole; SSp, primary somatosensory cortex; SSs, suplemental somatosensory cortex; Mop, primary somatomotor cortex; MOs, secondary somatomotor cortex; ACCd, anterior cingulate cortex, dorsal part; ACCv: anterior cingulate cortex, ventral part; PL, prelimbic cortex; IL, infralimbic cortex; ORBm, orbital cortex, medial part; ORBI, orbital cortex, lateral part; ORBvI, orbital cortex, ventrolateral part; Ald, agranular insular cortex, dorsal part; Alp, agranular insular cortex, posterior part; Alv, agranular insular cortex, ventral part; RSPagl, retrosplenial cortex, lateral agranular part; RSPd, retrosplenial cortex, dorsal part; RSPv, retrosplenial cortex, ventral part; MCC, midcingulate cortex; GU, gustatory cortex; AUD, auditory cortex; VIS,visceral cortex; PTLp, posterior parietal cortex; ECT; ectorhinal cortex; AON, anterior olfactory nucleus; COA:, cortical amygdalar area, anterior part; DP, dorsal peduncular cortex; MOB, main olfactory bulb; PAA, piriform-amygdalar cortex; PIR, piriform cortex; TR, post-piriform transition; TTd, taenia tecta, dorsal part; TTv, taenia tecta, ventral part; ENTI, entorhinal cortex, lateral part.

Labelled neurons were identified in all thalamic groups (figure 12), especially within nuclei of the ventral (VENT; WT, 7.521 ± 2.888%; KO, 4.757 ± 0.3002%) and the anterior (ATN; WT, 4.557 ± 1.700%; KO, 8.801 ± 2.970%) thalamus. For the *Fmr1*KO group, we detected a significant increase in the proportion of presynaptic neurons within the anteromedial (AM; WT, 1.584 ± 0.839% *vs* KO, 3.730 ± 1.431%; $p<0.01$) nucleus, and a decrease of afferents from the mediodorsal (MD; WT, 3.858 ± 0.342% *vs* KO, 1.734 ± 0.261%; $p<0.01$) nucleus and posterior complex (PO; WT, 2.328 ± 0.024% *vs* KO, 0.378 ± 0.31%; $p<0.05$) of the thalamus.

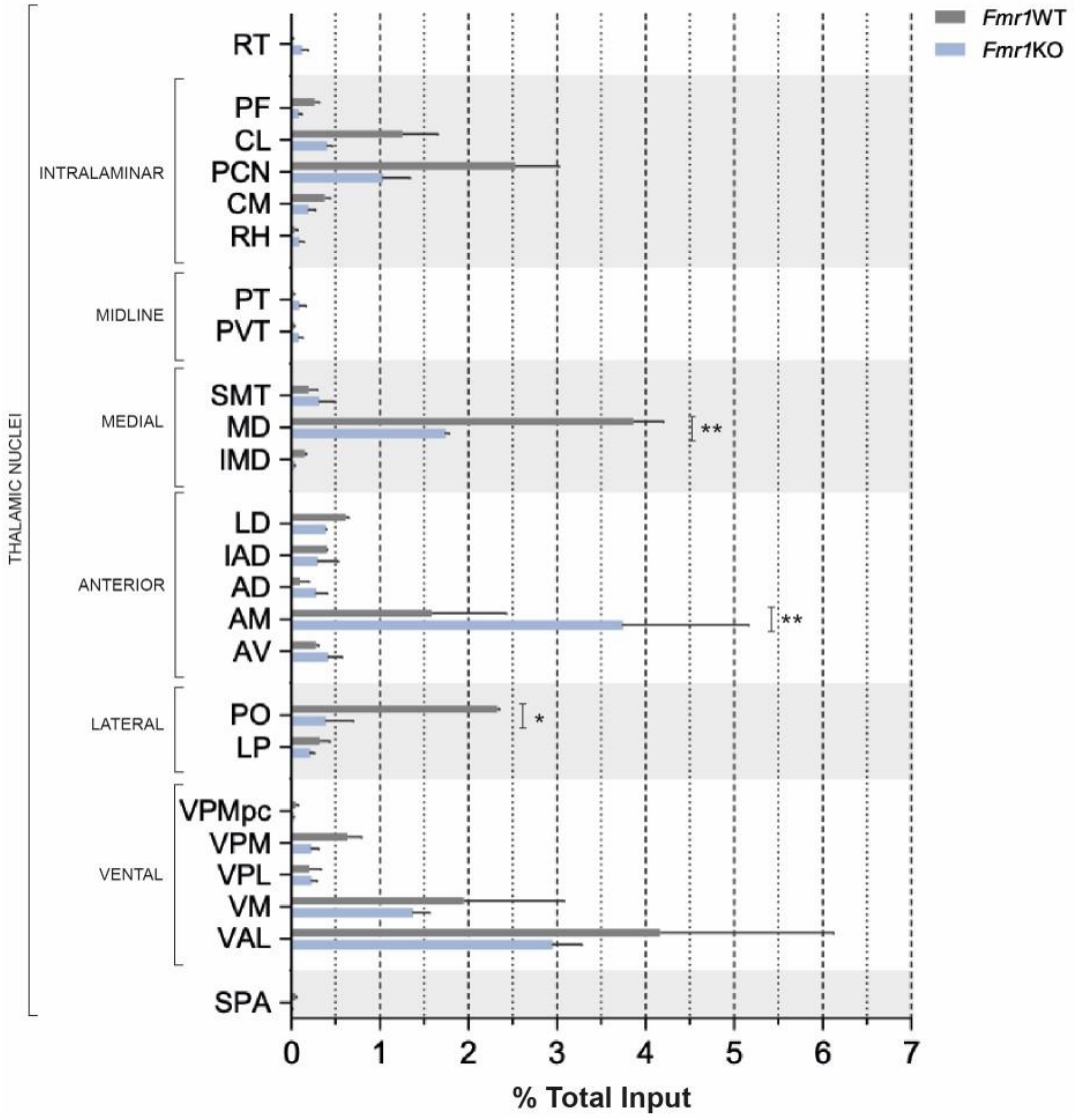

Figure 12. ACC presynaptic neurons engaged during TFC encoding throughout thalamic nuclei. *p<0.05; **p<0.01. RT, reticular nucleus; PF, parafascicular nucleus; CL, central lateral nucleus; PCN, paracentral nucleus; CM, central medial nucleus; RH, rhomboid nucleus; PT, parataenial nucleus; PVT, paraventricular nucleus; SMT, submedial nucleus; MD, mediodorsal nucleus; IMD, intermediodorsal nucleus; LD, lateral dorsal nucleus; IAD: interanterodorsal nucleus; AD, anterodorsal nucleus; AM, anteromedial nucleus; AV, anteroventral nucleus; PO, posterior complex; LP, lateral posterior nucleus; VPMpc, ventral posteromedial nucleus, parvicellular part;

VPM, ventral posteromedial nucleus; VPL, ventral posterolateral nucleus; VM, ventral medial nucleus; VAL, ventral anterior-lateral complex; SPA, subparafascicular nucleus.

Other sources of inputs to engaged neurons include structures of the cortical subplate, striatum, pallidum and hypothalamus (figures 13 and 14). For instance, amygdalar presynaptic neurons were visualized not only in the basolateral (BLA) and basomedial (BMA) amygdalar nuclei, but also within the central (CEA) and medial (MEA) amygdalar nuclei, and the anterior (AAA) amygdalar area; and the diagonal band nucleus (NDB; figure 13) is the pallidum structure with higher percentages of projections to the ACC (WT, 2.278 ± 0.04592; KO, 2.683 ± 0.1975). In addition, hypothalamic inputs (figure 14) were mainly from the hypothalamic lateral zone (LZ; WT, 1.655 ± 0.5504; KO, 1.671 ± 0.6853; p=0.0002 comparing other hypothalamic zones), which includes the lateral hypothalamic area (LHA), lateral preoptic area (LPO) and zona incerta (ZI). Midbrain and hindbrain represented less than 0.5% and 0.05% of the total input map, respectively. A few isolated labelled neurons were identified, for example, within the midbrain reticular nucleus, periaqueductal gray, ventral tegmental area, and pedunculopontine nucleus, as well as in the pontine reticular nucleus and tegmental reticular nucleus. Importantly, no major differences between the *Fmr1*WT and KO mice were detected among the aforementioned subcortical areas.

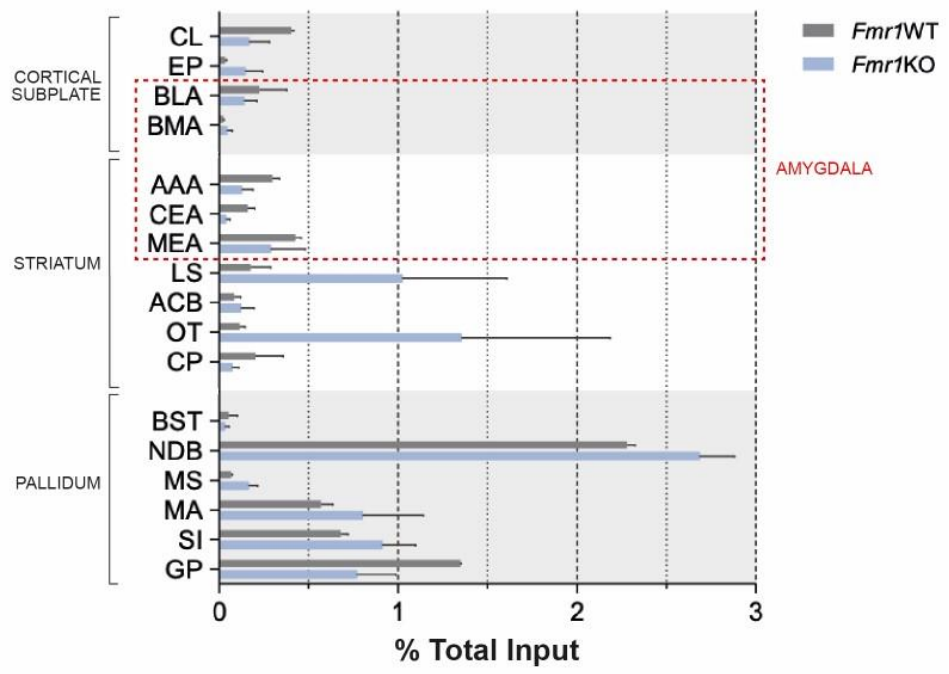

Figure 13. ACC presynaptic neurons engaged during TFC encoding throughout cortical subplate, striatum and pallidum substructures. CL, claustrum; EP, endopiriform nucleus; BLA, basolateral amygdalar nucleus; BMA, basomedial amygdalar nucleus; AAA, anterior amygdalar area; CEA, central amygdalar nucleus; MEA, medial amygdalar nucleus; LS, lateral septal nucleus; ACB, nucleus accumbens; OT, olfactory tubercle; CP, caudoputamen; BST, bed nuclei

of the stria terminallis; NDB, diagonal band nucleus; MS, medial septal nucleus; MA, magnocellular nucleus; SI, substantia innominate; GP, globus pallidus.

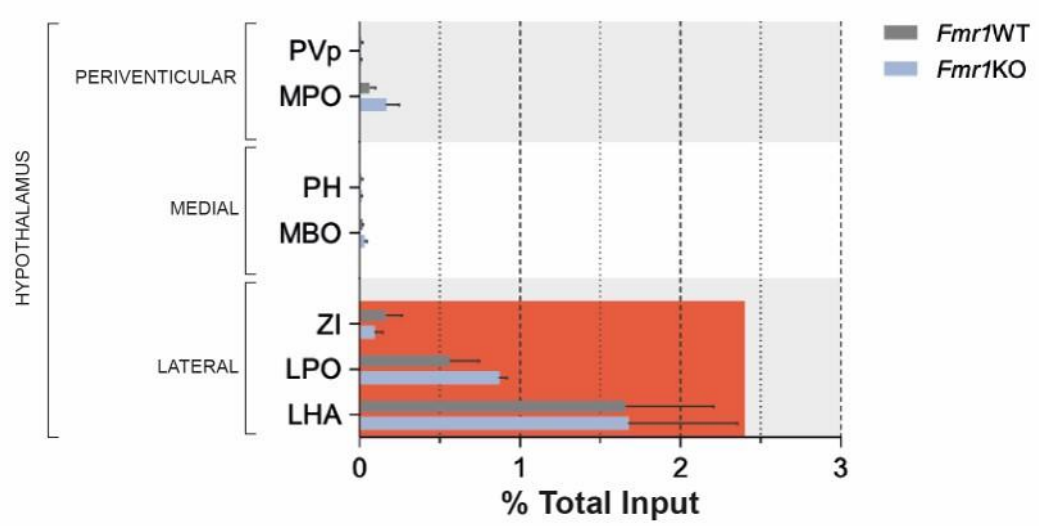

Figure 14. ACC presynaptic neurons engaged during TFC encoding throughout hypothalamus. Highlighted hypothalamic zone represent $p<0.01$ when compared to the others, independently of genotype. PVp, periventricular hypothalamic nucleus, posterior part; MPO, medial preoptic area; PH, posterior hypothalamic nucleus; MBO, mammillary body; ZI, zona incerta; LPO, lateral preoptic area; LHA, lateral hypothalamic area.

Optimization of the whole-brain mapping analysis approach

The mapping approach described above required the detection, and identification (assignment to a brain region, subzone or nuclei) of each fluorescently (mcherry expressing) labelled neurons. As an initial quality control, each brain slice was manually observed under a wide-field fluorescence microscope to confirm the injection site and presence of labelled neurons before mounting. This preliminary quality control evaluation allowed us to identify brain slices that would require confocal imaging (thus different mounting conditions) for a proper analysis, in addition to imaging using wide-filed fluorescence microscopy. Acquired images where then manually collated and assigned coordinates along the rostral caudal axis (with respect to Bregma). To do this, DAPI-stained images of our brain slices were manually compared with Nissl stained brain sections of the Allen Mouse Brain Atlas. Anatomical landmarks (see also below) were the used to identify the corresponding atlas image.

To map ACC presynaptic neurons, we used a custom-written python script developed within the host team. This script enables the overlay of each image with a reference atlas in order to assess the position of each manually selected labelled neuron. Since it is a semi-automatic method for brain mapping, the user is responsible for defining the A/P position for each brain slice in order to select the correspondent position of the reference atlas to overlay. This overlay is guided by the initial collation.

In addition, we took into consideration the thickness of the brain slices (i.e.: each brain slice is 50µm apart from the previous one), and easily identifiable anatomical borders and landmarks, such as the ventricles size, the hippocampus presence, size and position, the thalamus size and shape, or the presence and size of brain commissures. This step was hindered by changes in brain size as well as distortion caused by the perfusion and mounting procedure. In most of the brain slices, these artefacts made it impossible to correctly overlay regions containing the cortex (as highlighted in figure 15), thus for these brain areas, labelled neurons were counted and mapped manually. As exemplified in figure 16, mapping of labelled cortical neurons was made in close comparation with the Allen Mouse Brain Atlas, and manly guided by the cortical layer organization (e.g.: layer 4 presence/absence) and using the surrounding brain subcortical structures as reference.

While using the mapping script, some technical difficulties were encountered. Firstly, the script integrated a “down-sizing” to enable the handling of large imaging files. This resulted in a reduction of image quality within the viewer window. In addition, the script lacked many aspects related to user friendliness i.e. non-intuitive layout of the settings tool-bars, poor responsiveness for regulating settings such as brightness, contrast or scale, and errors during the export of results. In collaboration with students from the Bioinformatics Master’s program of the University of Bordeaux, I contributed to improvements in this mapping approach. In particular, by making concrete suggestions and then experimentally testing the corrections that they made to the script, we were able to markedly refine and improve the analysis approach. These modifications significantly improved the user-friendliness, thus increasing the accuracy of both neural selection and overlap with the reference atlas.

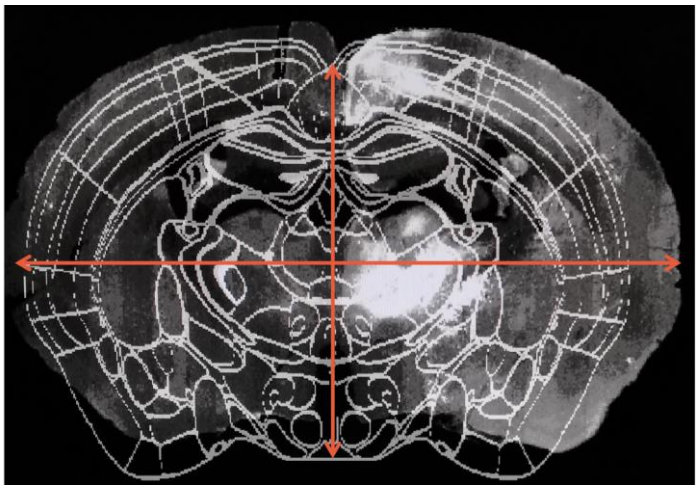

Figure 15. Distortion and changes in brain size caused by the perfusion and mounting procedures hindered the overlay with the reference atlas.

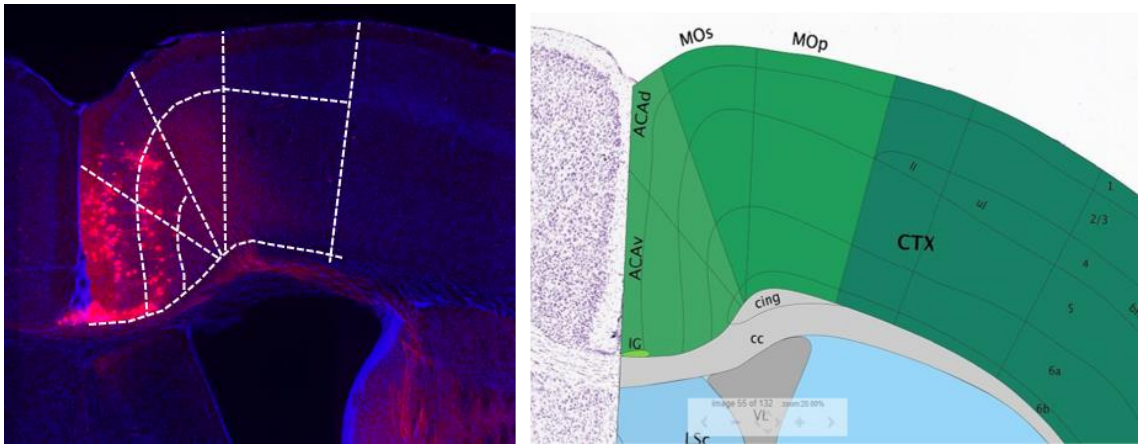

Figure 16. Manual mapping of cortical labelled neurons. Right image from Allen Mouse Brain Atlas, available online at https://mouse.brain-map.org/static/atlas.

Pharmacogenetic stimulation of thalamic nuclei afferents to ACC do not alter *Fmr1*KO phenotype

Our detailed examination of thalamic inputs into engaged ACC neurons (see above – figure 12) suggested that MD-ACC neural circuit may be altered in the *Fmr1*KO mouse model. Based on these viral tracing results and with reference to the existing literature examining the role of MD thalamic inputs for ACC network function, we decided to explore the consequences of functionally manipulating this circuit. To do this we aimed to pharmacogenetically manipulate the activity of ACC-projecting-MD neurons by using an intersectional approach in which Cre-dependent expression of hM3Dq excitatory DREADD was targeted to the input population of interesting (see *Experimental Design*). We opted for an excitatory DREADD since the neural density of MD afferents to ACC engaged neurons seems to be reduced. A similar strategy has been described for PFC-projecting amygdalar neurons in PTEN haplo-insufficient mice (Huang *et al*., 2016) [146] with the exception that this latter study used the approach of reducing the activity of a specific neuronal population. Our aim was to boost the neural activity of this specific ACC thalamic input during both TFC sessions (i.e.: encoding and novel-context) by CNO intraperitoneal injection 40 minute prior to behavioural testing. Freezing behaviour in the inter-trial intervals was scored in order to analyse consequences of this circuit manipulation.

Afterwards, both injection sites (i.e.: ACC and MD) were confirmed using wide-field microscopy (figure 17). These control revealed that although we tested and use stereotaxic coordinates to specifically target de MD, DREADD injection mistargeted this thalamic nuclei. mCherry+ neurons were observed in adjacent nuclei. Nevertheless, we

found interesting the analysis of the results obtained with this experience since our viral tracing results identified the thalamus as a main source of inputs to engaged ACC neurons.

This experiment included 4 experimental groups since both genotypes were tested for the administration of CNO (*Fmr1*WT_{CNO} and *Fmr1*KO_{CNO}) or vehicle solution (*Fmr1*WT_{VHC} and *Fmr1*KO_{VHC} as negative controls). In total 4 *Fmr1*WT and 2 KO mice received CNO, whereas the vehicle solution was injected in 2 WT mice and 1 KO mouse (one additional KO mouse died during anaesthesia). This limited group size reflects the significant constraints in place both during and following the confinement period at the University of Bordeaux and Neurocentre Magendie. In particular, access to experimental space was extremely limited due to quotas of the number of people present at any time. In addition, the production of mice in the transgenic breeding facility had been significantly reduced during the confinement in accordance with national INSERM guidelines. Given these constraints and the limitation of the size and composition of each experimental group (small and not equal between genotypes and experimental conditions such as CNO vs. VHC), their statistical comparation would not be appropriate. Yet, a qualitative analysis of our results reveals that the 4 experimental groups presented increased freezing throughout the TFC encoding trials (figure 18A). Although the *Fmr1*KO_{CNO} mice showed a slight superior freezing time compared to the respective WT and *Fmr1*KO_{VHC} mice between ITI-2 and ITI-7, average freezing of *Fmr1*WT and KO mice of each condition, during the encoding session (figure 18B; WT_{CNO}, 39.21 ± 4.121; KO_{CNO}, 44.33 ± 7.865; WT_{VHC}, 33.54 ± 6.556; KO_{VHC}, 36.77 ± 7.568) suggests that there were no differences among them. The same similarity in average freezing was displayed in the novel-context session (figure 18B; WT_{CNO}, 22.60 ± 2.053; KO_{CNO}, 18.83 ± 4.070; WT_{VHC}, 14.87 ± 1.689; KO_{VHC}, 30.96 ± 4.833). Therefore, the results obtained indicate that manipulating the excitability of thalamical-ACC circuits did not affect TFC outcome.

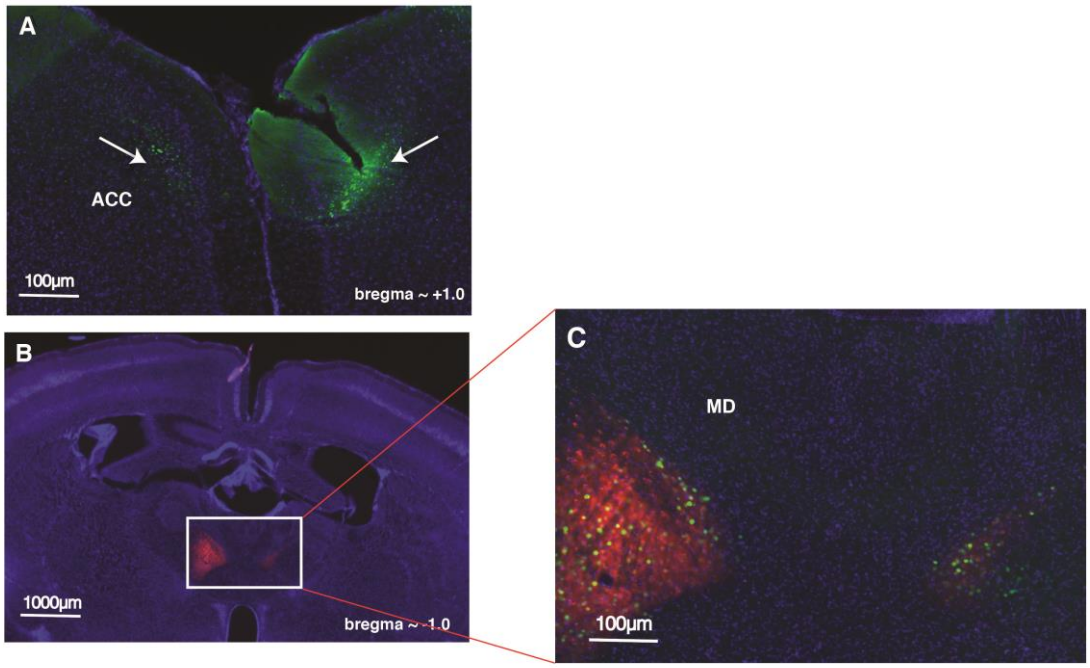

Figure 17. Posthoc verification of DREADD targeting strategy. (**A**) Image presenting injection site in ACC. AAV-retro2 Cre-nls-GFP labeled neurons, characterized by nuclear staining, at the site of injection; (**B**) Low magnification image demonstrating localization of DREADD expressing neurons (red) in thalamus; (**C**) Higher magnification image of thalamus regions expressing both DREADD (mCherry=red) and Cre (nuclear eGFP=green). Blue = DAPI staining of cell nuclei. Images were obtained using an inverted epi-fluroescence microscope (Nikon Eclipe Ti-U) equipped with a DSQi2 CMOS camera.

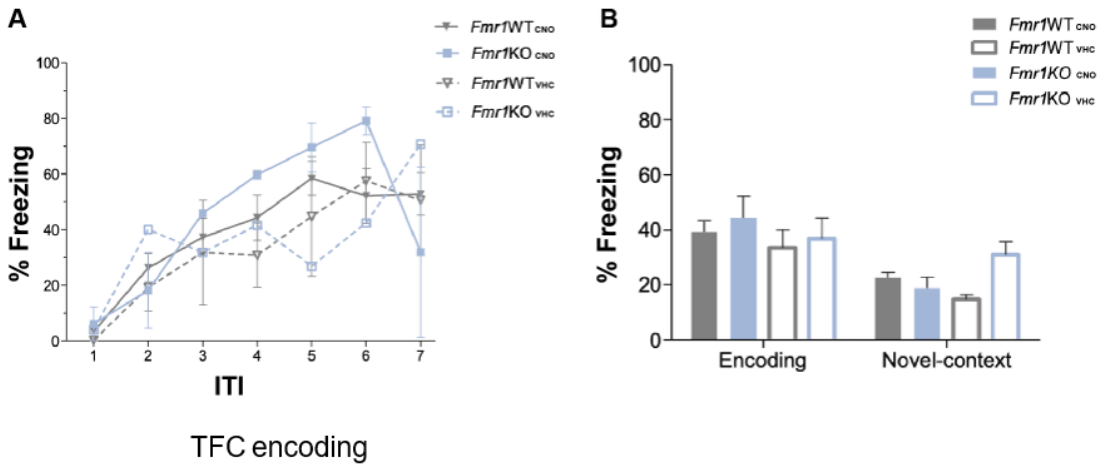

Figure 18. Percentage of time spent freezing during inter-trial intervals (ITI) in the *Fmr*1WT and *Fmr1*KO groups after intraperitoneal injection of CNO (Fmr1WT$_{CNO}$ and Fmr1KO$_{CNO}$) or vehicle solution (*Fmr1*WT$_{VHC}$ and *Fmr1*KO$_{VHC}$) for DREADD-dependent manipulation of ACC thalamic inputs. (**A**) Time course of TFC encoding, and (**B**) average freezing during TFC encoding.

6. DISCUSSION

The aim of this study was to examine alterations in the structural connectivity of prefrontal cortex circuits in *Fmr1*KO mice and to explore the functional consequences of these changes for cognitive abilities and behavioural outcome. We investigated these questions in the ACC part of the PFC. The reasons for this choice were that while defects in PFC function are poorly described in mouse models of ASD, there is existing literature demonstrating electrophysiological alterations in ACC function in the *Fmr1*KO mouse (e.g.: Zhao, *et al*., 2005; Koga *et al*., 2015) [135,137], and in the structural/functional connectivity of the ACC in the *Cntnap2*KO mouse model of ASD [62,206]. Moreover, the ACC has been described as a hub of connectivity [12] crucially implicated in cognitive abilities that are deficient in ASD, and is thus a likely target for pathophysiological changes leading to alterations in circuit function.

Inputs into engaged ACC neurons involved in the performance of a behavioural task

Using an innovative intersectional viral approach, combined with high throughput imaging, we explored the inputs specifically into those ACC neurons that were engaged in the TFC task. Although the dataset obtained is from a small experimental cohort it provides some interesting observations about the circuit underlying attention-dependent associative learning in *Fmr1*KO mice. Overall, the brain regions we identified as source of ACC inputs (appendix 1) are consistent with previous descriptions of afferent projections to a general ACC neuronal population (not linked to any specific behavioural task) [126,127]. Interestingly, our data revealed the MCC as a main cortical input into ACC engaged neurons. This input, as well as its potential function, is not clearly described in the literature. This is likely due to the fact that most rodent studies fail to mention the MCC (area 24') as a separate brain area, and rather include this area together with the ACC (area 24). So far, preclinical functional studies have implicated the MCC in pain processing, and the control of attentional and visual spatial orientation [207]. MCC thus seems to functionally complement the ACC, and to correspond to what is known about the human MCC [207]. Another main cortical input into engaged ACC neurons was from the RSP cortex. RSP activity is critical for trace (and contextual) fear memory formation and, taking into consideration our results, this might involve projections into the ACC [208,209]. Several studies have also elucidated the role of both hippocampus (namely the CA1 field) and basolateral amygdala in TFC [210]. Yet, in contrast to RSP, their connectivity with the ACC was relatively sparse. This is consistent with previous studies identifying light labelling within the hippocampus, but

somewhat contrary to findings suggesting a greater density of amygdalar inputs, in particular from the basolateral amygdala [126,127]. This finding may reflect a functional selection of circuits involved in the encoding of the trace fear memory, but not fear *per se*.

Additional quantitative differences between previous results and ours were observed in thalamic inputs. Hoover and Vertes (2007) showed that ACC afferents from the thalamus (in the rat) implicates the anteromedial, mediodorsal, central lateral, paracentral, and reuniens nuclei [127]. Our analysis (in the mouse) suggests that the thalamic inputs to ACC neurons engaged in the TFC task arise primarily from the anteromedial, mediodorsal, and paracentral nuclei, and from the posterior and ventral anterior-lateral complexes of the thalamus. These differences might reflect the fact that specific circuits are required for the TFC task (e.g. as suggested by the work of Ye *et al*., 2016) [211], but also differences between rat and mouse brain connectivity, or in the subzone of the ACC that was targeted (e.g. as suggested in Fillinger *et al*. 2017) [126].

Two neuromodulator ACC inputs that stood out were the NDB pallidum nuclei and the lateral hypothalamus. Both are likely very relevant for TFC. NDB cholinergic projections are part of the mPFC's acetylcholine neuromodulation supporting cognitive functions such as attention, learning and memory [212–214]. Similarly, the lateral hypothalamus includes many groups of orexin neurons that are known to target the mPFC [215] and mediate attention through selective activations of thalamocortical terminals [216].

Potential alterations in ACC circuits in the *Fmr1*KO mouse

According to our findings, specific aspects of the ACC connectivity may be altered in the *Fmr1*KO mouse model. Although the small sample size prevents a robust statistical analysis, our data proposes changes in the proportion of labelled presynaptic neurons with respect to the total number of neurons throughout the brain of *Fmr1*KO mice. In particular, the percentage of total inputs stemming from the PO, AM and MD thalamic nuclei seem to be affected. In fact, recent studies support an important role of thalamocortical circuits for cognitive integration, from learning and memory to flexible adaptation [217,218].

PO projections to the neocortex have been correlated with sensory-motor processes. For example, projections from this thalamic complex to vibrissae-related domains of the motor and somatosensory cortices are known to impact the sensory processing and affect active whisker exploration in rodents [219]. Our results pointed to a

reduction of afferents from this source, potentially leading to an alteration in the ACC processing of sensory information.

The anterior thalamic nuclei (which includes the AM nucleus), via its connections with the ACC and the orbitoprefrontal cortex, contributes to reciprocal hippocampal-prefrontal cortex interactions underlying memory processing and spatial navigation in rodents [217,218]. Notably, Wright *et al*. (2015) explored the role of the anterior thalamus in directing attention to task-relevant stimuli and proposed that ACC might contribute to this function [220]. Interestingly, our data suggests that inputs from this region may be increased. The functional implication of this alteration remains speculative at this point, since a greater percentage of presynaptic neurons does not necessarily mean a greater efficiency of this projection. Additional studies are required to probe the functional consequence of this potential connectivity reorganization.

The contribution of the MD thalamic nucleus to learning and memory has been extensively confirmed [217]. The role of an extensive forebrain circuit involving the MD, the basolateral nucleus of the amygdala, and the mPFC, for both the establishment and extension of fear-related memories is very well supported by many studies. Work by Mátyás *et al*. (2015) using tracer injections shows that in this fear circuit, the basolateral nucleus of the amygdala and the MD might interact via mutual reciprocal connections with the insular cortex and the ACC [221]. On other hand, the optogenetic activation of MD inputs to the ACC exacerbated pain-related aversion, according to Meda *et al* (2019) [222]. Numerous studies have also demonstrated that reciprocal interaction between MD nucleus and the mPFC (including the ACC) supports working memory, and that these MD inputs have a circuit-specific role in sustaining the PFC activity during the delay period of working memory task [223–225]. The possible reduction of MD inputs in *Fmr1*KO mice could thus be expected to impact a number of cognitive processes

Structural and electrophysiological data revealed that, within the mPFC, MD inputs drive direct excitation of prefrontal pyramidal neurons, as well as feedforward inhibition (through the direct innervation of inhibitory interneurons) [222,226]. Additionally, glutamatergic projections from the cerebellum to the MD nucleus activate, in turn, MD glutamatergic afferents to the medial PFC, thereby modulating mesocortical dopaminergic terminal release in this brain region [227]. Interestingly, *Fmr1*KO mice display an attenuation in this cerebellar-evoked medial PFC dopamine release compared to WT controls [227]. Local depletion of dopamine in the mPFC can cause cognitive deficits. Specifically, Granon *et* al. (2000) reported impaired attentional performance after infusion into the mPFC of an antagonist of D1 dopaminergic

receptors, while Pezze *et al*. (2015) confirmed that the infusion of a D1 agonist into the ACC can improve attentional performance during trace conditioning tasks [228–230].

This body of evidence (including our own findings) highlights the MD as a particularly interesting brain structure for further investigations into the functional role of connectivity alterations with the ACC in the establishment of cognitive deficits in the *Fmr1*KO mouse model (i.e.: experimental task 2).

Functional consequences of altered ACC circuit for *Fmr1*KO behavioural outcome

Our findings suggested that thalamic projections to ACC are altered in the *Fmr1*KO mouse model. Namely, there was a decrease in the number of MD inputs into ACC neurons engaged during the acquisition of TFC. To probe the contribute of this specific input disruption on Fmr1KO phenotype, we proposed to analyse the consequences of its DREADD-mediated neural activation on behavioural outcome.

Before this experience, MD coordinates were tested through the stereotaxic delivery of a fluorescent probe. Yet, imaging of the site of injection revealed that virus transduction and DREADD expression occurred in ACC efferents sent from surrounding nuclei. To limit the viral injection to a specific thalamic nuclei represents a challenge since this brain regions is composed by several adjacent and small nuclei, it is easier to target a thalamic group of nuclei. In addition, due to the limited time frame we had to perform this experience, experimental conditions were adapted from previous protocols implemented at the lab, and not tested and optimized to our propose. For instance, we did not test if the AAV serotype used was appropriate to target the MD neurons – different AAV serotypes have tropism for different brain cell populations according with the brain regions [231]. And experimental details such as the targeting approach (e.g.: needle or glass capillary) and volume of AAV delivered also dictate extension of neural transfection, and thus the magnitude of the circuit manipulation [232].

Although based on small and unbalanced experimental groups, we found that stimulation of different thalamic-ACC pathways during both encoding and retrieval of TFC might not affect behavioural performance, even though we have interfered with the neural activity of one of the main brain sources of inputs to ACC neurons engaged during TFC.

Choice of the trace fear conditioning paradigm

We employed TFC as a behavioural model for attention related cognitive deficits. TFC is an associative learning paradigm that introduces a time delay (the trace interval) between the conditional stimulus and the unconditional stimulus. Clinical and preclinical studies have established a requirement of ACC activation for attention [118,123,124]. In addition, Han, *et al*. (2003) demonstrated the necessity of both attention and ACC activation for intact TFC [125]. Other behavioural tasks, such as the five-choice serial reaction time task [described in Robbins (1998)], are employed to explore attention on a sustained basis. However, these protocols include several days of training, which are not compatible with tet-tagging technical approaches and may be difficult to establish in transgenic mice. Another issue which merits discussion is that it has been very well documented that behavioural phenotypes in the *Fmr1*KO mouse vary across publications [202]. One of the current challenges for research in this field is to identify phenotypes, or phenotyping approaches, that are reproducible between laboratories. To this extent, we find it to be a strength of our findings that we were able to reproduce phenotypes in the second generation *Fmr1*KO mouse line through methods established by independent laboratories which used first generation *Fmr1*KO mice. Based on these findings we tested two different protocols that only differ on the foot shock strength used.

Previous studies that tested *Fmr1*KO mice for their performance in TFC do not agree at which stage (encoding or response to the tone in a novel-context) of the task this experimental model displays the impairment. For instance, Zhao *et al*. (2005) and Nolan, *et al*. (2017) suggested that *Fmr1*KO mice have difficulties in the acquisition of trace fear memory during the encoding session, as well as in the expression of trace fear memory 24 hours later [137,204]. Hayashi *et al*. (2007), on the other hand, described that *Fmr1*KO mice exhibit normal memory acquisition but a significant reduction in tone-induced freezing [203]. Beyond the fact that the three publications use different methodological protocols (e.g.: number of conditioning trials and stimuli strength), the genetic background of the *Fmr1*KO mouse model might be a main raison for discrepant results since both Zhao *et al*. (2005) and Nolan, *et al*. (2017) used a FVB mouse strain, and Hayashi *et al*. (2007) used a B6 mouse strain. In fact, the genetic background has been described to play a relevant role in the way the *Fmr1*KO mouse model manifests certain phenotypes (explored in Pietropaolo, *et al*., 2011) [202,233], and our findings reinforce this notion. While Nolan, *et al*. (2017) applied a less aversive stimulus and found deficits in both learning and memory in *Fmr1*KO mice on a FVB background [204], a similar protocol ($TFC_{0.4mA}$) did not fear conditioned the *Fmr1*WT mice and did not

reproduce the same impairments in the *Fmr1*KO when applied to our B6 mouse strain model. Nevertheless, this result could be different if our experimental group was larger and balanced across genotypes (3WT *vs* 6KO). Kazdoba, *et al*. (2014) approached the possibility of phenotyping variances observed in the *Fmr1*KO mouse model reflecting the variability of FXS/ASD-related clinical symptoms, rather than only differences in procedures or genetic background. In addition, it is possible that other phenotypic aspects of FXS obscure the measurement of behaviourally expressed attention deficits. For example, *Fmr1*KO mice also exhibit novelty-related hyperactivity [234], which could lead to lower freezing scores. On other hand, freezing behaviour is only one of several means of evaluating the expression of fear. Other fear-related responses could include fear-related shivering or alterations in heart-rate, which might present differently in *Fmr1*KO and WT mice, and which would not be measured during the scoring of freezing. Lastly, *Fmr1*KO have a greater sensitivity to mild acoustic stimuli [235] and this might also complicate their expression of a test that was intended to detect alterations in attention (in this case, to acoustic stimuli).

A robust difference between *Fmr1*KO and WT mice was only achieved using the TFC paradigm when using a foot shock of 0.7mA instead of the less aversive approach (0.4mA). Both times we tested $TFC_{0.7mA}$ encoding (i.e.: when testing protocols and for the viral tracing experiment), genotype had a significant impact over conditional trials and *Fmr1*KO mice showed significantly reduced freezing time in the overall encoding session, suggesting that this mouse model has deficits in associative learning (during day1). This difference between genotypes was also observed in the novel-context session, indicating that the *Fmr1*KO mice also has deficits in memory retrieval (day2). Since the cohort used for both experimental sets was small and the second group of animals did not undergo the novel-context session, further experiments can be done to confirm if the second generation *Fmr1*KO mouse model has indeed impairments related to difficulties in the integration of multiple sources of information (needed for TFC acquisition) which might consequently impact the retrieval of the cued memory.

Shortcomings, technical limitations and further controls

Some of the individual experimental approaches employed in this project have shortcomings. For instance, undersampling of labelled presynaptic neurons is a main limitation of rabies virus-based mono-trans-synaptic tracing (reviewed in Ginger *et al*., 2013). Possible explanations are low levels of RG expression, or a possible viral tropism that affects the synaptic crossing according to its properties (strength, anatomy or molecular signature) [156]. To minimize the impact of under-sampling, the number of

labelled presynaptic neurons should be normalized to the number of starter cells (the ACC neurons transfected to express the TVA and RG molecules). Since it was not possible to use confocal imaging of our brain slices in order to count the starter cells, this important analysis was not performed – figure19 illustrates this point, showing the density of labelling and technical complexity of detecting starter cells (green nuclei and red cell body in same focal plane) within the intensely labelled network. The identification of starter cells would also be crucial to localize them and confirm if TVA and RG expression was restricted to the ACC or included portions of other medial prefrontal cortical regions – although we tested the injection site prior to start the experiments, and our tracing results, as a whole, are qualitatively and quantitatively consistent with previous descriptions of ACC inputs. In addition, our sample size is small and not balanced between experimental groups (i.e.: 2 WT *vs* 3 KO), thus impacting the power of statistical analysis. Future experiments should encompass additional control groups in which animals are stereotaxically injected with a vector expressing TVA only, or in which the animals remain on the doxycycline diet during the task (to test the leakiness of the doxycycline regulation), or are doxycycline deprived, but remain in the home cage (to identified "background" labelling). It may be also pertinent to compare our findings with the inputs into ACC neurons activated during the novel-context session the task since the neural substrates for TFC encoding and retrieval probably differ.

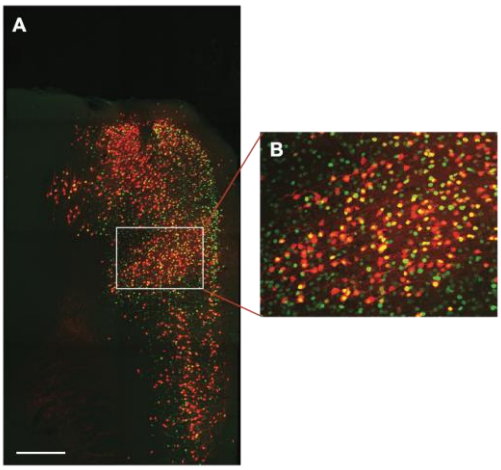

Figure 19. Visualization of starter cells in ACC. (**A**) Maximum projection derived from confocal image showing cfos (nuclear eGFP=green) expressing neurons and RABV ΔG transduced neurons (mcherry=red); (**B**) Zoom of selected region permitting starter cells visualization (identified by the presence of a yellow nucleus and red cell body). Scale = 250μm. Images were obtained with a Leica SP8 confocal microscope equipped with 20X 0.7 NA objective. Courtesy of Doctor Melanie Ginger.

Another shortcoming of our work relates to the tissue processing and mapping procedures. A better alternative to the traditional and mainly manual procedure we used to count and map the labelled neurons, are approaches that use automated light microscopy systems, namely serial block-face two-photon scanning microscopy, or tissue clearing and light-sheet fluorescence microscopy (described in *Neurocircuit Mapping and Characterization*) [178]. These methods allow the standardization and increase the throughput of mesoscopic connectivity mapping projects. Likewise, it would be interesting to integrate automated mapping approaches based on machine learning for the detection and mapping of neurons [178]. Another main challenge of brain mapping is the variability among brain atlases (e.g.: Allen Mouse Brain Atlas *vs* Paxinos and Franklin Mouse Brain Atlas) regarding the ontology of nomenclature, abbreviations and hierarchical organization of brain structures, which makes it difficult to compare data with the existing literature. In this context, it is also relevant to mentioned that the distinction between mouse ACC and MCC was estimated based on distances to bregma and landmarks referred in Vogt and Paxinos (2014). Yet, no cytoarchitectural analysis was done to confirm it.

Our pharmacogenetic manipulation of thalamic inputs to ACC were not conclusive mainly because DREADD expression occurred outside the MD. In addition to the experimental conditions (mentioned above, e.g.: serotype and volume of AAV), other technical details should have been taken in account. For instance, alternatives to CNO could also have been tested. According to Manvich *et* al. (2018) work on CNO pharmacokinetics in mice, this compound is rapidly metabolized to clozapine, which more easily converts into NDMC (N-desmethylclozapine) than into CNO again [236]. Both CNO metabolites have been related with off-target/interoceptive effects on behaviour or locomotion [236,237], for example. To detect these non-specific effects and verify CNO efficacy, an additional control group of animals only expressing mCherry, injected with CNO, should also be included [232]. In addition, excitatory DREADDs depolarize the neurons, without evoking action potentials, per se [186,232], and , since synaptic drive is still required for the neuron to fire, this may have not be enough to compensate the circuit deficits observed in the *Fmr1*KO mice. Optogenetic approaches, for instance, can lead to a more robust neural activity with higher spatial-temporal resolution [238]. In contrast, DREADD technology allows longer periods of neural activity modulation (from minutes to hours) without the risk of photo-toxicity [158,197,232]. Optogenetics also represent a more intrusive method since it additionally requires the surgical brain implantation of systems to delivery light, as well as behavioural installations adapt to it [158,197]. Additionally, DREADD-based approaches might have limitations depending on which cell-type or brain area is targeted. Alternative chemogenetic approaches based

on ligand-gated ion channels (such as PSAM/PSEM) might also be tested to overcome this problem [239]. Finally, we targeted the MD-ACC pathway based on evidences of its role in several cognitive processes. Lesions in the MD thalamic nuclei are described to affect contextual fear memory [240], and significantly impair trace eyeblink conditioning [241], yet the specific contribution of MD efferents in TFC was not explored before. Thus, a good starting point would be a loss of function experiment (e.g.: DREADD-mediated inhibition of MD input into ACC on WT mice) to confirm if it interferes in TFC outcome. This experiment would also be relevant since the MD input was not the only thalamic input found altered in the *Fmr1*KO mouse in our viral tracing results, and PO or AM thalamic nuclei could have been revealed as better targets for this functional analysis. Importantly, even though these circuit differences were detected by labelling presynaptic inputs of ACC neurons engaged in TFC it does not mean that the input itself was engaged by the task. To explore the role of this circuit in trace fear conditioning in *Fmr1*KO mice, a number of other approaches might also have been used such as classical cFOS staining approaches and electrophysiological recordings in awake behaving mice.

7. CONCLUSION

Core features of ASD, namely deficits in social behaviour and communication, stereotyped and repetitive patterns of movements and restricted interests, typically coexist with multiple medical and psychiatric comorbidities. Numerous studies have contributed to the theory that neurological comorbidities might have a bigger impact in function and outcome than core symptoms alone and, therefore, are extremely relevant for the phenotypic characterization of this disorder.

In addition, clinical and preclinical evidences support the hypothesis of generalized atypical neural connectivity contributing to the neuropathobiological basis of ASD. Alterations specifically in the ACC circuitry are correlated with social, behavioural and cognitive deficits of ASD, notably in selectivity of attention. Given that alterations in connectivity may explain various phenotypic features of ASD, they have been recently considered as an ASD biomarker that can aid in early diagnosis and prognosis of children with ASD.

Due to the variable nature of these changes, as well as the different spatial scales involved, further attention is required to more precisely study changes in connectivity in ASD. The development of methodology for cell-specific neural circuit mapping and manipulation (such sophisticated viral tracing approaches and chemogenetic systems) permits the analysis of mesoscale alterations in brain connectivity in animal models of ASD. Hence, preclinical studies may allow the correlation of alterations in neural circuits with specific genetic and non-genetic risk factors, under controlled experimental conditions (thus reducing the variation present in a heterogeneous clinical population).

The present project explored the neurobiological underpinning of altered cognition (a very common comorbidity in ASD) through the analysis of ACC connectivity. Our novel experimental strategy enabled us to limit the rabies-virus mediated mono-trans-synaptic tracing to neurons that are directly presynaptic to the ACC neurons activated during the acquisition of an attention-dependent associative learning task. Analysis of the number and location of these presynaptic neurons indicates that the *Fmr1*KO mouse has alterations in the anatomical input map of this brain region. Further work is needed to establish if these circuit alterations are in fact a cause of the observed TFC deficit (see future perspectives).

Studies like this, that relate connectivity differences to concrete ASD phenotypes, may contribute to an improved understanding and stratification of this heterogeneous and complex disorder. Such changes could subsequently lead to improvement of clinical treatment response or drug design.

8. FUTURE PERSPECTIVES

The detailed examination of inputs into a specific population of ACC neurons engaged during the acquisition of TFC (the first experimental task of this project), suggests that ACC connectivity is altered in the *Fmr1*KO mouse. Yet, further analysis is need do increase the sample size, include the starter cells and pre-synaptic labelled neurons surrounding the injection site, and add controls. Given that the whole brain mapping approaches applied (i.e.: manually or using a semi-automatic software) are time-consuming and underly large inter-variability between individuals performing the analysis, we would like to integrate an automated mapping approach for the analysis of two-dimension data.

Since our pharmacogenetic approach to assess the functional consequences of ACC circuit alteration on *Fmr1*KO mice phenotype failed probably mainly due to technical reasons, it needs to be optimized. A new experimental design should include a loss-of-function approach in WT mice to prove the relevance of each altered thalamic input (i.e.: AM, MD and PO nuclei afferents to the ACC) on TFC outcome; additional controls; and previously tested experimental conditions (e.g.: thalamic nuclei stereotaxic coordinates).

Additional studies should be done to specifically identify the type of presynaptic neurons targeted, as well as their presynaptic partners (e.g.: cerebellum > MD > ACC circuit).

BIBLIOGRAPHY

1. Park HR, Lee JM, Moon HE, et al. A Short Review on the Current Understanding of Autism Spectrum Disorders. *Exp Neurobiol*. 2016;25(1):1-13.
2. Lord C, Elsabbagh M, Baird G, Veenstra-Vanderweele J. Autism Spectrum Disorder. *Lancet*. 2018. doi:10.1016/S0140-6736(18)31129-2
3. Geschwind DH. Advances in Autism. *Annu Rev Med*. 2009;60(1):367-380. doi:10.1146/annurev.med.60.053107.121225
4. Simonoff E, Pickles A, Charman T, Chandler S, Loucas T, Baird G. Psychiatric disorders in children with autism spectrum disorders: prevalence, comorbidity, and associated factors in a population-derived sample. *J Am Acad Child Adolesc Psychiatry*. 2008;47(8):921-929. doi:10.1097/CHI.0b013e318179964f
5. Matson JL, Nebel-Schwalm MS. Comorbid psychopathology with autism spectrum disorder in children: An overview. *Res Dev Disabil*. 2007;28(4):341-352. doi:10.1016/j.ridd.2005.12.004
6. Chiarotti F, Venerosi A. Epidemiology of autism spectrum disorders: A review of worldwide prevalence estimates since 2014. *Brain Sci*. 2020;10(5). doi:10.3390/brainsci10050274
7. Durdon KG. Autism Risk Factors: genes, environmental, and gene-environmental interactions. *Occup Med Oxford Engl*. 2008;21(2):198-207. doi:10.1007/978-0-387-76495-5_19
8. Courchesne E, Pierce K. Why the frontal cortex in autism might be talking only to itself : local over-connectivity but long-distance disconnection. *Curr Opin Neurobiol*. 2005:225-230. doi:10.1016/j.conb.2005.03.001
9. Testa-silva G, Loebel A, Giugliano M, Kock CPJ De. Hyperconnectivity and Slow Synapses during Early Development of Medial Prefrontal Cortex in a Mouse Model for Mental Retardation and Autism. *Cereb Cortex*. 2013;22(6):1333-1342. doi:10.1093/cercor/bhr224.Hyperconnectivity
10. Belmonte MK. Autism and Abnormal Development of Brain Connectivity. *J Neurosci*. 2004;24(42):9228-9231. doi:10.1523/JNEUROSCI.3340-04.2004
11. Dalley JW, Cardinal RN, Robbins TW. Prefrontal executive and cognitive functions in rodents: Neural and neurochemical substrates. *Neurosci Biobehav Rev*. 2004;28(7):771-784. doi:10.1016/j.neubiorev.2004.09.006
12. Swanson LW, Hahn JD, Sporns O. Organizing principles for the cerebral cortex network of commissural and association connections. *Proc Natl Acad Sci*. 2017;114(45):E9692-E9701. doi:10.1073/pnas.1712928114
13. Fuster JM. *The Prefrontal Cortex*. 5th ed. Elsevier; 2015.

https://books.google.pt/books?hl=pt-PT&lr=&id=-8-cBAAAQBAJ&oi=fnd&pg=PP1&dq=prefrontal+cortex&ots=9myXUBOLhE&sig=l83GNf2oiV4oRxtR1-b1la8486g&redir_esc=y#v=onepage&q=prefrontal cortex&f=false.

14. Krueger DD, Osterweil EK, Chen SP, Tye LD, Bear MF. Cognitive dysfunction and prefrontal synaptic abnormalities in a mouse model of fragile X syndrome. *Proc Natl Acad Sci*. 2011;108(6). doi:10.1073/pnas.1013855108
15. Haberl MG, Zerbi V, Veltien A, Ginger M, Heerschap A, Frick A. Structural-functional connectivity deficits of neocortical circuits in the Fmr1 − / y mouse model of autism. *Sci Adv*. 2015;(November).
16. Simms ML, Kemper TL, Timbie CM, Bauman ML, Blatt GJ. The anterior cingulate cortex in autism: Heterogeneity of qualitative and quantitative cytoarchitectonic features suggests possible subgroups. *Acta Neuropathol*. 2009;118(5):673-684. doi:10.1007/s00401-009-0568-2
17. Zhou Y, Shi L, Cui X, Wang S, Luo X. Functional Connectivity of the Caudal Anterior Cingulate Cortex Is Decreased in Autism. *PLoS One*. 2016;11(3):e0151879. doi:10.1371/journal.pone.0151879
18. Chan AS, Han YMY, Leung WWM, Leung C, Wong VCN, Cheung MC. Abnormalities in the anterior cingulate cortex associated with attentional and inhibitory control deficits: A neurophysiological study on children with autism spectrum disorders. *Res Autism Spectr Disord*. 2011;5(1):254-266. doi:10.1016/j.rasd.2010.04.007
19. Dichter GS, Felder JN, Bodfish JW. Autism is characterized by dorsal anterior cingulate hyperactivation during social target detection. *Soc Cogn Affect Neurosci*. 2009;4(3):215-226. doi:10.1093/scan/nsp017
20. Thakkar KN, Polli FE, Joseph RM, et al. Response monitoring, repetitive behaviour and anterior cingulate abnormalities in autism spectrum disorders (ASD). *Brain*. 2008;131(9):2464-2478. doi:10.1093/brain/awn099
21. American Psychiatric Association. *Diagnostic and Statistical Manual of Mental Disorders*. 5th ed. Arlington; 2013.
22. Vasa RA, Mostofsky SH, Ewen JB. The Disrupted Connectivity Hypothesis of Autism Spectrum Disorders: Time for the Next Phase in Research. *Biol Psychiatry Cogn Neurosci Neuroimaging*. 2016;1(3):245-252. doi:10.1016/j.bpsc.2016.02.003
23. DiCicco-Bloom E, Lord C, Zwaigenbaum L, et al. The Developmental Neurobiology of Autism Spectrum Disorder. *J Neurosci*. 2006;26(26):6897-6906. doi:10.1523/JNEUROSCI.1712-06.2006

24. Parliament E, Action EC. Autism Spectrum Disorders in the European Union (ASDEU). 2018.
25. Baio J, Wiggins L, Christensen DL, et al. Prevalence of Autism Spectrum Disorders Among Children Aged 8 Years. *MMWR Surveill Summ*. 2018;67(6):1-25. doi:10.15585/mmwr.ss6706a1
26. Krishnan MC. Sex differences in autism spectrum disorder. *Complex Autism Spectr Disord*. 2018;26(2):69-86. doi:10.4324/9780429454646
27. Geschwind DH, State MW. Gene hunting in autism spectrum disorder: On the path to precision medicine. *Lancet Neurol*. 2015;14(11):1109-1120. doi:10.1016/S1474-4422(15)00044-7
28. Geschwind DH. Autism: Many Genes, Common Pathways? *Cell*. 2008;135(3):391-395. doi:10.1016/j.cell.2008.10.016
29. Huguet G, Ey E, Bourgeron T. The genetic landscape of autism spectrum disorders. *Dev Med Child Neurol*. 2014;56(1):12-18. doi:10.1111/dmcn.12278
30. Amaral DG. Examining the Causes of Autism. *Cerebrum*. 2017.
31. Muhle RA, Reed HE, Stratigos KA, Veenstra-VanderWeele J. The emerging clinical neuroscience of autism spectrum disorder a review. *JAMA Psychiatry*. 2018;75(5):514-523. doi:10.1001/jamapsychiatry.2017.4685
32. Alonso-Gonzalez A, Rodriguez-Fontenla C, Carracedo A. De novo mutations (DNMs) in autism spectrum disorder (ASD): Pathway and network analysis. *Front Genet*. 2018;9(SEP). doi:10.3389/fgene.2018.00406
33. De Rubeis S, He X, Goldberg AP, et al. Synaptic, transcriptional and chromatin genes disrupted in autism. *Nature*. 2014;515(7526):209-215. doi:10.1038/nature13772
34. Li X, Zou H, Brown WT. Genes associated with autism spectrum disorder. *Brain Res Bull*. 2012;88(6):543-552. doi:10.1016/j.brainresbull.2012.05.017
35. Yoo H. Genetics of Autism Spectrum Disorder: Current Status and Possible Clinical Applications. *Exp Neurobiol*. 2015;24(4):257. doi:10.5607/en.2015.24.4.257
36. Gross C, Hoffmann A, Bassell GJ, Berry-Kravis EM. Therapeutic Strategies in Fragile X Syndrome: From Bench to Bedside and Back. *Neurotherapeutics*. 2015;12(3):584-608. doi:10.1007/s13311-015-0355-9
37. Pirone A, Alexander JM, Koenig JB, et al. Social Stimulus Causes Aberrant Activation of the Medial Prefrontal Cortex in a Mouse Model With Autism-Like Behaviors. *Front Synaptic Neurosci*. 2018;10(October):1-10. doi:10.3389/fnsyn.2018.00035
38. O'Roak BJ, Deriziotis P, Lee C, et al. Multiplex Targeted Sequencing Identifies

Recurrently Mutated Genes in Autism Spectrum Disorder. *Nat Genet*. 2011;43(6):585-589. doi:10.1038/ng.835

39. Larsen E, Menashe I, Ziats MN, Pereanu W, Packer A, Banerjee-Basu S. A systematic variant annotation approach for ranking genes associated with autism spectrum disorders. *Mol Autism*. 2016;7(1):1-8. doi:10.1186/s13229-016-0103-y
40. He X, Sanders SJ, Liu L, et al. Integrated Model of De Novo and Inherited Genetic Variants Yields Greater Power to Identify Risk Genes. *PLoS Genet*. 2013;9(8). doi:10.1371/journal.pgen.1003671
41. SFARI. Criteria - SFARI Gene. https://gene.sfari.org/about-gene-scoring/criteria/. Accessed July 23, 2019.
42. Karimi P, Kamali E, Mousavi SM. Environmental factors influencing the risk of autism. *J Res Med Sci*. 2017:22-27. doi:10.4103/1735-1995.200272
43. Akshoomoff N, Pierce K, Courchesne E. The neurobiological basis of autism from a developmental perspective. *Dev Psychopathol*. 2002;14(3):613-634. doi:10.1017/s0954579402003115
44. Varghese M, Keshav N, Jacot-Descombes S, Warda T, Wicinski B, Dickstein DL. Autism Spectrum Disorder: Neuropathology and animal models. *Acta Neuropathol*. 2017;134:537-566. doi:1doi:10.1007/s00401-017-1736-4
45. Nancy J. Minshew; Diane L. Williams. The New Neurobiology of Autism. *Neurol Rev*. 2012;64(7):945-950. doi:10.1001/archneur.64.7.945.The
46. Zikopoulos B, Barbas H. Altered neural connectivity in excitatory and inhibitory cortical circuits in autism. *Front Hum Neurosci*. 2013;7(September):1-24. doi:10.3389/fnhum.2013.00609
47. Courchesne E, Campbell K, Solso S. Brain growth across the life span in autism: Age-specific changes in anatomical pathology. *Brain Res*. 2011;1380:138-145. doi:10.1016/j.brainres.2010.09.101
48. Herbert MR, Ziegler DA, Deutsch CK, et al. Dissociations of cerebral cortex, subcortical and cerebral white matter volumes in autistic boys. *Brain*. 2003;126(5):1182-1192. doi:10.1093/brain/awg110
49. Casanova MF, Buxhoeveden DP, Switala AE, Roy E. Minicolumnar pathology in autism. *Neurology*. 2002;58(3):428-432. doi:10.1212/WNL.58.3.428
50. Rubenstein J, Merzenich M. Model of autism: increased ratio of excitation/inhibition in key neural systems. *Genes Brain Behav*. 2003;2(5):255-267. doi:10.1046/j.1601-183X.2003.00037.x
51. Ben-Ari Y, Woodin M, Sernagor E, et al. Refuting the challenges of the developmental shift of polarity of GABA actions: GABA more exciting than ever! *Front Cell Neurosci*. 2012;6(JULY 2012):1-18. doi:10.3389/fncel.2012.00035

52. Nelson SB, Valakh V. Excitatory/Inhibitory balance and circuit homeostasis in Autism Spectrum Disorders A theory of excitatory/inhibitory imbalance in Autism HHS Public Access. *Neuron*. 2015;87(4):684-698. doi:10.1016/j.neuron.2015.07.033
53. Yizhar O, Fenno LE, Prigge M, Schneider F, Davidson T. Neocortical excitation/inhibition balance in information processing and social dysfunction. *Nature*. 2011;477(7363):171-178. doi:10.1038/nature10360
54. El Idrissi A, Ding XH, Scalia J, Trenkner E, Brown WT, Dobkin C. Decreased GABAA receptor expression in the seizure-prone fragile X mouse. *Neurosci Lett*. 2005;377(3):141-146. doi:10.1016/j.neulet.2004.11.087
55. Gibson JR, Bartley AF, Hays SA, Huber KM. Imbalance of neocortical excitation and inhibition and altered UP states reflect network hyperexcitability in the mouse model of fragile X syndrome. *J Neurophysiol*. 2008;100(5):2615-2626. doi:10.1152/jn.90752.2008
56. Gogolla N, Takesian A, Feng G, Fagiolini M, Hensch T. Sensory integration in mouse incular cortex reflects GABA circuit maturation. *Neuron*. 2014;83(4):894-905. doi:10.1016/j.neuron.2014.06.033.Sensory
57. Peñagarikano O, Abrahams BS, Herman EI, et al. Absence of CNTNAP2 leads to epilepsy, neuronal migration abnormalities, and core autism-related deficits. *Cell*. 2011;147(1):235-246. doi:10.1016/j.cell.2011.08.040
58. Hashemi E, Ariza J, Rogers H, Noctor SC, Martínez-Cerdeño V. The Number of Parvalbumin-Expressing Interneurons Is Decreased in the Medial Prefrontal Cortex in Autism. *Cereb cortex*. 2017;27(3):1931-1943. doi:10.1093/cercor/bhw021
59. Stoodley CJ. The Cerebellum and Neurodevelopmental Disorders. *Cerebellum*. 2016;15(1):34-37. doi:10.1007/s12311-015-0715-3
60. Rogers TD, McKimm E, Dickson PE, Goldowitz D, Blaha CD, Mittleman G. Is autism a disease of the cerebellum? An integration of clinical and pre-clinical research. *Front Syst Neurosci*. 2013;7(May):1-16. doi:10.3389/fnsys.2013.00015
61. Geschwind DH, Levitt P. Autism spectrum disorders: developmental disconnection syndromes. *Curr Opin Neurobiol*. 2007;17(1):103-111. doi:10.1016/j.conb.2007.01.009
62. Zerbi V, Ielacqua GD, Markicevic M, et al. Dysfunctional autism risk genes cause circuit-specific connectivity deficits with distinct developmental trajectories. *Cereb Cortex*. 2018;28(7):2495-2506. doi:10.1093/cercor/bhy046
63. Liska A, Gozzi A. Can mouse imaging studies bring order to autism connectivity chaos? *Front Neurosci*. 2016;10(NOV):1-8. doi:10.3389/fnins.2016.00484

64. D'Albis MA, Guevara P, Guevara M, et al. Local structural connectivity is associated with social cognition in autism spectrum disorder. *Brain*. 2018;141(12):3472-3481. doi:10.1093/brain/awy275
65. Di Martino A, Kelly C, Grzadzinski R, Zuo X-N, Mennes M, Mairena MA. Aberrant Striatal Functional Connectivity in Children with Autism. *Biol Psychiatry*. 2011;69(9):847-856. doi:doi:10.1016/j.biopsych.2010.10.029
66. Nair A, Carper RA, Abbott AE, et al. Regional Specificity of Aberrant Thalamocortical Connectivity in Autism. *Hum Brain Mapp*. 2015;36(11):4497-3511. doi:doi:10.1002/hbm.22938
67. Dajani DR, Uddin LQ. Local brain connectivity across development in autism spectrum disorder: A cross-sectional investigation. *Autism Res*. 2016;9(1):43-54. doi:10.1002/aur.1494
68. Paakki JJ, Rahko J, Long X, et al. Alterations in regional homogeneity of resting-state brain activity in autism spectrum disorders. *Brain Res*. 2010;1321:169-179. doi:10.1016/j.brainres.2009.12.081
69. O'Reilly C, Lewis JD, Elsabbagh M. Is functional brain connectivity atypical in autism? A systematic review of EEG and MEG studies. *PLoS One*. 2017;12(5):1-28. doi:10.1371/journal.pone.0175870
70. Strimbu K, Tavel JA. What are Biomarkers? *Curr Opin HIV AIDS*. 2010;5(6):463-466. doi:10.1097/COH.0b013e32833ed177
71. Del Valle Rubido M, McCracken JT, Hollander E, et al. In Search of Biomarkers for Autism Spectrum Disorder. *Autism Res*. 2018;11(11):1567-1579. doi:10.1002/aur.2026
72. Beversdorf DQ. Phenotyping, Etiological Factors, and Biomarkers: Toward Precision Medicine in Autism Spectrum Disorders. *J Dev Behav Pediatr*. 2016;37(8):659-673. doi:10.1097/DBP.0000000000000351
73. Ruggeri B, Sarkans U, Schumann G, Persico AM. Biomarkers in autism spectrum disorder: The old and the new. *Psychopharmacology (Berl)*. 2014;231(6):1201-1216. doi:10.1007/s00213-013-3290-7
74. Goldani AA, Downs SR, Widjaja F, Lawton B. Biomarkers in autism. *Int J PharmTech Res*. 2014;3(3):1281-1289. doi:10.3389/fpsyt.2014.00100
75. Ellegood J, Anagnostou E, Babineau BA, et al. Clustering autism: Using neuroanatomical differences in 26 mouse models to gain insight into the heterogeneity. *Mol Psychiatry*. 2015;20(1):118-125. doi:10.1038/mp.2014.98
76. Orekhova E V, Elsabbagh M, Jones EJ, Dawson G, Charman T, Johnson MH. EEG hyper-connectivity in high-risk infants is associated with later autism. *J Neurodev Disord*. 2014;6(1):1-11. doi:10.1186/1866-1955-6-40

77. Buckley AW, Scott R, Tyler A, et al. State-Dependent Differences in Functional Connectivity in Young Children With Autism Spectrum Disorder. *EBioMedicine*. 2015;2(12):1905-1915. doi:10.1016/j.ebiom.2015.11.004
78. Keown CL, Shih P, Nair A, Peterson N, Mulvey ME, Müller RA. Local functional overconnectivity in posterior brain regions is associated with symptom severity in autism spectrum disorders. *Cell Rep*. 2013;5(3):567-572. doi:10.1016/j.celrep.2013.10.003
79. Anderson JS, Nielsen JA, Froehlich AL, et al. Functional connectivity magnetic resonance imaging classification of autism. *Brain*. 2011;134(12):3739-3751. doi:10.1093/brain/awr263
80. Freitas BCG, Trujillo CA, Carromeu C, Yusupova M, Herai RH, Muotri AR. Stem cells and modeling of autism spectrum disorders. *Exp Neurol*. 2014;260(858):33-43. doi:10.1016/j.expneurol.2012.09.017
81. Yi F, Danko T, Botello SC, et al. Autism-Associated SHANK3 Haploinsufficiency Causes IhChannelopathy in Human Neurons. *Science (80-)*. 2016;352(6286):1-24. doi:10.1126/science.aaf2669
82. Chan WK, Griffiths R, Price DJ, Mason JO. Cerebral organoids as tools to identify the developmental roots of autism. *Mol Autism*. 2020;11(1):1-14. doi:10.1186/s13229-020-00360-3
83. Qian X, Song H, Ming GL. Brain organoids: Advances, applications and challenges. *Dev*. 2019;146(8). doi:10.1242/dev.166074
84. van der Staay FJ, Arndt SS, Nordquist RE. Evaluation of animal models of neurobehavioral disorders. *Behav Brain Funct*. 2009;5:1-23. doi:10.1186/1744-9081-5-11
85. Meshalkina DA, N. Kizlyk M, V. Kysil E, et al. Zebrafish models of autism spectrum disorder. *Exp Neurol*. 2018;299:207-216. doi:10.1016/j.expneurol.2017.02.004
86. Patel J, Lukkes JL, Shekhar A. *Overview of Genetic Models of Autism Spectrum Disorders*. Vol 241. 1st ed. Elsevier B.V.; 2018. doi:10.1016/bs.pbr.2018.10.002
87. Tian Y, Zhang ZC, Han J. Drosophila Studies on Autism Spectrum Disorders. *Neurosci Bull*. 2017;33(6):737-746. doi:10.1007/s12264-017-0166-6
88. Coll-Tané M, Krebbers A, Castells-Nobau A, Zweier C, Schenck A. Intellectual disability and autism spectrum disorders ‘on the fly’: insights from *Drosophila*. *Dis Model Mech*. 2019;12(5):dmm039180. doi:10.1242/dmm.039180
89. Zhao H, Jiang YH, Zhang YQ. Modeling autism in non-human primates: Opportunities and challenges. *Autism Res*. 2018;11(5):686-694. doi:10.1002/aur.1945

90. Perlman RL. Mouse Models of Human Disease: An Evolutionary Perspective. *Evol Med Public Heal*. 2016:eow014. doi:10.1093/emph/eow014
91. Shinoda Y, Sadakata T, Furuichi T. Animal Models of Autism Spectrum Disorder (ASD): A Synaptic-Level Approach to Autistic-Like Behavior in Mice. *Exp Anim*. 2013;62(2):71-78. doi:10.1538/expanim.62.71
92. Hutsler JJ, Zhang H. Increased dendritic spine densities on cortical projection neurons in autism spectrum disorders. *Brain Res*. 2010;1309:83-94. doi:10.1016/j.brainres.2009.09.120
93. Ajram LA, Horder J, Mendez MA, et al. Shifting brain inhibitory balance and connectivity of the prefrontal cortex of adults with autism spectrum disorder. *Transl Psychiatry*. 2017;7(5):e1137. doi:10.1038/tp.2017.104
94. Martínez-Cerdeño V. Dendrite and spine modifications in autism and related neurodevelopmental disorders in patients and animal models. *Dev Neurobiol*. 2017;77(4):393-404. doi:10.1002/dneu.22417
95. Bernardet M, Crusio WE. Fmr1 KO mice as a possible model of autistic features. *ScientificWorldJournal*. 2006;6:1164-1176. doi:10.1100/tsw.2006.220
96. Ey E, Leblond CS, Bourgeron T. Behavioral profiles of mouse models for autism spectrum disorders. *Autism Res*. 2011;4(1):5-16. doi:10.1002/aur.175
97. Ellegood J, Pacey LK, Hampson DR, Lerch JP, Henkelman RM. Anatomical phenotyping in a mouse model of fragile X syndrome with magnetic resonance imaging. *Neuroimage*. 2010;53(3):1023-1029. doi:10.1016/j.neuroimage.2010.03.038
98. Bromley RL, Mawer G, Clayton-Smith J, Baker GA. Autism spectrum disorders following in utero exposure to antiepileptic drugs. *Neurology*. 2008;73(12):1923-1924. doi:10.1212/WNL.0b013e3181af0b95
99. Jakob Christensen et al. Prenatal Valproate Exposure and Risk of Autism Spectrum Disorders and Childhood Autism. 2015;309(16):1696-1703. doi:10.1001/jama.2013.2270.Prenatal
100. Braunschweig D, Ashwood P, Krakowiak P, et al. Autism: Maternally derived antibodies specific for fetal brain proteins. *Neurotoxicology*. 2008;29(2):226-231. doi:10.1016/j.neuro.2007.10.010
101. Singer HS, Morris CM, Gause CD, Gillin PK, Crawford S, Zimmerman AW. Antibodies against fetal brain in sera of mothers with autistic children. *J Neuroimmunol*. 2008;194(1-2):165-172. doi:10.1016/j.jneuroim.2007.11.004
102. Martínez-Cerdeño V, Camacho J, Fox E, et al. Prenatal Exposure to Autism-Specific Maternal Autoantibodies Alters Proliferation of Cortical Neural Precursor Cells, Enlarges Brain, and Increases Neuronal Size in Adult Animals. *Cereb*

Cortex. 2016;26(1):374-383. doi:10.1093/cercor/bhu291

103. Atladóttir HÓ, Thorsen P, Østergaard L, et al. Maternal infection requiring hospitalization during pregnancy and autism spectrum disorders. *J Autism Dev Disord*. 2010;40(12):1423-1430. doi:10.1007/s10803-010-1006-y
104. Zerbo O, Iosif AM, Walker C, Ozonoff S, Hansen RL, Hertz-Picciotto I. Is Maternal Influenza or Fever during Pregnancy Associated with Autism or Developmental Delays? Results from the CHARGE (childhood Autism Risks from Genetics and Environment) Study. *J Autism Dev Disord*. 2013;43(1):25-33. doi:10.1007/s10803-012-1540-x
105. Crawley JN. Designing mouse behavioral tasks relevant to autistic-like behaviors. *Ment Retard Dev Disabil Res Rev*. 2004;10(4):248-258. doi:10.1002/mrdd.20039
106. DiCicco-Bloom E. International Journal of Developmental Neuroscience: Preface. *Int J Dev Neurosci*. 2005;23(2-3 SPEC. ISS.):117-124. doi:10.1016/j.ijdevneu.2005.01.004
107. Winslow JT, Insel TR. The social deficits of the oxytocin knockout mouse. *Neuropeptides*. 2002;36(2-3):221-229. doi:10.1054/npep.2002.0909
108. Wrenn CC, Harris AP, Saavedra MC, Crawley JN. Social transmission of food preference in mice: Methodology and application to galanin-overexpressing transgenic mice. *Behav Neurosci*. 2003;117(1):21-31. doi:10.1037/0735-7044.117.1.21
109. Blanchard DC, Griebel G, Blanchard RJ. The Mouse Defense Test Battery: Pharmacological and behavioral assays for anxiety and panic. *Eur J Pharmacol*. 2003;463(1-3):97-116. doi:10.1016/S0014-2999(03)01276-7
110. Petrulis A, Alvarez P, Eichenbaum H. Neural correlates of social odor recognition and the representation of individual distinctive social odors within entorhinal cortex and ventral subiculum. *Neuroscience*. 2005;130(1):259-274. doi:10.1016/j.neuroscience.2004.09.001
111. Presti MF, Watson CJ, Kennedy RT, Yang M, Lewis MH. Behavior-related alterations of striatal neurochemistry in a mouse model of stereotyped movement disorder. *Pharmacol Biochem Behav*. 2004;77(3):501-507. doi:10.1016/j.pbb.2003.12.004
112. Orefice LL, Zimmerman AL, Chirila AM, Sleboda SJ, Head JP, Ginty DD. Peripheral Mechanosensory Neuron Dysfunction Underlies Tactile and Behavioral Deficits in Mouse Models of ASDs. *Cell*. 2016;166(2):299-313. doi:10.1016/j.cell.2016.05.033
113. Sinclair D, Oranje B, Razak K, Siegel S, Schmid S. Sensory processing in

autism spectrum disorders and Fragile X syndrome - From clinic to animal models. *Neurosci Biobehav Rev*. 2017;76 (Pt B):235-253. doi:10.1016/j.neubiorev.2016.05.029.Sensory

114. Lovelace J, Ethell I, Binder D, Razak K. Translation-relevant EEG phenotypes in a mouse model of Fragile X Syndrome. *Neurobiol Dis*. 2018;115:39-48. doi:doi:10.1016/j.nbd.2018.03.012
115. Wen T, Lovelace J, Ethell I, Binder D. Developmental changes in EEG phenotypes in a mouse model of Fragile X Syndrome. *Neuroscience*. 2019;398:136-143. doi:10.1016/j.neuroscience.2018.11.047.Developmental
116. Modi ME, Sahin M. Translational use of event-related potentials to assess circuit integrity in ASD. *Nat Rev Neurol*. 2017;13(3):160-170. doi:10.1038/nrneurol.2017.15
117. Oddi D, Subashi E, Middei S, et al. Early Social Enrichment Rescues Adult Behavioral and Brain Abnormalities in a Mouse Model of Fragile X Syndrome. *Neuropsychopharmacology*. 2015;40:1113-1122. doi:10.1038/npp.2014.291
118. Fuster JM. The prefrontal cortex - An update: Time is of the essence. *Neuron*. 2001;30(2):319-333. doi:10.1016/S0896-6273(01)00285-9
119. Heidbreder CA, Groenewegen HJ. The medial prefrontal cortex in the rat: Evidence for a dorso-ventral distinction based upon functional and anatomical characteristics. *Neurosci Biobehav Rev*. 2003;27(6):555-579. doi:10.1016/j.neubiorev.2003.09.003
120. Carlén M. What constitutes the prefrontal cortex? *Science (80-)*. 2017;358(6362):478-482. doi:10.1126/science.aan8868
121. Laubach M, Amarante LM, Swanson K, White SR. What, If Anything, Is Rodent Prefrontal Cortex? *eNeuro*. 2018;5(5).
122. Vogt BA, Paxinos G. Cytoarchitecture of mouse and rat cingulate cortex with human homologies. *Brain Struct Funct*. 2014;219(1):185-192. doi:10.1007/s00429-012-0493-3
123. Gehring WJ, Knight RT. Prefrontal-cingulate interactions in action monitoring. 2000;3(5):1-5.
124. Ito S, Ito S, Stuphorn V, Brown JW, Schall JD. Performance Monitoring by the Anterior Cingulate Cortex During Saccade Countermanding. *Science*. 2011;120(2003):120-122. doi:10.1126/science.1087847
125. Han CJ, Tuathaigh CMO, Trigt L Van, et al. Trace but not delay fear conditioning requires attention and the anterior cingulate cortex. *Proc Natl Acad Sci*. 2003;100(22):13087-13092. doi:10.1073/pnas.2132313100
126. Fillinger C, Yalcin I, Barrot M, Veinante P. Afferents to anterior cingulate areas

24a and 24b and midcingulate areas 24a′ and 24b′ in the mouse. *Brain Struct Funct*. 2017;222(3):1509-1532. doi:10.1007/s00429-016-1290-1

127. Hoover WB, Vertes RP. Anatomical analysis of afferent projections to the medial prefrontal cortex in the rat. *Brain struct Funct*. 2007;212:149-179.
128. Riga D, Matos MR, Glas A, Smit AB, Spijker S, Van den Oever MC. Optogenetic dissection of medial prefrontal cortex circuitry. *Front Syst Neurosci*. 2014;8(DEC):1-19. doi:10.3389/fnsys.2014.00230
129. Reep RL, Corwin J V., King V. Neuronal connections of orbital cortex in rats: Topography of cortical and thalamic afferents. *Exp Brain Res*. 1996;111(2):215-232. doi:10.1007/BF00227299
130. Barthas F, Kwan AC. Secondary motor cortex: where “sensory” meets “motor” in the rodent frontal cortex. *Trends Neurosci*. 2017;40(3):181-193. doi:10.1016/j.tins.2016.11.006
131. Kolb B, Mychasiuk R, Muhammad A, Li Y, Frost DO, Gibb R. Experience and the developing prefrontal cortex. *Proc Natl Acad Sci*. 2012;109(Supplement_2):17186-17193. doi:10.1073/pnas.1121251109
132. Bailey A, Luthert P, Dean A, et al. A clinicopathological study of autism. *Brain*. 1998;121(5):889-905. doi:10.1093/brain/121.5.889
133. Kemper TL, Bauman ML. Neuropathology of infantile autism. *Mol Psychiatry*. 2002;7:12-13. doi:10.1038/sj.mp.4001165
134. Zikopoulos B, Barbas H. Changes in Prefrontal Axons May Disrupt the Network in Autism. *J Neurosci*. 2010;30(44):14595-14609. doi:10.1523/jneurosci.2257-10.2010
135. Koga K, Liu MG, Qiu S, et al. Impaired presynaptic long-term potentiation in the anterior cingulate cortex of Fmr1 knock-out mice. *J Neurosci*. 2015;35(5):2033-2043. doi:10.1523/JNEUROSCI.2644-14.2015
136. Xu Z hui, Yang Q, Ma L, et al. Deficits in LTP Induction by 5-HT2A Receptor Antagonist in a Mouse Model for Fragile X Syndrome. *PLoS One*. 2012;7(10):3-8. doi:10.1371/journal.pone.0048741
137. Zhao M, Toyoda H, Ko SW, Ding H, Wu L, Zhuo M. Deficits in Trace Fear Memory and Long-Term Potentiation in a Mouse Model for Fragile X Syndrome. *J Neurosci*. 2005;25(32):7385-7392. doi:10.1523/JNEUROSCI.1520-05.2005
138. Vargas DL, Nascimbene C, Krishnan C, Zimmerman AW, Pardo CA. Neuroglial activation and neuroinflammation in the brain of patients with autism. *Ann Neurol*. 2005;57(1):67-81. doi:10.1002/ana.20315
139. Murphy DGM, Daly E, Schmitz N, et al. Cortical serotonin 5-HT2A receptor binding and social communication in adults with Asperger’s syndrome: An in vivo

SPECT study. *Am J Psychiatry*. 2006;163(5):934-936. doi:10.1176/ajp.2006.163.5.934

140. Haznedar MM, Buchsbaum MS, Wei TC, et al. Limbic circuitry in patients with autism spectrum disorders studied with positron emission tomography and magnetic resonance imaging. *Am J Psychiatry*. 2000;157(12):1994-2001. doi:10.1176/appi.ajp.157.12.1994
141. Kennedy DP, Redcay E, Courchesne E. Failing to deactivate: Resting functional abnormalities in autism. *Proc Natl Acad Sci*. 2006;103(21):8275-8280. doi:10.1073/pnas.0600674103
142. Medalla M, Barbas H. Specialized prefrontal "auditory fields": Organization of primate prefrontal-temporal pathways. *Front Neurosci*. 2014;8(8 APR):1-15. doi:10.3389/fnins.2014.00077
143. Ghashghaei H, Hilgetag C, Babas H. Sequence of information processing for emotions based on the anatomic dialogue between prefrontal cortex and amygdala. *Neuroimage*. 2007;34(3):905-923.
144. Kana RK, Keller TA, Minshew NJ, Just MA. Inhibitory Control in High-Functioning Autism: Decreased Activation and Underconnectivity in Inhibition Networks. *Biol Psychiatry*. 2007;62(3):198-206. doi:10.1016/j.biopsych.2006.08.004
145. Tanji J, Hoshi E. Role of the Lateral Prefrontal Cortex in Executive Behavioral Control. *Physiol Rev*. 2008;88(1):37-57. doi:10.1152/physrev.00014.2007
146. Huang W, Chen Y, Page DT. Hyperconnectivity of prefrontal cortex to amygdala projections in a mouse model of macrocephaly / autism syndrome. *Nat Commun*. 2016;7:1-15. doi:10.1038/ncomms13421
147. Shofty B, Bergmann E, Zur G, et al. Loss of function in the autism and learning disabilities associated gene Nf1 disrupts corticocortical and corticostriatal functional connectivity in human and mouse. *bioRxiv*. 2019:618223. doi:10.1101/618223
148. Bertero A, Liska A, Pagani M, et al. Autism-associated 16p11.2 microdeletion impairs prefrontal functional connectivity in mouse and human. *Brain*. 2018;141(7):2055-2065. doi:10.1093/brain/awy111
149. Rinaldi T. Hyper-connectivity and hyper-plasticity in the medial prefrontal cortex in the valproic acid animal model of autism. *Front Neural Circuits*. 2008;2(October):1-7. doi:10.3389/neuro.04.004.2008
150. Smith SM. The future of FMRI connectivity. *Neuroimage*. 2012;62(2):1257-1266. doi:10.1016/j.neuroimage.2012.01.022
151. Jonckers E, Shah D, Hamaide J, Verhoye M, Van der Linden A. The power of

using functional fMRI on small rodents to study brain pharmacology and disease. *Front Pharmacol*. 2015;6(OCT):1-19. doi:10.3389/fphar.2015.00231

152. Harris AP, Lennen RJ, Marshall I, et al. Imaging learned fear circuitry in awake mice using fMRI. *Eur J Neurosci*. 2015;42(5):2125-2134. doi:10.1111/ejn.12939
153. Dum RP, Strick PL. Transneuronal tracing with neurotropic viruses reveals network macroarchitecture. *Curr Opin Neurobiol*. 2013;23(2):245-249. doi:10.1038/jid.2014.371
154. Ugolini G. Advances in viral transneuronal tracing. *J Neurosci Methods*. 2010;194(1):2-20. doi:10.1016/j.jneumeth.2009.12.001
155. Morecraft RJ, Ugolini G, Lanciego JL, Wouterlood FGG, Pandya DN. *Classic and Contemporary Neural Tract-Tracing Techniques*. Elsevier Inc.; 2013. doi:10.1016/B978-0-12-396460-1.00017-2
156. Ginger M, Haberl M, Conzelmann K-K, Schwarz MK, Frick A. Revealing the secrets of neuronal circuits with recombinant rabies virus technology. *Front Neural Circuits*. 2013;7(January):1-15. doi:10.3389/fncir.2013.00002
157. Ekstrand MI, Enquist LW, Pomeranz LE. The alpha-herpesviruses: molecular pathfinders in nervous system circuits. *Trends Mol Med*. 2008;14(3):134-140. doi:10.1016/j.molmed.2007.12.008
158. Luo L, Callaway EM, Svoboda K. Genetic Dissection of Neural Circuits: A Decade of Progress. *Neuron*. 2018;98(2):256-281. doi:10.1016/j.neuron.2018.03.040
159. Tervo G, Huang B-Y, Viswanathan S, Gaj T, Lavzin M. A designer AAV variant permits efficient retrograde access to projection neurons. *Neuron*. 2016;92(2):372-382. doi:110.1016/j.neuron.2016.09.021
160. Ruigrok TJH, van Touw S, Coulon P. Caveats in Transneuronal Tracing with Unmodified Rabies Virus: An Evaluation of Aberrant Results Using a Nearly Perfect Tracing Technique. *Front Neural Circuits*. 2016;10(July):1-19. doi:10.3389/fncir.2016.00046
161. Wickersham IR, Lyon DC, Barnard RJO, et al. Monosynaptic Restriction of Transsynaptic Tracing from Single, Genetically Targeted Neurons. *Neuron*. 2007;53(5):639-647. doi:10.1016/j.neuron.2007.01.033
162. Dodt HU, Leischner U, Schierloh A, et al. Ultramicroscopy: Three-dimensional visualization of neuronal networks in the whole mouse brain. *Nat Methods*. 2007;4(4):331-336. doi:10.1038/nmeth1036
163. Hama H, Kurokawa H, Kawano H, et al. Scale: A chemical approach for fluorescence imaging and reconstruction of transparent mouse brain. *Nat Neurosci*. 2011;14(11):1481-1488. doi:10.1038/nn.2928

164. Miyamichi K, Amat F, Moussavi F, et al. Cortical representations of olfactory input by trans-synaptic tracing. *Nature*. 2011;472(7342):191-199. doi:10.1038/nature09714
165. Ragan T, Kadiri LR, Venkataraju KU, et al. Serial two-photon tomography for automated ex vivo mouse brain imaging. *Nat Methods*. 2012;9(3):255-258. doi:10.1038/nmeth.1854
166. Callaway EM, Luo L. Monosynaptic Circuit Tracing with Glycoprotein-Deleted Rabies Viruses. *J Neurosci*. 2015;35(24):8979-8985. doi:10.1523/jneurosci.0409-15.2015
167. Osakada F, Mori T, Cetin AH, Marshel JH, Virgen B, Callaway EM. New rabies virus variants for monitoring and manipulating activity and gene expression in defined neural circuits. *Neuron*. 2011;71(4):617-631. doi:10.1016/j.neuron.2011.07.005
168. Kumsar P. Retrograde Tracing. *Mater Methods*. 2019;9. doi://dx.doi.org/10.13070/mm.en.9.2713
169. Wall NR, Wickersham IR, Cetin A, De La Parra M, Callaway EM. Monosynaptic circuit tracing in vivo through Cre-dependent targeting and complementation of modified rabies virus. *Proc Natl Acad Sci*. 2010;107(50):21848-21853. doi:10.1073/pnas.1011756107
170. Praag H Van, Schinder AF, Christie BR, et al. Functional neurogenesis in the adult hippocampus. *2Nature*. 2002;32415:1030-1024.
171. Choi J, Callaway EM. Monosynaptic Inputs to ErbB4 Expressing Inhibitory Neurons in Mouse Primary Somatosensory Cortex. *Bone*. 2011;519(17):3402-3414. doi:doi:10.1002/cne.22680
172. Choi J, Young JAT, Callaway EM. Selective viral vector transduction of ErbB4 expressing cortical interneurons in vivo with a viral receptor-ligand bridge protein. *Proc Natl Acad Sci*. 2010;107(38):16703-16708. doi:10.1073/pnas.1006233107
173. Metzger D, Chambon P. Site- and time-specific gene targeting in the mouse. *Methods*. 2001;24(1):71-80. doi:10.1006/meth.2001.1159
174. Baron U, Bujard H. Tet Repressor-Based System for Regulated Gene Expression in Eukaryotic Cells: Principles and Advances. *Methods in enxymology*. 2000;327:401-421.
175. Kistnert A, Gossentt M, Zimmermannt F, et al. Doxycycline-mediated quantitative and tissue-specific control of gene expression in transgenic mice (tet system/genetic switch/kinetics of induction/liver-specific control). *Proc Natl Acad Sci USA*. 1996;93(October):10933-10938. doi:10.1073/pnas.93.20.10933

176. Jaisser F. Inducible gene expression and gene modification in transgenic mice. *J Am Soc Nephrol*. 2000;11 Suppl 1:S95-S100. http://www.ncbi.nlm.nih.gov/pubmed/11065338.
177. Mikula S. Progress towards mammalian whole-brain cellular connectomics. *Front Neuroanat*. 2016;10(JUNE):1-7. doi:10.3389/fnana.2016.00062
178. Osten P, Margrie TW. Mapping brain circuits with light microscope. *Nat Methods*. 2013;10(6):515-523.
179. Amato SP, Pan F, Schwartz J, Ragan TM. Whole brain imaging with serial two-photon tomography. *Front Neuroanat*. 2016;10(MAR):1-11. doi:10.3389/fnana.2016.00031
180. Perrin-Terrin AS, Jeton F, Pichon A, et al. The c-FOS protein immunohistological detection: A useful tool as a marker of central pathways involved in specific physiological responses in vivo and ex vivo. *J Vis Exp*. 2016;2016(110):1-9. doi:10.3791/53613
181. Kawashima T, Okuno H, Bito H. A new era for functional labeling of neurons: activity-dependent promoters have come of age. *Front Neural Circuits*. 2014;8(April):1-9. doi:10.3389/fncir.2014.00037
182. Liu X, Ramirez S, Pang PT, et al. Optogenetic stimulation of a hippocampal engram activates fear memory recall. *Nature*. 2012;484(7394):381-385. doi:10.1038/nature11028
183. Reijmers LG, Perkins BL, Matsuo N, Mayford M. Localization of a stable neural correlate of associative memory. *Science (80-)*. 2007;317(5842):1230-1233. doi:10.1126/science.1143839
184. Guenthner CJ, Miyamichi K, Yang HH, Heller HC, Luo L. Permanent genetic access to transiently active neurons via TRAP: Targeted recombination in active populations. *Neuron*. 2013;78(5):773-784. doi:10.1016/j.neuron.2013.03.025
185. Alexander GM, Rogan SC, Abbas AI, et al. Remote Control of Neuronal Activity in Transgenic Mice Expressing Evolved G Protein-Coupled Receptors. *Neuron*. 2009;63(1):27-39. doi:10.1016/j.neuron.2009.06.014
186. Roth B. DREADDs for Neuroscientists. *Neuron*. 2016;118(24):6072-6078. doi:10.1002/cncr.27633.Percutaneous
187. Zhu H, Roth BL. Silencing Synapses with DREADDs. *Neuron*. 2014;82(4):723-725. doi:10.1016/j.neuron.2014.05.002
188. Stachniak TJ, Ghosh A, Sternson SM. Chemogenetic synaptic silencing of neural circuits localizes a. 2014;82(4):797-808.
189. Ferguson SM, Phillips PEM, Roth BL, Wess J, Neumaier JF. Direct-Pathway Striatal Neurons Regulate the Retention of Decision-Making Strategies. *J*

Neurosci. 2013;33(28):11668-11676. doi:10.1523/jneurosci.4783-12.2013

190. Guettier J, Gautam D, Scarselli M, et al. A chemical-genetic approach to study G protein regulation of β cell function in vivo. *PNAS*. 2009;106(45):19197-19202.
191. Vardy E, Robinson JE, Li C, Olsen RHJ, DiBerto JF, Giguere PM. A New DREADD Facilitates the Multiplexed Chemogenetic Interrogation of Behavior. *Neuron*. 2015;86(4):936-946. doi:10.1016/j.neuron.2015.03.065
192. Campbell EJ, Marchant NJ. The use of chemogenetics in behavioural neuroscience: receptor variants, targeting approaches and caveats. *Br J Pharmacol*. 2018;175(7):994-1003. doi:10.1111/bph.14146
193. Chen X, Choo H, Huang XP, et al. The first structure-activity relationship studies for designer receptors exclusively activated by designer drugs. *ACS Chem Neurosci*. 2015;6(3):476-484. doi:10.1021/cn500325v
194. Hello Bio. DREADD agonist 21 (Compound 21) | Effective agonist for muscarinic-based DREADDs. https://www.hellobio.com/dreadd-agonist21.html. Accessed July 21, 2019.
195. Peñagarikano O, Lázaro MT, Lu X, et al. Exogenous and evoked oxytocin restores social behavior in the Cntnap2 mouse model of autism. *Sci Transl Med*. 2015;7(271):1-26. doi:10.1126/scitranslmed.3010257.Exogenous
196. Urban DJ, Zhu H, Marcinkiewcz CA, et al. Elucidation of the Behavioral Program and Neuronal Network Encoded by Dorsal Raphe Serotonergic Neurons. *Neuropsychopharmacology*. 2016;41(5):1404-1415. doi:10.1038/npp.2015.293
197. Chow BY, Han X, Boyden ES. *Genetically Encoded Molecular Tools for Light-Driven Silencing of Targeted Neurons*. Vol 196. 1st ed. Elsevier B.V.; 2012. doi:10.1016/B978-0-444-59426-6.00003-3
198. Josselyn SA. Genetic control of active neural circuits. *Front Mol Neurosci*. 2009;2(December):1-8. doi:10.3389/neuro.02.027
199. Kim H, Kim M, Im S-K, Fang S. Mouse Cre-LoxP system: general principles to determine tissue-specific roles of target genes. *Lab Anim Res*. 2018;34(4):147. doi:10.5625/lar.2018.34.4.147
200. Li M, Snider BJ. *Gene Therapy Methods and Their Applications in Neurological Disorders*. Elsevier Inc.; 2018. doi:10.1016/B978-0-12-809813-4.00001-6
201. del Rio D, Beucher B, Lavigne M, et al. CAV-2 vector development and gene transfer in the central and peripheral nervous systems. *Front Mol Neurosci*. 2019;12(March):1-16. doi:10.3389/fnmol.2019.00071
202. Kazdoba TM, Leach PT, Silverman JL, Crawley JN. Modeling fragile X syndrome in the Fmr1 knockout mouse. *Intractable Rare Dis Res*. 2014;3(4):118-133. doi:10.5582/irdr.2014.01024

203. Hayashi ML, Rao BSS, Seo JS, et al. Inhibition of p21-activated kinase rescues symptoms of fragile X syndrome in mice. *Proc Natl Acad Sci U S A*. 2007;104(27):11489-11494. doi:10.1073/pnas.0705003104
204. Nolan SO, Reynolds CD, Smith GD, et al. Deletion of Fmr1 results in sex-specific changes in behavior. *Brain Behav*. 2017;7(10):1-13. doi:10.1002/brb3.800
205. Aloisi E, Le Corf K, Dupuis J, et al. Altered surface mGluR5 dynamics provoke synaptic NMDAR dysfunction and cognitive defects in Fmr1 knockout mice. *Nat Commun*. 2017;8(1). doi:10.1038/s41467-017-01191-2
206. Liska A, Bertero A, Gomolka R, et al. Homozygous loss of autism-risk gene cntnap2 results in reduced local and long-range prefrontal functional connectivity. *Cereb Cortex*. 2018;28(4):1141-1153. doi:10.1093/cercor/bhx022
207. van Heukelum S, Mars RB, Guthrie M, et al. Where is Cingulate Cortex? A Cross-Species View. *Trends Neurosci*. 2020;43(5):285-299. doi:10.1016/j.tins.2020.03.007
208. Vann SD, Aggleton JP, Maguire EA. What does the retrosplenial cortex do? *Nat Rev Neurosci*. 2009;10(11):792-802. doi:10.1038/nrn2733
209. Kwapis JL, Jarome TJ, Lee JL, Helmstetter FJ. The retrosplenial cortex is involved in the formation of memory for context and trace fear conditioning. *Neurobiol Learn Mem*. 2015;123:110-116. doi:10.1016/j.nlm.2015.06.007
210. Lugo JN, Smith GD, Holley AJ. Trace fear conditioning in mice. *J Vis Exp*. 2014;(85):1-7. doi:10.3791/51180
211. Ye L, Allen WE, Thompson KR, Tian Q. Wiring and Molecular Features of Prefrontal Ensembes Representing Distinct Experiences. *Cell*. 2016;165(7):1776-1788. doi:10.1016/j.cell.2016.05.010
212. Paolone G, Mallory CS, Koshy Cherian A, Miller TR, Blakely RD, Sarter M. Monitoring cholinergic activity during attentional performance in mice heterozygous for the choline transporter: A model of cholinergic capacity limits. *Neuropharmacology*. 2013;75:274-285. doi:10.1016/j.neuropharm.2013.07.032
213. Bloem B, Poorthuis RB, Mansvelder HD. Cholinergic modulation of the medial prefrontal cortex: The role of nicotinic receptors in attention and regulation of neuronal activity. *Front Neural Circuits*. 2014;8(MAR):1-16. doi:10.3389/fncir.2014.00017
214. Chaves-Coira I, Martín-Cortecero J, Nuñez A, Rodrigo-Angulo ML. Basal Forebrain Nuclei Display Distinct Projecting Pathways and Functional Circuits to Sensory Primary and Prefrontal Cortices in the Rat. *Front Neuroanat*. 2018;12(August):1-15. doi:10.3389/fnana.2018.00069

215. Jin J, Chen Q, Qiao Q, et al. Orexin neurons in the lateral hypothalamus project to the medial prefrontal cortex with a rostro-caudal gradient. *Neurosci Lett*. 2016;621:9-14. doi:10.1016/j.neulet.2016.04.002
216. Lambe EK, Aghajanian GK. Hypocretin (orexin) induces calcium transients in single spines postsynaptic to identified thalamocortical boutons in prefrontal slice. *Neuron*. 2003;40(1):139-150. doi:10.1016/S0896-6273(03)00598-1
217. Wolff M, Vann SD. The cognitive thalamus as a gateway to mental representations. *J Neurosci*. 2019;39(1):3-14. doi:10.1523/JNEUROSCI.0479-18.2018
218. Saalmann YB, Kastner S. The cognitive thalamus. *Front Syst Neurosci*. 2015;9:1-2. doi:10.1038/nn957
219. Casas-Torremocha D, Porrero C, Rodriguez-Moreno J, et al. Posterior thalamic nucleus axon terminals have different structure and functional impact in the motor and somatosensory vibrissal cortices. *Brain Struct Funct*. 2019;224(4):1627-1645. doi:10.1007/s00429-019-01862-4
220. Wright NF, Vann SD, Aggleton JP, Nelson AJD. A critical role for the anterior thalamus in directing attention to task-relevant stimuli. *J Neurosci*. 2015;35(14):5480-5488. doi:10.1523/JNEUROSCI.4945-14.2015
221. Mátyás F, Lee J, Shin H-S, Acsády L. The fear circuit of the mouse forebrain: connections between the mediodorsal thalamus, frontal cortices and basolateral amygdala. *Eur J Neurosci*. 2014;39:1810-1823.
222. Meda KS, Patel T, Braz JM, Seikifar H, Basbaum AI, Sohal V. Microcircuit Mechanisms through which Mediodorsal Thalamic Input to Anterior Cingulate Cortex Exacerbates Pain-Related Aversion. *Neuron*. 2019;102:944-959.
223. Parnaudeau S, O'Neill PK, Bolkan SS, et al. Inhibition of medio-dorsal thalamus disrupts thalamo-frontal connectivity and cognition. *Neuron*. 2013;77(6):1151-1162.
224. Schmitt LI, Wimmer RD, Nakajima M, Mofakham S, Halassa MM. Thalamic amplification of cortical connectivity sustains attentional control. *Nature*. 2017;545(7653):219-223.
225. Bolkan SS, Stujenske JM, Parnaudeau S, et al. Thalamic projections sustain prefrontal activity during working memory maintenance. *Nat Neurosci*. 2017.
226. Delevich K, Tucciarone J, Huang ZJ, Li XB. The Mediodorsal Thalamus Drives Feedforward Inhibition in the Anterior Cingulate Cortex via Parvalbumin Interneurons. 2015;35(14):5743-5753. doi:10.1523/JNEUROSCI.4565-14.2015
227. Rogers TD, Dickson PE, McKimm E, et al. Reorganization of Circuits Underlying Cerebellar Modulation of Prefrontal Cortical Dopamine in Mouse Models of

Autism Spectrum Disorder. *Cerebellum*. 2013;12:547-556.

228. Granon S, Passetti F, Thomas KL, Dalley JW, Everitt BJ, Robbins TW. Enhanced and Impaired Attentional Performance After Infusion of D1 Dopaminergic Receptor Agents in Rat Prefrontal Cortex. *J Neurosci*. 2000;20(3):1208-1215.
229. Pezze MA, Marshall HJ, Domonkos A, Cassaday HJ. Effects of dopamine D1 modulation of the anterior cingulate cortex in a fear conditioning procedure. *Prog Neuropsychopharmacol Biol Psychiatry*. 2015;65:60-67.
230. Pezze MA, Marshall HJ, Cassaday HJ. Dopaminergic modulation of appetitive trace conditioning: the role of D1 receptors in medial prefrontal cortex. *Psychopharmacology (Berl)*. 2015.
231. Castle M, Turunen H, Vandenberghe L, Wolfe J. Controlling AAV Tropism in the Nervous System with Natural and Engineered Capsids. 2016;1382(1382):133-149. doi:10.1007/978-1-4939-3271-9
232. Smith KS, Bucci DJ, Luikart BW, Mahler S V. DREADDs: Use and application in behavioral neuroscience. *Behav Neurosci*. 2016;130(2):137-155. doi:10.1037/bne0000135
233. Pietropaolo S, Guilleminot A, Martin B, D'Amato FR, Crusio WE. Genetic-background modulation of core and variable autistic-like symptoms in Fmr1 knock-out mice. *PLoS One*. 2011;6(2):1-11. doi:10.1371/journal.pone.0017073
234. Carreno-Munoz MI, Martins F, Medrano MC, et al. Potential Involvement of Impaired BK Ca Channel Function in Sensory Defensiveness and Some Behavioral Disturbances Induced by Unfamiliar Environment in a Mouse Model of Fragile X Syndrome. *Neuropsychopharmacology*. 2017;43(3):492-502. doi:10.1038/npp.2017.149
235. Michalon A, Sidorov M, Ballard TM, et al. Chronic Pharmacological mGlu5 Inhibition Corrects Fragile X in Adult Mice. *Neuron*. 2012;74(1):49-56. doi:10.1016/j.neuron.2012.03.009
236. Manvich DF, Webster KA, Foster SL, et al. The DREADD agonist clozapine N-oxide (CNO) is reverse-metabolized to clozapine and produces clozapine-like interoceptive stimulus effects in rats and mice. *Sci Rep*. 2018;8(1):1-10. doi:10.1038/s41598-018-22116-z
237. Goutaudier R, Coizet V, Carcenac C, Carnicella S. Dreadds: The power of the lock, the weakness of the key. favoring the pursuit of specific conditions rather than specific ligands. *eNeuro*. 2019;6(5):1-5. doi:10.1523/ENEURO.0171-19.2019
238. Fiala A, Suska A, Schlüter OM. Optogenetic approaches in neuroscience. *Curr*

Biol. 2010;20(20):897-903. doi:10.1016/j.cub.2010.08.053

239. Atasoy D, Sternson SM. Chemogenetic tools for causal cellular and neuronal biology. *Physiol Rev*. 2018;98(1):391-418. doi:10.1152/physrev.00009.2017

240. Li XB, Inoue T, Nakagawa S, Koyama T. Effect of mediodorsal thalamic nucleus lesion on contextual fear conditioning in rats. *Brain Res*. 2004;1008(2):261-272. doi:10.1016/j.brainres.2004.02.038

241. Powell DA, Churchwell J. Mediodorsal thalamic lesions impair trace eyeblink conditioning in the rabbit. *Learn Mem*. 2002;9(1):10-17. doi:10.1101/lm.45302

APPENDIX 1. List of inputs into ACC neurons engaged during TFC

ISOCORTEX	Frontal pole (FRP)			
	Somatomotor cortex	Primary (MOp)		
		Secondary (MOs)		
	Somatosensory cortex	Primary (SSp)		
		Supplemental (SSs)		
	Gustatory cortex (GU)			
	Visceral cortex (VISC)			
	Auditory cortex (AU)			
	Visual cortex (VIS)	Anterolateral (VISal)		
	Anterior cingulate Cortex	Dorsal (ACCd)		
		Ventral (ACCv)		
	Prelimbic cortex (PL)			
	Infralimbic cortex (ILA)			
	Orbital cortex	Lateral (ORBl)		
		Medial (ORBm)		
		Ventrolateral (ORBvl)		
	Agranular insular cortex	Dorsal (AId)		
		Posterior (AIp)		
		Ventral (AIv)		
	Retrosplenial cortex	Lateral agranular (RSPagl)		
		Dorsal (RSPd)		
		Ventral (RSPv)		
	Midcingulate cortex (MCC)			
	Posterior parietal association areas (PTLp)			
	Ectorhinal area (ECT)			
OLFACTORY AREAS	Main olfactory bulb (MOB)			
	Anterior olfactory nucleus (AON)			
	Taenia tecta	Dorsal (TTd)		
		Ventral (TTv)		
	Dorsal peduncular area (DP)			
	Piriform area (PIR)			
	Cortical amygdalar area (COA)			
	Piriform-amygdalar area (PAA)			
	Post-piriform transition area (TR)			
HIPPOCAMPAL FORMATION	Hippocampal region	Ammon's horn	CA1	
			CA3	
	Retrohippocampal region	Entorhinal area	Lateral (ENTl)	
CORTICAL SUBPLATE	Claustrum (CL)			
	Endopiriform nucleus (EP)			
	Basolateral amygdalar nucleus (BLA)			
	Basomedial amygdalar nucleus (BMA)			
STRIATUM	Dorsal region	Caudoputamen (CP)		
	Ventral region	Nucleus accumbens (ACB) Olfactory tubercle (OT)		
	Lateral septal complex	Lateral septal nucleus (LS)		
	Striatum-like amygdalar nuclei	Anterior amygdalar area (AAA) Central amygdalar nucleus (CEA)		
		Medial amygdalar nucleus (MEA)		
PALLIDUM	Dorsal region	Globus pallidus (GP)		
	Ventral region	Substantia innominata (SI)		
		Magnocellular nucleus (MA)		
	Medial region	Medial septal complex	Diagonal band nucleus (NDB)	
			Medial septal nucleus (MS)	
	Caudal region	Bed nuclei of the stria terminalis (BST)		
THALAMUS	Sensory-motor cortex related	**Ventral group**	Ventral anterior-lateral complex (VAL)	
			Ventral medial nucleus (VM)	
			Ventral posterior complex	Ventral posterolateral nucleus (VPL)
				Ventral posteromedial nucleus (VPM)
				Ventral posteromedial nucleus, parvicellular part (VPMpc)
		Subparafascicular area (SPA)		
	Polymodal association cortex related	**Lateral group**	Lateral posterior nucleus (LP)	
			Posterior complex (PO)	
		Anterior group	Anteroventral nucleus (AV)	
			Anteromedial nucleus (AM)	
			Anterodorsal nucleus (AD)	
			Interanterodorsal nucleus (IAD)	
			Lateral dorsal nucleus (LD)	
		Medial group	Intermediodorsal nucleus (IMD)	
			Mediodorsal nucleus (MD)	
			Submedial nucleus (SMT)	
		Midline group	Paraventricular nucleus (PVT)	
			Parataenial nucleus (PT)	
		Intralaminar nuclei	Rhomboid nucleus (RH)	
			Central medial nucleus (CM)	
			Paracentral nucleus (PCN)	
			Central lateral nucleus (CL)	
			Parafascicular nucleus (PF)	
		Reticular nucleus (RT)		
HYPOTHALAMUS	Periventricular zone	Medial preoptic area (MPO)		
		Periventricular hypothalamic nucleus (PVp)		
	Hypothalamic lateral zone	Lateral hypothalamic area (LHA)		
		Lateral preoptic area (LPO)		
		Zona incerta (ZI)		
	Hypothalamic medial zone	Mammillary body Posterior hypothalamic nucleus (PH)		
MIDBRAIN	Motor related	Substantia nigra, reticular part (SNr)		
		Ventral tegmental area (VTA)		
		Midbrain reticular nucleus (MRN)		
		Superior colliculus, motor related (SCm)		
		Periaqueductal gray (PAG)		
		Pretectal region (PRT)	Anterior pretectal nucleus (APN)	
			Nucleus of the posterior comissure (NPC)	
		Red nucleus (RN)		
		Ventral tegmental nucleus (VTN)		
	Behavioral state related	Substantia nigra, compact part (SNc)		
		Midbrain raph nuclei	Interpeduncular nucleus (IPN)	
			Central linear nucleus raphe (CLI)	
			Interfascicular nucleus raphe (IF)	
		Pedunculopontine nucleus (PPN)		
HINDBRAIN	Pons	Pons behavioral state related	Pontine reticular nucleus (PNr)	
			Superior central nucleus raphe (CS)	
		Pons motor related	Pontine central gray (PCG)	
			Tegmental reticular nucleus (TRN)	